Investigating the role of Wnt/ß-catenin pathway in pluripotency and somatic cell reprogramming

Francesco Aulicino

Tesi Doctoral UPF - 2016

Thesis Director:

Dr. Maria Pia Cosma

Gene Regulation, Stem Cells and Cancer DepartmentCenter for Genomic Regulation (CRG) - Barcelona

To my family

Acknowledgements

Thanks to Pia for giving me the opportunity to join her lab. I grew a lot during these years and she gave me the possibility to develop and satisfy my scientific interests posing no limits to my ideas. She had always encouraged me to develop my own hypotheses and to acquire a number of technical skills to prove or confute them, with a freedom rarely granted to PhD students.

Thanks to all Pia Cosma's lab. Whe have been friends more than simple co-workers and glad to share expertise and suggestions amongst us. Thanks to Luigi, who guided my first steps in the lab and to Fredi, who gradually made me able to work independently. Thanks to Ilda, for sharing the joys and pains of a paper with a seemingly endless revision,

Thanks to Elisa, amongst other things for cigarette-breaks passed discussing the whereabouts of ß-catenin in the nucleus. We shared many scientific "disgraces" but we worked them out together. Thanks to Giacoma for being Giacoma. Thanks to Valeria, Birgit, Jack, Lorenzo, Jordi and to my flat-mates Jara and Angie.

A special thank goes to Franky, who "forced" me to after-work beers and always helped me practically and technically. Sorry for all the useless experiments I have dragged you in (they all seemed good ideas in principle). As your mug says "you are the one who knocks". I wish you all the best.

A personal thank goes to my parents, who always supported me since when I left home 10 years ago. It has been a long journey and it has not finished yet. Although distant they are always close to me, and keep alive a special place in Italy, the only one I will always consider "home". No matter where I go, the values they taught me will always be with me and made the person who I am, and will be.

Thanks to Lucia, who helped me in so many ways I cannot even recall. She always listened to me and did not let me down even when I was too proud to ask for help, often with nothing in return. I am sorry for putting her aside during the last year, too much work almost drove me mad, but she always stood there for me.

Thanks to my brother, who is amongst the person I most appreciate. I have rarely met his sincerity and his love for life in other people. He is a modern philosopher from whom I often inspire, even if he does not know it. I wish him all the best and hope to roam with him on mountains and forests (no caves though, thanks) for many days to come.

Thanks to all the friends I left behind in Italy or all over the world, Antonio, Felice, Lorenzo, Bruno, Giovanni, Giovanni (no it is not a mistake), Toru (aka Davide) and all the others I will remember tomorrow, when this thesis will be already printed. Sorry.

Abstract

The adaptive response of cells to external stimuli is an intriguing mechanism at the basis of the existence of life itself. For this purpose, signalling pathways and gene regulatory networks elegantly evolved translating extracellular signals into finely tuned cellular responses. Among them, the Wnt/ß-catenin signalling pathway converges on the regulation of ß-catenin protein, which, in turn regulates target gene expression. In particular the Wnt/ß-catenin pathway plays a pivotal role in sustaining pluripotency and somatic cell reprogramming.

Here we identified a temporal of Wnt/ß-catenin activity during somatic cell reprogramming, controlling the expression levels of mesenchymal-to-epithelial transition and senescence-associated genes through TCF1.

We demonstrated that the "Wnt-OFF" state is an early reprogramming marker and that dynamic modulation can be effectively used to increase the reprogramming efficiency.

Furthermore the Wnt/ß-catenin pathway is a key regulator of pluripotency and self-renewal of mouse embryonic stem cells (mESCs) and a small-molecule activator of the Wnt pathway is widely used to maintain embryonic stem cells in a ground state of pluripotency.

The role of ß-catenin in mESCs is however still controversial. We noticed available ß-catenin knock-out models are flawed by the production of N-terminally truncated proteins with unknown functions. We therefore generated a novel ß-catenin knock-out using CRISPR/Cas9 technology, hoping to have clearer insight of ß-catenin functions in mESCs.

We have also found that ground state pluripotency promoted by sustained Wnt pathway activation cannot be maintained indefinitely, resulting in a "lapsed" ground state possibly due, among other factors, to regulatory negative feedback loops that impair Wnt/ß-catenin activity.

Resumen

La respuesta adaptativa de las células a estímulos externos es un mecanismo fundamental de la existencia de la vida en sí misma. Para este fin, rutas de señalización y redes de regulación génica evolucionaron elegantemente, traduciendo señales extracelulares en respuestas celulares calibradas con precisión. Entre ellas, la ruta de señalización de Wnt/ß-catenin converge en la regulación de la proteína ß-catenin, que a su vez regula la expresión de genes diana. En particular, la ruta de Wnt/ß-catenin tiene un rol fundamental en el mantenimiento de la pluripotencia y la reprogramación de células somáticas. En esta tesis hemos identificado un papel temporal de actividad de Wnt/ß-catenin durante la reprogramación de células somáticas, lo que controla los niveles de expresión de genes asociados a transición mesenquima-epitelial y senescencia a través de TCF1. Además, la ruta de Wnt/ß-catenin es un regulador clave de la pluripotencia y la auto-renovación de células madre embrionarias de ratón (mESCs). Una pequeña molécula, activadora de la ruta Wnt es usada comúnmente para mantener las células madre embrionarias en *"ground state"* de pluripotencia. Sin embargo, el rol de la ß-catenin en las mESCs es aún controvertido. Observamos que los modelos disponibles de *Knock-Out* de ß-catenin producen proteínas truncadas en N-terminal con funciones desconocidas. Por ello, generamos un nuevo *Knock-Out* usando CRISPR/Cas9, al fin de clarificar funciones de ß-catenina en mESCs.

Hemos encontrado también que el *"ground state"* de pluripotencia promovido por la activación sostenida de Wnt no puede ser mantenido indefinidamente, resultando esto en un*" lapsed ground state"*; debido posiblemente, entre otros factores, a feedback-loop negativos que afectan negativamente la actividad de Wnt/ß-catenin.

Preface

Wnt/ß-catenin signalling is involved in a variety of cellular processes spanning from cancer initiation to proliferation and development. Moreover its function has been extensively characterized in pluripotency regulation of embryonic stem cell and in regulating both direct and cell-fusion mediated somatic cell reprogramming.

To date it is still not clear how the Wnt/ß-catenin pathway regulates different processes in different cell types; however the answer could arise by considering levels and dynamics of activation as well as the context specific ß-catenin pathway responses, from Wnt ligands to nuclear interactors.

Giving the importance of Wnt/ß-catenin signalling in controlling cell-fate identitiy, a detailed study of its molecular components, mechanisms and functions is key to understand and harness pluripotent stem cells biology and somatic cell reprogramming.

Table of contents

PART I – INTRODUCTION

CHAPTER 1 – Wnt pathways and genes

Wingless, int-1 and Wnts

Back in 1984, Roel Nusse and Harold Varmus (Nusse et al. 1984) were studying the genomic integration sites of mouse mammary tumour virus (MMTV) to identify genes responsible for cancer initiation. The MMTV proviral genome was found integrated in the chromosome 15 of many tumour cell lines at the 5' or 3' of a new gene that the authors called "int-1". Int-1 was identified as a potential oncogene, whose reactivation after MMTV infection could lead to tumour initiation. This approach led to the identification of two additional genes (int-2 and int-3) (Peters et al. 1983, Gallahan et al. 1987), which did not share sequence or functional conservation among them. Int-2 (later named Fgf3) and Int-3 (later annotated as Notch4) were found to be a fibroblast growth factor and a trans-membrane protein, respectively.

Int-1 was instead proved to be a secreted glycoprotein, and in 1987 researchers realized that the gene they accidentally identified was the homologous of the Drosophila Wingless (Wgl) gene (Rijsewijk et al. 1987), discovered and mapped in 1973 (Sharma 1973, Sharma et al. 1976) and characterized as a segment polarity gene by Christiane Nüsslein-Volhard and Eric Wieschaus in 1980 (Nusslein-Volhard et al. 1980) (Nobel laureates later in 1995 for their pioneering studies on developmental genes).

In 1991 multiple int-1 family genes had already been identified in different species (10 in mouse and 3 in human) and a new nomenclature was necessary: Wingless and int-1 names finally fused into Wnt, to be pronounced "wint" (Nusse et al. 1991). While Nüsslein-Volhard and Eric Wieschaus already pointed out that Wgl was important in Drosophila

development, the Wnt proteins were only at their baptisms, a new field ahead would have shed light on their functions, mechanisms and evolutionary importance.

1.1 Conservation and structure of Wnt proteins

While it soon became clear that Wnt genes were a conserved class of secreted glycoproteins, unravelling their specie-specific roles and functions required a significant amount of research.

Wnt genes are conserved in all animals from hydra to humans, but they are absent from plants, unicellalur eukaryots and prokaryots. In human and mouse 19 Wnt genes have been mapped, mostly spread on different chromosome locations, an hint that their evolutionary diversification occurred by genome duplication or gene translocation rather than local duplication (Miller 2002) (Table 1).

A certain degree of functional conservation across species was found, but in Drosophila Wingless mostly related to segment polarity regulation (Nusslein-Volhard et al. 1980), while in mouse Wnt1 was found to be fundamental for embryo development and spermatogenesis (Nusse et al. 1991), and also related to cancer initiation, as firstly reported by Nusse et al. (Nusse et al. 1984). It is indeed intriguing how Wnt family genes can control multiple processes in different species and, within the same organism, in different cell types.

Human		Mouse	
Gene name	**Chromosome**	**Gene name**	**Chromosome**
WNT1	12q13	***Wnt1***	15
WNT2	7q31	***Wnt2***	6
WNT2b/13	1p13	***Wnt2b/13***	3
WNT3	17q21	***Wnt3***	11
WNT3a	1q42.13	***Wnt3a***	11
WNT4	1p35	***Wnt4***	4
WNT5a	3p14-p21	***Wnt5a***	14
WNT5b	12p13.3	***Wnt5b***	6
WNT6	2q35	***Wnt6***	1
WNT7a	3p25	***Wnt7a***	6
WNT7b	22q13.3	***Wnt7b***	15
WNT8a/d	5q31	***Wnt8a***	18
WNT8b	10q24	***Wnt8b***	19
WNT10a	2q35	***Wnt10a***	1
WNT10b/12	12q13.1	***Wnt10b***	15
WNT11	11q13.5	***Wnt11***	7
WNT14/WNT9a	1q42	***Wnt14(Wnt9a)***	11
WNT15	17q21	***Wnt15***	11
WNT16	7q31	***Wnt16***	6

Table 1 – Homologues Wnt genes between human and mouse, adapted from Miller R.J.(1992).

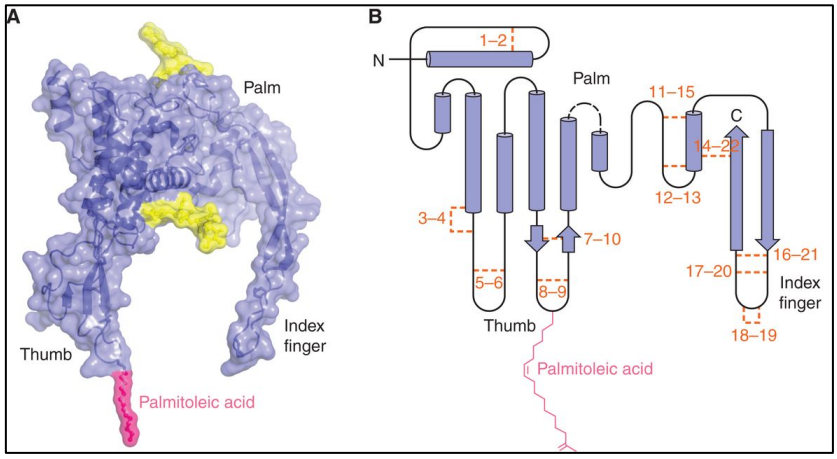

Figure 1 - Space-filling model (A) and secondary structure (B) of Xenopus Xwnt8a in its receptor-bound conformation (receptor not shown). Yellow cluster show N-glycosilation, palmytoleic acid is shown in purple and cysteine residues (22 for Xwnt8) and disulphide bridges are shown in orange. Adapted from Wilert et al. 2012.

Wnt proteins range from 39 to 43 KDa, but little is known about their structure, except for Xenopus Xwnt8 (Janda et al. 2012) and Drosophila WntD. Regarding amino acid composition, between 23 and 24 cysteine residues have been found to be spaced by sequence of conserved length, suggesting that the formation of disulphide bonds could be a dominating factor in regulating Wnt proteins folding and a conserved central serine is indispensable for palmitoylation (Willert et al. 2012) (Figure 1). I will discuss in further details the nature and importance of Wnts post-translational modification in a separate section.

Wnt genes evolved from a common ancestor, which is reflected by the core structure, to fulfil different biological tasks. This is the first level of complexity of Wnt pathway, surely one of the most important. Different Wnts can bind to different receptors, triggering partially overlapping functions or completely different cellular responses.

For instance, overexpression of Xwnt8 into Xenopus embryos ventralized by UV irradiation is able to rescue axis formation through the reactivation of the homeobox protein *goosecoid* (Gsc). In contrast, overexpression of Xwnt5 in wild-type embryos leads to dorso-anterior structures defects, without affecting Gsc expression. Interestingly, the overexpression of a chimeric protein with N-terminal Xwnt8 and C-terminal Xwnt5 mimics the effects of wild-type Xwnt8 overexpression, and vice versa (Du et al. 1995, Miller 2002), suggesting that C-terminal Wnt portion is responsible for selective binding between Wnts and their cognate receptors.

Deletion of C-terminal Xwnt8 moreover results in a dominant-negative protein which can still interact with the receptor but fails to activate it, confirming the importance of carboxyl-terminal residues in Wnt/receptor specificity but also suggesting that the N-terminus is required for proper ligand-receptor interaction (Hoppler et al. 1996, Miller 2002).

1.2 Major biological processes and phenotypes in mouse

Wnt proteins regulate different biological processes and concur to regulate development, cell-fate determination and cell-cycle control. Moreover the same molecule can trigger different, or opposite cellular responses depending on the downstream signalling components, levels and timing of Wnts availability. For the sake of clarity, I will resume briefly the major phenotypes found in association with specific Wnts knock-out/loss of function mice as listed by Roel Nusse in his Wnt-dedicated internet page (Bibliography: Nusse"The Wnt-homepage") (Table 2).

Gene KO	Phenotype
Wnt1	• loss midbrain, loss cerebellum • deficiency in neural crest derivatives, reduction in dorsolateral neural precursors in the neural tube together with Wnt-3A KO • decrease in the number of thymocytes (with Wnt-4 deletion)
Wnt2	• placental defects • Defective lung development (with Wnt2b)
Wnt2b/13	• Retinal cell differentiation • Defective lung development (with Wnt2b) • Olfactory bulb reduction
Wnt3	• Early gastrulation defect; Axis formation • Hair growth • Defect in establishing the apical ectodermal ridge (AER) • medial-lateral retinotectal topography • hippocampal neurogenesis
Wnt3a	• Somites, tailbud defects through loss expression Brachyury (Lef1-mediated) • Deficiency in neural crest derivatives, reduction in dorsolateral neural precursors in the neural tube together with Wnt-1 KO • Loss hippocampus • Segmentation oscillation clock • Left right asymmetry • HSC self-renewal defect

Wnt4	• kidney defects, renal vesicle induction • Sex determination defects in female development; • absence Mullerian Duct. Ectopic Testosterone synthesis in females. • Side-branching in mammary gland • Decrease in the number of thymocytes (with Wnt-1 deletion) • Repression of the migration of steroidogenic adrenal precursors into the gonads • Lung development
Wnt5	• truncated limbs, truncated AP axis, reduced number proliferating cells • Distal lung morphogenesis • Chondrocyte differentiation, longitudinal skeletal outgrowth • Inhibits B cell proliferation and functions as a tumour suppressor • Defects in posterior growth of the female reproductive tract • shortened and widened cochlea (planar polarity) • Mammary gland phenotype • prostate gland development • intestinal elongation Cervantes • endothelial differentiation of ES cells Yang
Wnt6	• stromal cell proliferation in embryo
Wnt7a	• Limb polarity • female infertility; failure regression of the Mullerian duct because the receptor for Mullerian-inhibiting substance is not expressed • maintenance appropriate uterine patterning during the development of the mouse female reproductive tract • Delayed maturation synapses in Cerebellum • High levels cell death in response to DES in the Female Reproductive Tract • May promote neuronal differentiation • CNS vasculature (with Wnt7b)
Wnt7b	• Placental developmental defects • Respiratory failure; defects in early mesenchymal proliferation leading to lung hypoplasia • macrophage-induced programmed cell death also in LRP5 and LEF1 mutants • Lung development • CNS vasculature (with Wnt7a) • Cortico-medullary axis in the kidney
Wnt9a	• Loss of function mutant: Joint integrity

Wnt9b	• Regulation of mesenchymal to epithelial transitions • Renal vesicle induction • Planar cell polarity of the kidney epithelium
Wnt10	• Loss of function mutant: decreased trabecular bone, loss bone mass • Taste Papilla Development • Loss gene promotes coexpression of myogenic and adipogenic program
Wnt11	• Ureteric branching defects • Cardiogenesis
Wnt16	• Bone Density phenotype

Table 2 - Genetic ablation and loss of function experiments demonstrate that Wnts are involved in many biological processes throughout development and cell-fate specification. Adapted from R.Nusse "The Wnt Homepage".

The severe phenotypes induced by ablation of several Wnts highlight the importance of these proteins in controlling mouse embryo development and cell fate-specification. As anticipated in the previous paragraphs, Wnts can control partially overlapping or completely different cellular programs, as reflected by the variety of phenotypes triggered by genetic loss of Wnt proteins. In addition Wnt proteins display some degree of functional redundancy, for instance Wnt1 is important for midbrain patterning and Wnt3a for formation of the paraxial mesoderm, however Wnt1/Wnt3a double knock-out triggers deficiency in neural crest derivatives and a reduction in dorsolateral neural precursors in the neural tube (Ikeya et al. 1997). Of course, from an evolutionary point of view, redundancy is reflected into signalling flexibility, and the possibility to overcome dangerous mutations, at least in part, promoting adaptation of the biological system. Wnt signalling redundancy is to be found at almost any level of signal transduction, from ligands to downstream effectors. It is not rare, for instance, to find two protein homologs having different roles that can easily compensate for the absence of the other and vice versa.

1.3 Wnts post-translational modification and secretion

Before providing further details about Wnt signalling, I will briefly resume the nature of Wnt proteins post-translational modifications, and their impact on Wnt signalling functions.

Wnt proteins undergo extensive post-translational modification, mainly through glycosylation and acylation (Willert et al. 2003). It has been speculated that N-glycosylation could be related to extracellular Wnt transport, increasing the interaction with heparan sulfate proteoglycans present on target cells in Drosophila (Binari et al. 1997). To date, is still unclear to which extent Wnt N-glycosylation is required for proper folding or extracellular transport; also, its relevance has been challenged by the observation that, in Drosophila, N-glycosylation appears to be dispensable for proper Wnt secretion and signalling, while lipid modifications play a major role in both processes (Tang et al. 2012).

The primary structure of Wnt proteins suggest they are quite soluble, but also extremely hydrophobic, due to the addition of palmitate and/or palmitoleic acid to one or two residues (Cys77 and/or Ser209 in Wnt3a) (Janda et al. 2012). The palmitoylation is necessary for Wnt signalling, since enzymatic digestion of the palmitate modification in purified extracts results in neither hydrophobic nor biologically active Wnt protein (Willert et al. 2003). Where palmitoylation is required for proper Wnt secretion, membrane positioning and target cells anchoring have been extensively debated (Mikels et al. 2006). Palmytoilation seems to be essential for Wnt N-glycosylation, suggesting that it serves as an anchor to the endoplasmic reticulum (ER), helping to keep Wnt protein in close proximity to the oligosaccharyl transferase complex (Willert et al. 2003). Besides, the structural analysis of XWnt8 with its receptor Fzd, had shed new lights on the role of this post-translational modification. The

palmitate moiety of XWnt8 protrudes from the Wnt structure into a deep grove of Fzd/CRD receptor (Janda et al. 2012), and seems to be required for the stabilization of the ligand-receptor complex and effective signal transduction in a unique mechanism of ligand-receptor interaction (Figure 2).

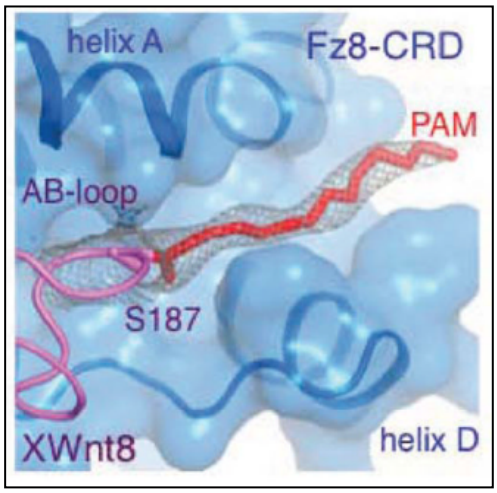

Figure 2 – The palmitate (PAM, in red) protrude from Xwnt8 serine 187 to a deep grove in Fzd receptor, highlighting a function in ligand-receptor interaction. Adapted from Janda et al. 2012

Within the ER, Wnt proteins are palmitoylated by *porcupine*, a seven helices trans-membrane protein localized in the ER itself. Porcupine was identified in Drosophila and C.elegans (*mom-1*), and mutants of this gene showed reduced or aberrant Wnt signalling with increased ER retention of Wnt proteins. These results suggest that producing cells are unable to correctly secrete Wnts (Tanaka et al. 2000); as a consequence, less Wgl (Wnt Drosophila ortholog) is found on target cell membrane (Zhai et al. 2004).

Furthermore, Porcupine mutants showed embryo lethality in mouse, ablating all Wnt activity (Willert et al. 2012).

Wntless/eveness/mom-3 (wls/evi/mom-3), a multipass transmembrane protein, plays a major role in Wnt secretion. RNA interference of wls/evi/mom-3 shows a phenotype similar to porcupine ablation in both Drosophila and mammalian cell culture (Banziger et al. 2006), including increase retention of Wnts into the ER and reduced Wnt signalling activity. However, unlike porcupine, wls/evi/mom-3 does not localize in the ER and does not alter N-glycosilation, while palmytoilation seems to be required for Wls interaction with Wnt proteins in the Golgi, where it acts as a sorting receptor, guiding Wnts toward the cell-membrane (Willert et al. 2012).

The final steps of Wnts intracellular journey toward the membrane are

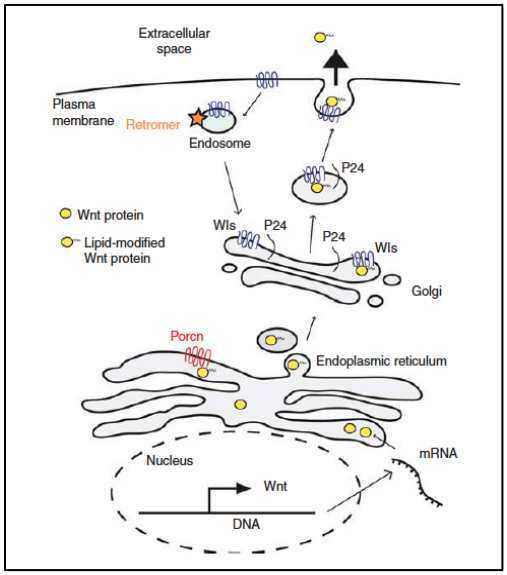

Figure 3 - Wnts secretion. In the endoplasmic reticulum (ER), Wnts mRNA are translated and readily acylated by Porcupine. Wls binds acylated Wnts and guide them out the Golgi toward the cell-surface together with the p24 cargo protein. At the cell surface, Wnts are released in the extracellular space, while Wls is recycled through the retromer complex, which repositionsWls back in the Golgi to bind newly synthetized Wnts. Adapted from Willert and Nusee 2012.

members of the p24 family of cargo proteins, which take part in the anterograde transport of Wnt proteins and do not seem to regulate other secreted factors (Buechling et al. 2011), pointing out that Wnts require an active mechanism of secretion. Once Wnts reach the cell membrane, they are finally released and Wls is recycled through the retromer complex to escort newly processed Wnts to the cell surface (Coudreuse et al. 2006) (Figure 3).

1.4 Wnts Receptors

Two distinct families of cell membrane associated receptors are involved in Wnt signalling transduction: Frizzled and LRP. Frizzled (Fzd) proteins are seven helices transmembrane receptors, with an amino-terminal cysteine rich-domain (CRD) that recognizes Wnt ligands and a short cytoplasmic C-terminal tail with a PDZ binding motif domain. Fzd is very similar to G-protein-coupled receptor, suggesting that heterotrimeric G proteins might also be involved in transducing Wnt signalling (Liu et al. 2001, Miller 2002). As Wnt proteins, also Fzd receptors have diversified to fulfil different functions; a total of 10 Fzd genes have been identified in mouse and human.

On the other hand, members of the LDL-receptor-related (LDLR) proteins can bind Wnts forming ternary complex with Fzd and Wnt ligands (Tamai et al. 2000, Miller 2002). In particular, Lrp5 and Lrp6 have been proved to be important for Wnt signalling transduction. LRP-6 mutations in mice produce developmental defects, phenocopying the absence of several Wnt genes while *arrow*, the Drosophila ortholog of LRP-5 and 6, is required for succesfull Wnt signalling (Wehrli et al. 2000).

Lrp5/6 are anchored to the plasma membrane and possess a 207aa cytoplasmic domain. Their structure contains a large extracellular domain, accounting for up to 85% of all the aminoacids of both proteins. The N-terminus is projected into the extracellular space and contains four

epidermal growth factor-like repeats that create binding sites for Wnts or other ligands (Bhat et al. 2007, Williams et al. 2009).

Furthermore Lrp5/6 responsiveness to Wnt ligands is regulated by members of the Dickkopf (Dkk) family, in particular Dkk1, Dkk2 and Dkk4, which can act as competitors for Wnts binding, occupying the receptor and thus preventing signal transduction (Niehrs 2006).

Specific Wnts can in addition bind to another class of membrane bound threonine kinase receptors (RTK) such as Ror1/2, functioning as a Fzd co-receptor or working in a Fzd-independent way (De 2011).

1.5 Non-canonical Wnt pathways

Distinct sets of Wnts can interact and activate different receptors, triggering different cellular responses.

Three main pathways are under control of Wnt signalling: a canonical Wnt/ß-catenin pathway and two non-canonical Wnt pathways, the planar cell polarity pathway and the Wnt/Ca2+ pathway. The canonical pathway (that I will describe in detail in Chapter 2) acts in the downstream regulation of ß-catenin protein stability and transcriptional activity, while non-canonical pathways by definition, act through mechanisms independent from ß-catenin (Rao et al. 2010). To date Wnt4, Wnt5a and Wnt11 have been found to be involved in non-canonical Wnt/pathways (Tao et al. 2005).

1.6.1 The planar cell-polarity pathway

Wnt/Planar cell polarity pathway controls coordinated behaviour of a population of polarized cells. It is required for the generation of highly ordered cellular structures during development and morphogenesis. Most of the proteins involved in the planar cell polarity (PCP) pathway have been identified from studies in Drosophila; defects in these proteins result in a range of phenotypes, from randomized orientation of epithelial

structures (Seifert et al. 2007) to defects in hair follicles orientation and hexagonal array of the ommatidia in the eye (Mlodzik 2002). The role of PCP in vertebrates regulates instead the organization of hair follicles and the migratory behaviour of dorsal mesodermal cells during gastrulation (Wang et al. 2007). The PCP pathway regulates the actin cytoskeleton, regulating cell polarization and migration. In non-canonical pathways, Wnts mainly interact with the Fzd co-receptor independently of Lrp5/6 (He et al. 2004). The signal is then transduced to Dishevelled (Dsh), which in turn activates the GTPases Rho and Rac (Cadigan et al. 2006). From this point on, two branches emerge from the same signal. Activation of Rho leads to the activation of the Rho-associated kinase (ROCK) (Marlow et al. 2002), which, in turn, modifies actin polymerization, consequently reshaping the cytoskeleton. On the other hand, Rac stimulates c-Jun N-terminal kinase (JNK), converging on cytoskeleton rearrangement (Komiya et al. 2008) (Figure 4) .

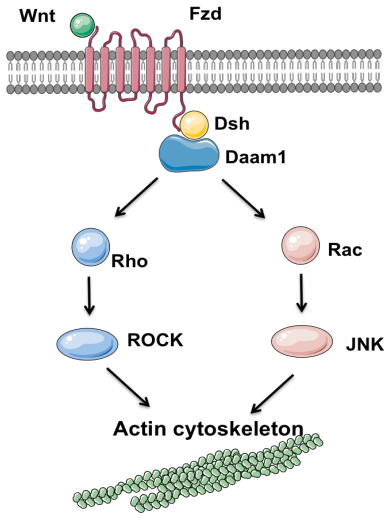

Figure 4 A simplified version of the Wnt/planar cell-polarity pathway. Adapted from Komiya 2008.

1.6.2 The Wnt/Ca^{2+} pathway

Wnt ligands can also regulate the intracellular concentration of Ca^{2+}. When Wnt binds to Frizzled receptor, in association with Ror1/2 co-receptor, heterotrimeric G proteins lead to the activation of phospholipase C, which in turn converts phosphatidylinositol 4,5-biphosphate into inositol 1,4,5-triphosphate (IP3) and 1,2 diacylglycerol (DAG) (De 2011). IP3 diffuses through the cytosol interacting with the calcium channels on the membrane of the endoplasmic reticulum (ER) resulting in release of calcium ions from ER to cytosol. Calcium is a potent second messenger, and its concentration levels inside the cells can quickly trigger different cellular responses. Together with calmodulin, Ca^{2+} activates calmodulin-dependent protein kinase II (CaMKII) (Kuhl et al. 2000) while, in complex with DAG, activates protein kinase C (PKC) (Sheldahl et al. 1999). Both CaMKII and PKC can activate nuclear transcription factors such as NFkB and CREB. Furthermore increased calcium levels activate calcineurin phosphatase, which by dephosphorilation, activates NFAT transcription factor (Figure 5).

Regarding the specific components of the pathway, only a subset of Wnt ligands and receptors is able to stimulate intracellular Calcium levels increase as a second messenger. The Wnt/Ca^{2+} pathway is mainly activated by Wnt5a and Wnt11, acting through Fzd-2, Fzd-4 and Fzd-6 (Kohn et al. 2005). Moreover Ror2 (Hikasa et al. 2002) co-receptor and Knypek (Topczewski et al. 2001) have also been found to be involved in Wnt/calcium pathway.

Experimental evidences suggest that Wnt5a, acting through Wnt/Ca^{2+} signalling, is able to interfere with canonical Wnt/ß-catenin signalling (Hikasa et al. 2002), making it difficult to study isolated pathways components.

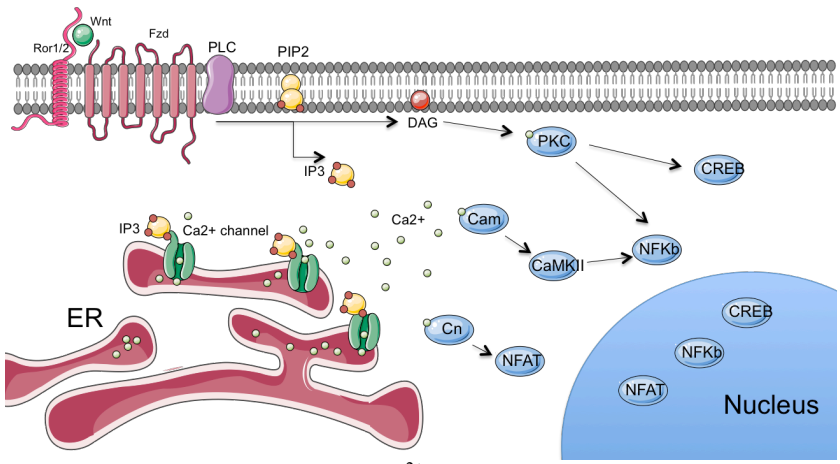

Figure 5 – Topology of the Wnt /Ca^{2+} signalling pathway. Wnt ligands form a ternary complex with Fzd receptor and Ror1/2 co-receptor, that triggers a cascade of events converging on intracellular Calcium levels increase and regulating many Calcium-dependent proteins.

CHAPTER 2 – The canonical Wnt pathway

2.1 ß-catenin structure and functions

ß-catenin (Armadillo in drosophila) is a dual function protein, involved in both cell-cell adhesion and transcriptional regulation of target genes. In adherens junctions, ß-catenin plays an important role binding to the intracellular domain of E-cadherin trans-membrane protein and to α-catenin, which in turn connect the adherens junctions to the actin cytoskeleton (Brembeck et al. 2006).

In vertebrates, two Armadillo homologs have been found: ß-catenin and γ-catenin (plakoglobin), both of them being able to bind cadherins and to establish cell adhesion. It has been demonstrated that, although with a weaker transcriptional activity, γ-catenin can partially compensate for ß-catenin loss in malignant cell lines (Maeda et al. 2004). Deregulation of ß-catenin activity is associated with cancer and constitutive activation of ß-catenin transcriptional activity has been found in 80% of colon cancer (Bienz et al. 2000).

ß-catenin is a 781 amino-acids protein containing 12 armadillo domain repeats (Huber et al. 1997) and it has been found to interact with more than 20 protein partners mostly related to cell-adhesion or Wnt signalling (Xing et al. 2008). Crystal structure showed that ß-catenin possesses a positively charged groove that spans the super-helical armadillo repeats region, with a C-terminal helix capping the last armadillo repeat and a N-terminal helix (Xing et al. 2008) (Figure 6).

The armadillo repeats mediate many ß-catenin interactions with other proteins such as E-cadherin, Axin, APC and TCF/LEFs whose importance will be discussed later in this chapter.

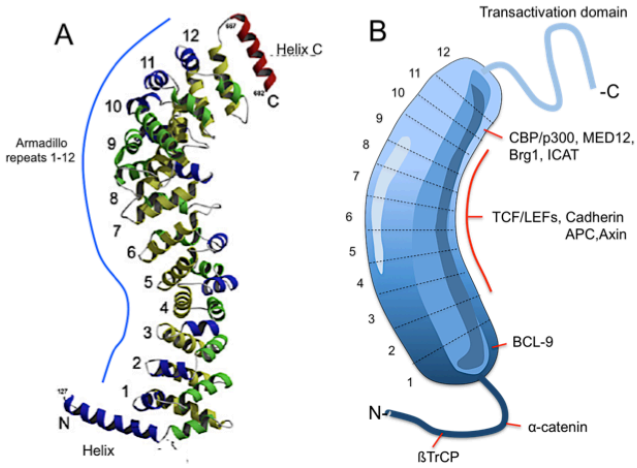

Figure 6 A) Crystal structure of full-length zebrafish ß-catenin showing armadillo repeats 1-12 and N and C terminal structures B) A schematic representation of ß-catenin main structural motifs with a subset of its respective interacting partners. Adapted from Xing et al. 2008.

N-terminal ß-catenin domain mediates protein-protein interactions that, together with the armadillo repeats, enables ß-catenin to work as a scaffolding protein for multi-protein complexes assembling; also, it is essential for interactions with α-catenin (Yamada et al. 2005). N-terminus is also involved in ß-catenin post-translational modification, harbouring four phosphorylation sites keys for proteasome-mediated degradation (Wu et al. 2003).

Regarding ß-catenin transcriptional activity, the armadillo repeats 3-10 is necessary for interaction whit TCF/LEFs DNA binding protein, a class of downstream Wnt nuclear effectors which recruit ß-catenin on specific gene promoters (Willert et al. 2006). In addition, armadillo repeats 1 (R1) and 11 (R11) are essential for the transactivation of Wnt target genes (Stadeli et al. 2006, Willert et al. 2006).

R1 armadillo repeat interacts with BCL-9, which in turn recruits Pygopus, a transcriptional co-activator of Wnt target genes (Kramps et al. 2002). On the other hand, armadillo repeat R11 is able to interact with many

transcriptional co-activators such as CBP/p300, MED12, Brg1 or inhibitors such as ICAT (Barker et al. 2001).

2.2 ß-catenin post-translational modifications

ß-catenin molecular functions, protein degradation, interactions and sub-cellular localization are finely controlled through different post-translational modifications orchestrated by several enzymes (Gao et al. 2014) (Table 3).

CK1, Gsk3ß and ß-TrCP act in a cascade of events to achieve ß-catenin proteasome-mediated degradation. In particular, CK1 phosphorylates S45, a priming phosphorylation for the subsequent Gsk3ß phosphorylation on the S33/S37/T41 residues. Importantly, the phosphorylation on S33/S37/T41 enables the binding of ß-catenin with ß-TrCP, which in turn ubiquitinates K19/K49 residues, targeting ß-catenin for proteasome mediated degradation (Willert et al. 2006, Gao et al. 2014).

ß-catenin stability is also positively controlled by PKA phosphorylation on S675, EDD ubiquitination on K11/K29 and Rad6B ubiquitination on K394 (Gao et al. 2014).

Phosphorylation on S552 by AKT promotes ß-catenin dissociation from adherens junctions, loosening the interaction with E-cadherin, while S191 and S605 phosphorylation by JNK2 are critical for ß-catenin nuclear localization (Gao et al. 2014).

Also ß-catenin transcriptional activity is tightly controlled through post-translational modifications which enhance or inhibit ß-catenin binding with its nuclear interactors.

Phosphorylation on T120 by PKD1 may suppress ß-catenin expression and activity, while ubiquitination on K11/K63 by FANCL is correlated with an increase in transcriptional activity. In addition, acetylation on K345 by P300 (a nuclear ß-catenin interactor) enhances ß-catenin interaction with TCF4, while acetylation on K49 by CBP inhibits ß-

catenin ability to activate c-myc gene (one of its downstream transcriptional targets) (Gao et al. 2014).

Residue and type of modification	Domain	Enzyme	Function
Phosphorylation			
S45	-	CK1	Primes phosphorylation by GSK3
S33/S37/T41	-	GSK3	Required for β-TrCP recognition
S675	-	PKA	Increases stability
S552	ARM	AKT	Promotes β-catenin disassociation from cell-cell contact and accumulation in both the cytosol and nucleus
S191/S605	ARM	JNK2	Critical for β-catenin nuclear localization
T120	-	PKD1	May suppress β-catenin transcription activity
Ubiquitination			
K19/K49 (K48-linked chain)	-	β-TrCP	Targets for degradation
- (K11/K29-linked chain)	-	EDD	Increases stability
K394 (K63-linked chain)	-	Rad6B	Increases stability
- (K11/K63-linked chain)	-	FANCL	May increase β-catenin expression and activity
-	-	Jade-1	Targets for degradation
Acetylation			
K49	-	CBP	Inhibits β-catenin ability to activate c-myc gene
K345	ARM	P300	Enhances β-catenin interaction with TCF-4
K19/K49	-	PCAF	Increases stability

Table 3 Summary of ß-catenin post-translational modifications. Adapted from Gao et al. 2014.

2.3 Wnt-dependent ß-catenin stabilization

The canonical Wnt signalling tightly regulates the stability of ß-catenin and its nuclear translocation, necessary for its transcriptional activity. Of note, ß-catenin does not have a DNA binding motif itself and relies, for activating target genes, on association with transcriptional co-factors.

In absence of Wnt ligands, most of the ß-catenin is found at adherens junctions, interacting with E-cadherin and α-catenin to regulate cell adhesion. A multiprotein complex, named ß-catenin destruction complex, tightly controls ß-catenin cytoplasmic levels. Members of this complex are Axin, Adenomatous polyposis coli (APC), protein phosphatase 2A

(PP2A) and two protein kinases, the glycogen synthase kinase 3 ß (Gsk3ß) and the casein kinase 1 α (CK1α) (Willert et al. 2006).

Within the destruction complex, ß-catenin is phosphorylated at Ser-45 by CK1α (priming phosphorylation) and subsequently at Ser-33, Ser-37 and Thr-41 by Gsk3ß. Once phosphorylated, ß-catenin is recognized and ubiquitinated by the ß-transducing repeat-containing protein (ß-TrCP) E3 ubiquitin ligase and, finally, targeted for proteasome mediated degradation (Price 2006).

In presence of Wnt ligands, a ternary complex between Wnt, Frizzled and LRP5/6 triggers a series of events that converge on the inactivation of ß-catenin destruction complex. Activation of Frizzled receptors by Wnt ligands rapidly recruits Dishevelled (Dsh) at the receptor level. Activated Dsh binds to Axin, CK1, Par-1 and Ck2 and may help sequestering these proteins from the destruction complex (Cadigan 2002). The mechanism through which the Wnt signal is transduced from the receptor to Dsh is not fully understood; given the coupling between G-protein and Frizzled, G-protein signalling might be involved in such process (Ahumada et al. 2002, Jernigan et al. 2010). In addition, Dsh mediates clustering of Fz/LRP5/6 receptors to form signalosomes at the plasma membrane and transmitting input signals received from the Wnt receptor (Kishida et al. 1999).

Axin is stabilized by Gsk3ß dependent phosphorylation: upon Wnt signalling stimulation, activated Dsh inhibits Gsk3ß, increasing Axin degradation and ß-catenin stabilization. Anyway, physiological ß-catenin stabilization seems to be accomplished efficiently through sequestration of scaffolding complexes rather than by direct inhibition of Gsk3ß activity (Willert et al. 2006). In particular, binding of Wnt ligands to LRP/6 induces phosphorylation of the LRP5/6 intracellular domain by the combined action of CK1γ (a membrane associated kinase) and Gsk3ß (Davidson et al. 2005, Zeng et al. 2005). Once activated, LRP5/6 can bind

Axin, sequestering it away from the destruction complex (Lee et al. 2003) and stopping ß-catenin degradation (Figure 7).

Furthermore it has recently been observed that LRP6 polymerization at the cell membrane is necessary and sufficient for activation of Wnt signalling at high levels, even in absence of external Wnt stimuli (Metcalfe et al. 2010). DIX domain dependent LRP6 clustering, in absence of Wnt ligands, increases Gsk3ß-dependent LRP6 phosphorylation, triggering Axin relocalization at the cell membrane and subsequent ß-catenin stabilization and nuclear translocation.

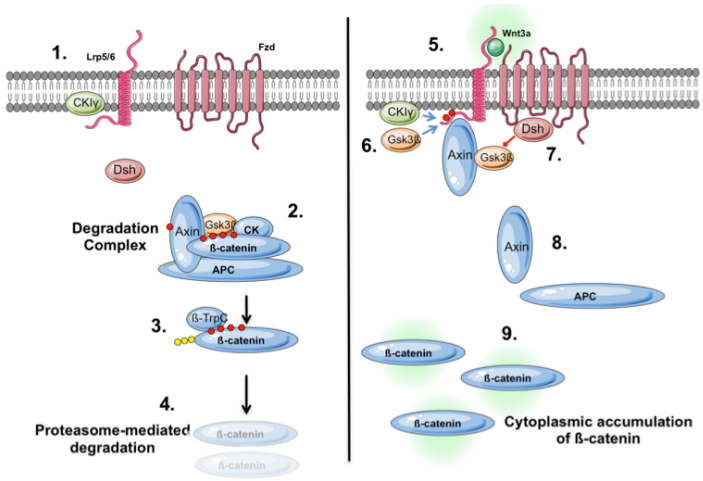

Figure 7 - Canonical Wnt-signalling regulates the degradation rate of ß-catenin. In absence of Wnt ligands (1.) ß-catenin is constantly phosphorylated by CKI and Gsk3ß (2.). Red dots indicate phosphorylation on Serine or Threonine residues. Once phosphorylated, ß-catenin is ubiquitinated (yellow dots) (3.) and targeted for proteasome-mediated degradation (4.). In presence of Wnt ligands (5.) a ternary complex between LRP5/6 and Fzd is formed, LRP5/6 is phosphorylated (6.) and subtracts Axin from the destruction complex, while Dsh (7.) inhibits Gsk3 and reduces both Axin stability and ß-catenin phosphorylation leading to the disassembling of the destruction complex (8.) and ß-catenin accumulation into the cytoplasm (9.)

2.4 ß-catenin nuclear translocation

Upon Wnt signalling stimulation, stabilized and hypophosphorylated ß-catenin accumulates into the cytoplasm and translocates into the nucleus, where it exerts a transcriptional activity on target genes. The molecular mechanisms by which ß-catenin is shuttled between cytoplasmic and nuclear compartment are not completely understood.

ß-catenin itself lacks a nuclear localization signal; however, many molecular components of the Wnt pathway can be found in both compartments, suggesting a possible role in mediating ß-catenin translocation.

For instance, Axin and APC contain nuclear import and export sequences that allow them to shuttle in and out the nucleus. Nuclear APC directly counteracts ß-catenin dependent activation of target genes, by accelerating the rate of ß-catenin export from the nucleus (Sierra et al. 2006), and is necessary for the periodic activation of target genes Also Axin has been detected in the nucleus and promotes the accumulation of cytoplasmic ß-catenin, thus providing a negative feedback on Wnt activation enhancing ß-catenin cytoplasmic retention (Cong et al. 2004).

It is therefore possible that Axin and APC shuttle as part of a complex that controls ß-catenin nuclear translocation. The existence of such a complex, however, has not been proved yet, but it could possibly include also the Bcl-9 adaptor protein, which can mediate nuclear import of ß-catenin by targeting it to the nuclear Pygopus protein (Townsley et al. 2004).

Additional ß-catenin partners and regulators, such as Dsh, α-catenin, ICAT, CK1, CK2 and Gsk3ß, can shuttle in and out the nucleus (Willert et al. 2006). Is therefore important to which these proteins might control ß-catenin nuclear translocation dynamics; the challenge is decoupling the effect that each protein has on ß-catenin cytoplasmic stabilization from the nuclear translocation mechanism.

While the existence of a ß-catenin nuclear translocation complex has not been proven, experimental evidences suggest a possible alternative landscape for nuclear ß-catenin accumulation upon Wnt signalling, where the balance between nuclear, cytoplasm and membrane ß-catenin interactors influence the nuclear to cytoplasmic ß-catenin ratio.

Photobleaching experiments on fluorescence-tagged ß-catenin in NHI3T3 cells demonstrated that Wnt activation (through Wnt ligands or Gsk3ß chemical inhibitors) does not affect ß-catenin nuclear import, but enhances its nuclear retention instead by reducing the normal ß-catenin export rate (Jamieson et al. 2011). However, this effect is not direct, since a mutant ß-catenin insensitive to Gsk3ß inhibition does not show an increased nuclear retention, but is mediated by the presence of nuclear ß-catenin partners that increase upon Wnt stimulation. In particular, Jamieson and colleagues (Jamieson et al. 2011) showed that Lef1, a member of the TCF/LEFs transcription factors, increases its expression upon Wnt stimulation and retains ß-catenin in the nucleus, triggering a positive feedback loop.

Whether the Lef1/ß-catenin complex assembles in the nucleus or not is still debated. However, the positive feedback of Lef1 on ß-catenin nuclear localization has been observed also in 2-cells mouse embryo (Huber et al. 1996), in which ectopic ß-catenin clearly localizes in the nucleus only in presence of ectopic Lef1 expression.

On the other hand, genetic ablation of E-cadherin, the major membrane ß-catenin interactor, triggers aberrant ß-catenin nuclear localization (Orsulic et al. 1999), suggesting once again that ß-catenin relocation is dependent on its protein interactors at various cell-compartments levels.

The experimental evidence that ß-catenin can freely shuttle between nucleus and cytoplasmic compartments is furthermore confirmed by the finding that, even in absence of a nuclear localization signals, it is able to interact with the nuclear pore complex in a NLS and

importing/karyopherin independent way (Fagotto et al. 1998). Possibly, all the above mentioned molecular mechanisms concur to finely tune ß-catenin nuclear translocation, and apparent contradictory results could be explained by the different cellular models used. It is very plausible that, as for the outcome of the Wnt signalling activity in different cell lines, also ß-catenin nuclear translocation can be regulated differently depending on the Wnt downstream components availability, thus achieving efficient nuclear translocation by different means depending on the intracellular context.

2.5 Transactivation of Wnt-target genes

Inside the nucleus, ß-catenin cannot bind directly to DNA, but substantially works as a scaffolding protein, linking members of the TCF/LEFs familiy to specific chromatin remodelling complexes and to Wnt co-activators such as Bcl-9 and Pygopus.

ß-catenin structure can be discretised in three different regions with three distinct tasks, which work together in connecting multiple proteins and assembling nuclear complexes: i) the N-terminal region, able to bind Bcl-9; ii) the ARM repeats, which bind TCF/LEFs factors; iii) the C-terminal region, that interacts with chromatin remodelling complexes and enables genes transactivation.

In detail, ß-catenin N-terminal region binds Bcl-9 and creates a chain of adaptors that connect Lef1 to Pygopus PHD finger protein (Stadeli et al. 2005), while TCF/LEFs bind to the ß-catenin ARM repeats (in a region that spans the binding of APC and E-cadherin) (Willert et al. 2006).

APC, which can be also found in the nucleus, by virtue of competing with TCF/LEFs for the same binding region, can influence ß-catenin transcriptional activity by inhibiting the formation of active transcriptional complexes between TCF/LEFs and ß-catenin. Confirming this hypothesis, CK1 phosphorylation on APC increases its affinity for ß-catenin (Ha et al.

2004), consequently inhibiting its transcriptional activity (Willert et al. 2006).

In addition to TCF/LEFs and Bcl-9, ß-catenin has been also demonstrated to bind other nuclear partners such as the DNA ATPase/helicase TIP49a/Pontin52 (Bauer et al. 2000), Brg-1 and CBP/p300 (Bienz et al. 2003).

On the other hand, ß-catenin C-terminal region contains a very strong transactivation domain, able to bind to multiple chromatin remodeling subunits. MALDI-TOF mass spectrometry identified members of the ISWI remodelling complex and the MLL1/2 hystone methyltransferase complexes (HMT) containing the SET1-type proteins (Sierra et al. 2006). SET1 proteins mediate hystone 3 lysine 4 trimethylation (H3K4Me3) which is a chromatin modification found in highly active genes and associated with open chromatin structure in vitro (Sims et al. 2004). ß-catenin has been found to recruit MLL1/2 complexes on target genes, by strongly inducing H3K4me3 (Sierra et al. 2006).

On the other hand, transcriptional corepressors for Wnt dependent transactivation include the C-terminal binding protein (CtBP) co-repressor (which recruits Polycomb co-repressors (Chinnadurai 2002)) and Groucho/TLE1 (which directly interacts with TCF/LEFs).

2.6 Wnt/ß-catenin target genes

ß-catenin signalling can trigger different cellular responses depending on the intracellular context. Therefore, ß-catenin nuclear translocation and activation of target genes can result in very different outcomes depending on the cell-type. This makes very difficult to define a universal set of canonical Wnt “target genes” indicating that is the cell, rather than the signal, that determines the nature of the response (Logan et al. 2004).

Nevertheless, some genes robustly respond to Wnt/ß-catenin signalling in almost all the cell types studied so far.

Among them cell-cycle regulators cMyc and CyclinD1 are up-regulated upon canonical Wnt activation in colon cancer cells, providing a mechanism by which ß-catenin activity promotes cell-proliferation and cancer progression (He et al. 1998)

Furthermore canonical Wnt targets include Wnt pathway components, providing extensive feedback control of the Wnt pathways, although regulation of these genes is cell-type dependent.

Among them Frizzled, Dkk and TCF/LEF genes can be regulated by Wnt signalling (Logan et al. 2004). In particular LEF1, up-regulated upon Wnt signalling in colorectal cancer cells or immortalized mouse fibroblasts, provides a positive feedback loop strengthening both ß-catenin nuclear translocation and activity (Hovanes et al. 2001, Jamieson et al. 2011).

On the other hand, Axin2 activation in response to ß-catenin nuclear activity provides a negative feedback loop that limits excessive transcriptional response (Jho et al. 2002, Aulehla et al. 2003). To date, Axin2 is the only ß-catenin target gene whose expression is robustly up-regulated in all the cell-types upon Wnt signalling and Axin2 promoter has been successfully used to dive lacZ or GFP expression to report Wnt pathway activity *in vitro* and *in vivo* (Jho et al. 2002).

Reliable ß-catenin cell-type specific target identification requires a multistep approach that considers ß-catenin and TCF/LEFs (and other nuclear ß-catenin partners) genomic binding sites in both presence and absence of Wnt ligands and gene expression data for the same experimental conditions. This approach reliably identifies ß-catenin transcriptional targets within the context of a specific cell type, and has been successfully applied in mouse embryonic stem cells (Wu et al. 2013) for the identification of ß-catenin TCF dependent and independent targets.

Although highly informative, this approach is nevertheless expensive and time consuming for cell-types in which all these information are not available and have to be generated *de novo*.

Another approach for the identification of Wnt activity relies on the usage of reporter genes under the control of a multimerized TCF/LEFs DNA binding motif (called TOP) (Staal et al. 1999). The expression of a downstream gene (usually LacZ or GFP) efficiently reports Wnt activity and correlates with the levels of nuclear ß-catenin, providing an indirect mean to follow Wnt signal without any previous knowledge of its cell-type specific transcriptional targets.

2.7 Wnt/ß-catenin signalling in cancer

Wnt signalling pathway has been linked to various human cancers, including colon cancer, hepatocellular carcinomas, leukemia and melanoma (Moon et al. 2004). Over 90% of colon cancers contains mutations in one or multiple Wnt pathway components (Klaus et al. 2008).

Mutation in adenomatous polyposis coli (APC), a component of the ß-catenin destruction complex, were discovered and linked to colon cancer back in 1987-1989, but the link connecting APC and ß-catenin was not discovered until 1993, providing the foundation for the mechanistic insight for APC mutation (Klaus et al. 2008). Inherited or sporadic mutations in APC have been found in most colorectal cancer. Mutations in the APC Axin binding domain, render APC unable to correctly assemble in the ß-catenin destruction complex, triggering ß-catenin accumulation and continuous expression of the c-Myc oncogene and CyclinD1, inducing aberrant proliferation rate increase and tumour growth.

Also in absence of APC mutations, a fraction of colorectal cancer (about 1%) (Klaus et al. 2008) is characterized by mutations in the ß-catenin

phosphorylation sites responsible for its degradation, which cause bypassing of the wild-type APC tumour-suppression role, ß-catenin accumulation and nuclear translocation (Willert et al. 2006).

Mutations in ß-catenin (predominantly in the N-terminal region) have been found also in 700 out of 3500 different human cancers including colon cancer, melanoma, pilomatrixoma (hair tumours), hepatocellular carcinoma, medulloblastoma, hepatoblastoma and gastrointestinal tumours (Klaus et al. 2008).

However, the axiom "more Wnt activity means increased tumorigenicity" is not universal. As mentioned above, Wnt activity may have different outcomes depending on the cell type. Cancer initiation does not make an exception. While a higher Wnt activity is found in colorectal cancers and many other types of tumours, a suppressed Wnt activity may be responsible for the same outcome in different cell type. For instance, one third of human sebaceous gland tumours contain a dual-site mutation on LEF1 that impairs its interaction with ß-catenin, rendering it a dominant negative Wnt inhibitor (Takeda et al. 2006).

2.8 Wnt pathway modulation: ligands and small molecules

Given the variety and importance of processes in which canonical Wnt signalling is involved, an extensive research has been devoted to identify molecules that regulate Wnt activity, with implication for their therapeutic applications. As previously discussed, canonical Wnt pathway requires a multistep cascade of events from the cell membrane to the nucleus; several of these steps can be selectively modulated by both physiological ligands or small molecule inhibitors of various Wnt pathway components, providing invaluable tools to dissect canonical Wnt signalling at different signal transduction steps.

2.8.1 Activators

In cell culture, physiological activation of the canonical pathway can be achieved by the addition of purified recombinant Wnt ligands, such as Wnt3a. A multitude of small chemical inhibitors has furthermore been developed to target specific Wnt pathway components. Activation of the Wnt pathway can be promoted by selective inhibition of Gsk3, thus inhibiting Gsk3-dependent ß-catenin phosphorylation and promoting cytoplasmic ß-catenin accumulation and nuclear translocation. Lithium Chloride (LiCl) is the first Gsk3ß inhibitor discovered and it has extensively been used to activate Wnt pathway (Klein et al. 1996).

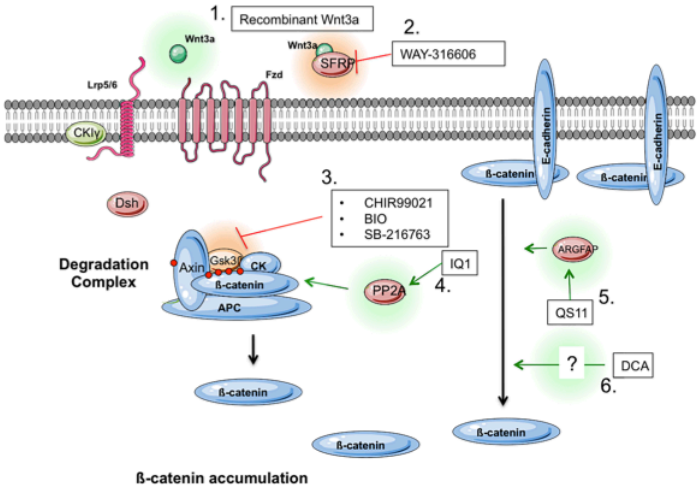

Figure 8 - Activation of the canonical Wnt pathway can be achieved by recombinant Wnt ligands (1.) or small molecule inhibitors. Inhibition of Wnt antagonist SFRP (2.) or Gsk3 inhibitors (3.) can be used to increase ß-catenin accumulation and subsequent nuclear translocation. Wnt3a synergistic molecules such as IQ1 and QS11 (4. and 5.) can improve ß-catenin transcriptional activity and subcellular localization in presence of Wnt. Deoxycholic acid regulates ß-catenin subcellular localization through a yet not fully characterized mechanism (6.). Adapted from the Wnt homepage (http://web.stanford.edu/group/nusselab/cgi-bin/wnt/).

Other metal ions, such as Zinc, can inhibit Gsk3 even more efficiently than Lithium. However, both Lithium and Zinc lack of specificity and they trigger many unspecific, Gsk3 independent cellular responses (Eldar-Finkelman et al. 2011).

The need for more selective Gsk3 inhibitors led to the development of small molecules inhibitors (see Figure 8 for a summary). ATP-competitive inhibitors of Gsk3 were identified mainly in the screening when searching for inhibitors for cyclin-dependent protein kinases (CDKs) with anti-tumour activity. The dual activity of inhibitors targeting Gsk3 and CDKs is a direct result of their structural similarity, within the ATP-binding sites of both kinases (about 86% similarity). (Eldar-Finkelman et al. 2011) Components of the indirubins family have been synthetized to increase their selectivity toward the Gsk3. The indirubin analogue 6-bromoindirubin-3'-oxime (BIO) is 16-fold more selective for Gsk3 with respect to CDKs. On the other hand, aminopyrimidines, such as CHIR99021 (Chiron), are even more selective toward Gsk3, making it to date the state of the art molecule to achieve Wnt pathway activation *in vitro*. Wnt pathway activation can be triggered also using small molecules inhibitors of secreted Frizzled-related proteins (sFRPs). The function of sFRP is to act as a secreted receptor, sequestering extracellular Wnts and preventing their binding to target cells. Inhibitors of sFRP, such as WAY-316606, have been successfully used to activate Wnt pathway *in vivo* (Bodine et al. 2009).

Many other molecules can activate canonical Wnt signalling at various levels. IQ1 is a small molecule, which activates PP2A; the latter can synergize with Wnt3a to enhance ß-catenin nuclear response through association with CBP. The alternative QS11 small molecule activates the GTPase activating protein ADP-ribosylation factor 1 (ARGFAP), resulting in an increased ß-catenin mobilization from the membrane to the nucleus in a Wnt3a-dependent fashion (Zhang et al. 2007).

Similarly, deoxycholic acid (DCA) stimulates Wnt signalling by regulating ß-catenin C-terminal phosphorylation and lowering its affinity for E-cadherin, resulting in increased nuclear translocation through a yet poorly characterized mechanism, which possibly depends on other signalling pathways involving the EGF receptor (Pai et al. 2004).

2.8.2 Inhibitors

As previously discussed, aberrant canonical Wnt pathway activation has been extensively linked to cancer initiation and progress. Therefore, the identification of small molecules capable of inhibiting Wnt activity *in vitro* and *in vivo* represents a crucial point for the development of new pharmaceutical approaches for cancer treatment.

Recombinant Dkk1 protein is able to bind Lrp6 (Figure 9), preventing Wnt binding to its receptor, and therefore upstream inhibiting Wnt signalling (i.e.at the receptor level). Several alternative strategies enable Wnt pathway inhibition. Tankyrase inhibitors, such as XAV, IWR or GOO7-LK, stabilise Axin, reinforcing the ß-catenin destruction complex (Madan et al. 2015) (Figure 9). Of note, long term Tankyrase inhibition in cultured cells increases DNA damage and telomeres shortening, discouraging potential therapeutic application (Kulak et al. 2015).

Selective inhibitors for ß-catenin binding to its transcriptional co-activators, such as CREBP/CBP, include PRI-724 (Figure 9), a molecule that is currently in phase I trial for acute myeloid leukemia and advanced solid tumors treatment (Chan et al. 2015). ß-catenin transcriptional activity can also be inhibited by iCRT, disrupting the ß-catenin binding with TCF/LEFs (Madan et al. 2015). Pyridinium selectively binds to all Casein Kinase (CK) and potentiates the action of CK1a, simultaneously increasing ß-catenin degradation rate, increasing Axin stability and decreasing Pygopus abundance (Figure 9) (Thorne et al. 2010). Wnt signalling can also be blocked at the source by targeting Porcupine; the

latter can be efficiently inhibited by several small-molecules including IWP, LGK974 and C59. Notably, this inhibition is highly specific since Porcupine function is entirely dedicated to Wnt functions, excluding potential off-targets. Porcupine inhibition leads to the abrogation of all Wnts exports, simultaneously inhibiting autocrine and paracrine Wnt functions (Kulak et al. 2015). On the other hand, Porcupine inhibition might not be sufficient to rescue aberrant Wnt-independent ß-catenin signalling (for instance, in cancers displaying APC and/or ß-catenin mutations) (Madan et al. 2015).

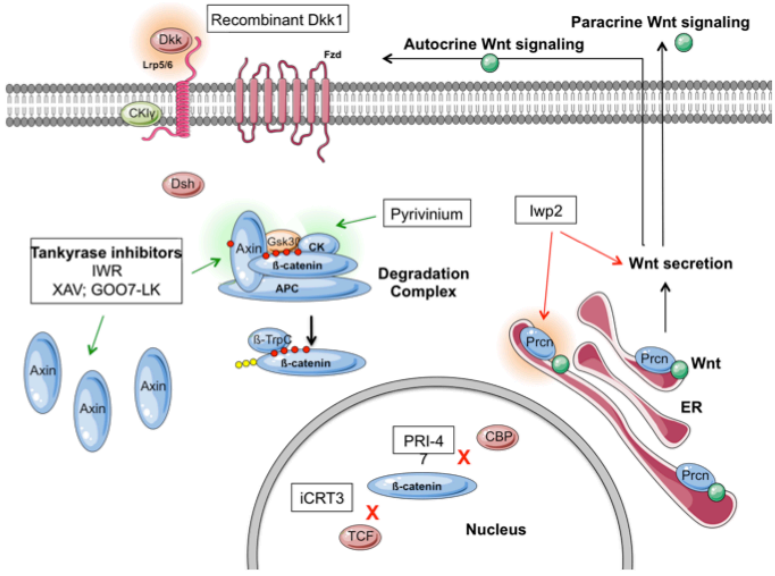

Figure 9 – Principal Wnt ß-catenin pathway inhibitors and their molecular targets. Adapted from Madan et al. 2015

CHAPTER 3 – TCF/LEFs family members

3.1 TCF/LEFs structural diversification

TCF/LEFs form a subfamily of the high-mobility group (HMG) box containing superfamily of transcription factors. They were first identified in the mammalian immune system (van de Wetering et al. 1991) and linked to ß-catenin only in 1996 (Behrens et al. 1996). TCF/LEFs factors bind a conserved DNA sequence called Wnt response element (WRE: C/T-C-T-T-T-G-A/T-A/T) through their HMG domain (van Beest et al. 2000).

In addition to DNA sequence specificity, the HMG box has a DNA bending function. It recognizes its specific nucleotide sequence in the minor groove of the DNA and enforces a bend in the helix between 90° and 120° (Giese et al. 1991).

Although TCF/LEFs have a well-conserved DNA binding motif, they are not transcription factors by themselves, since they can exert their transcriptional activity only by association with other transcriptional co-activators or co-repressors. In particular, they anchor ß-catenin to WRE containing region (Hoppler et al. 2007). In this context, ß-catenin itself serves as a scaffolding protein (anchored via TCF/LEFs to a precise locus) to recruit CBP/p300 and Bcl-9/Pygopus, remodelling the chromatin and activating transcription of target genes.

An interesting point of TCF/LEFs biology is that, as a general rule, they act as transcriptional repressors in absence of nuclear ß-catenin, assembling different multiprotein complexes, such has CtBP or groucho/TLE factors, with repressive functions (Brannon et al. 1999).

Of note, TCF/LEFs have additional transcriptional functions independent of ß-catenin, and ß-catenin itself has nuclear functions independent of

TCF/LEFs (Carlsson et al. 1993, Zorn et al. 1999). In vertebrates, four different TCF/LEFs can be found: Tcf1, Lef1, Tcf3 and Tcf4; however, the extensive isoform regulation gives rise to an astonishing diversity of functions despite shared DNA binding domain. The general structure of any TCF can be divided into an N-terminal ß-catenin binding domain, a central domain containing the HMG box and the nuclear localization signal (NLS), and a long C-terminal tail (Figure 10).

Dual promoter usage is also observed in Tcf1 and Lef1 genes, in which transcription can be selectively started from a downstream promoter, producing shorter, N-terminal truncated isoforms, missing the ß-catenin binding domain and behaving as constitutive transcriptional repressors (Van de Wetering et al. 1996). Alternative splicing of a central exon increases the complexity of Tcf1, Lef1 and Tcf4 genes, while Tcf3 shows no alternative splicing in this region. In addition, the central exon can be alternatively spliced in Tcf4 genes, differentiating between isoforms containing two additional conserved domains (LVPQ and SxxSS) that are instead constitutive in Tcf3 and absent in vertebrate Tcf1 and Lef1. Importantly, for Tcf4 only, the isoforms containing LVPQ and SxxSS are able to repress Wnt target genes (Hoppler et al. 2007).

Alternative splicing furthermore can be found at the C-terminal of Tcf1 and Tcf4, giving rise to a variety of C-terminal tails with or without the CRARF motif, the RKKKCIRY motif and a proposed binding site for the CtBP cofactor (Van de Wetering et al. 1996). Alternative C-tails have been named E, C and B; E-tails contain CRARF and RKKKCIRY, C only CRARF motif and B none of them. In addition, Tcf4-E isoforms differ for the presence of the CtBP motif in the latter which is not present in Tcf1-E isoforms (Hoppler et al. 2007).

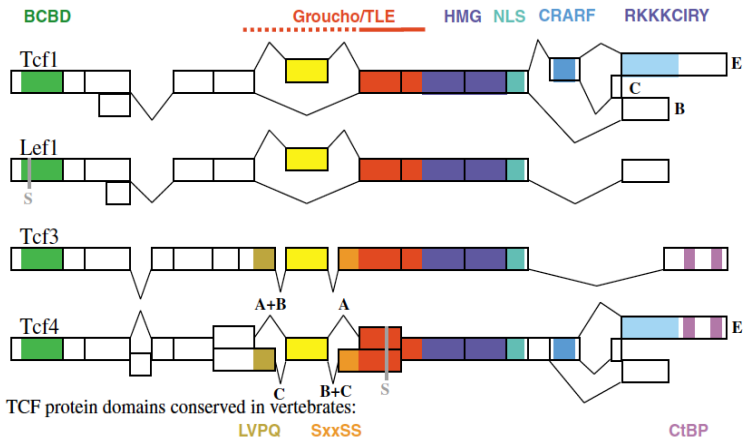

Figure 10 – Variety of vertebrates TCF splicing isoforms with major domains and motifs highlighted. Green: ß-catenin binding domain (BCBD); Yellow: central alternative exon with repressive function; Gold and Ordange: LVPQ and SxxSS repressive motifs respectively. Red: Groucho/TLE binding region; Purple: HMG DNA binding domain; Turquoise: nuclear localization signal (NLS); Dark blue: CRARF motif, Light blue: RKKKCIRY motif; Violet: CtBP domain. Adapted Hoppler et al. 2007.

3.2 Functional redundancy and divergence of TCF/LEFs

Vertebrates TCF/LEFs evolved and diversified to accomplish different functions and finely regulate the output of Wnt/ß-catenin signalling.

The mentioned extent of their transcriptional regulation (dual promoter usage, extensive alternative splicing) suggests that, unlike their invertebrate counterpart, vertebrate TCF/LEFs have different functions despite their common DNA binding motif.

As discussed above, TCF/LEFs exhibit over 95% amino-acid conservation in the HMG domain and NLS. It is therefore not surprising that the consensus DNA binding sequence is nearly identical for Tcf1, Lef1, Tcf3 and Tcf4 (Van de Wetering et al. 1996, van Beest et al. 2000). The

functional diversification of TCF/LEFs in vertebrates is majorly accountable to the extensive variety of isoforms and different accessory domain displayed by each member of this family. The C-terminal E-tail, produced from by all TCFs except Lef1, encodes a non-sequence specific DNA-binding domain that, among other functions, strengthens the interaction with p300 and the multiprotein complex containing ß-catenin (Atcha et al. 2003).

Surprisingly, the presence of this tail confers to TCFs selectivity towards some target genes instead of others. On the other side, the functions of the C-terminal B tails, although expressed by all TCF/LEFs except Tcf3, remain to date elusive, majorly because the most common optimal multimerized WRE has been used to follow Wnt activation in synthetic reporter constructs whose activation is tail independent.

Genetic experiments in mice, Zebrafish and Xenopus showed that TCF/LEFs are expressed in overlapping patterns with distinct and separate functions. For instance, ventral overexpression of xLef1 can induce a secondary axis formation in Xenopus embryos, but overexpression of xTcf3 and xTcf4 fails to do so (Molenaar et al. 1998).

The functional difference resides on the presence of the alternative central exon, flanked by LVPQ and SxxSS motifs in xTcf3 and xTcf4, which confers to these proteins a repressive activity not present in Lef1 (Gradl et al. 2002). Having said that all TCF/LEFs have the potential to inhibit transcription in absence of ß-catenin, Lef1 has a Wnt-dependent activating role, Tcf1 and Tcf4 have dual activities while Tcf3 functions as a constitutive repressor (Arce et al. 2006). This summary only takes into accounts full-length proteins, but, excluding Tcf3, all TCF/LEFs display the potential to express N-terminally truncated proteins, unable to bind ß-catenin and generally acting as dominant negative transcriptional repressors.

While the other TCF/LEFs have the potential to be converted from repressors to activators in a Wnt-dependent fashion, Tcf3 repressor activity is instead inhibited by the Wnt pathway either by transcriptional down-regulation, post-translational modification or nuclear exclusion (Arce et al. 2006).

In mice, deletion of TCF/LEFs highlights similarities and divergences. For instance, both Lef1 and Tcf1 are expressed in developing mouse thymocytes. Tcf1 depletion induces defects in thymocytes development, while Lef1 continues to be expressed. Instead, thymocytes differentiation can be completely blocked if both Tcf1 and Lef1 are depleted (Okamura et al. 1998). Similarly, experiments in natural killer T cells showed that Tcf1 and Lef1 are partially redundant, with Tcf1 contributing more to NK development than Lef1 [ref]. A redundancy is also observed for Tcf1 and Lef1 in the early stages of development: only the double knock-out is able to mimic Wnt3a KO at E9.5, with defects in paraxial mesoderm formation, limb buds and multiple neural tubes. Tcf4 knock-out in the intestine abrogates stem cell compartment, while Tcf1 knock-out show late effects promoting adenomas formation. Tcf4 therefore promotes stem cell maintenance in the intestine, while Tcf1 plays an opposing role (Arce et al. 2006).

On the other side, Tcf3 exhibits non-redundant actions in early development. Tcf3 knock-out embryos show defects in antero-posterior axis formation (duplication of the primitive streak) around E7.5/8.5, while some structures phenocopies aberrant ectopic Wnt signalling. In addition, Tcf3 represses target genes that are activated not by Wnt signalling but by other mechanisms, pointing out that TCF/LEFs in general can act independently of ß-catenin (Merrill et al. 2004, Pereira et al. 2006)

These evidences suggest that Tcf3 is a dedicated repressor different from other TCF/LEFs, or that is an activator with non-redundant repressor

activities. The similarities between Tcf3 and Pop1 (the C.Elegans TCF/LEFs ortholog) (Arce et al. 2006) reinforce the latter hypothesis.

3.3 Post-translational control of TCF/LEFs proteins

As previously discussed, post-translational modification of Wnt/ß-catenin pathway components play key roles in signalling transduction. The emerging complexity of TCF/LEFs biology and their context dependent functions are largely explained by alternative isoforms with distinct transcriptional activaton/repressor capacity and target selectivity. Nevertheless, post-translational modifications of TCF/LEFs proteins add another level of complexity to this family of DNA binding proteins.

Phosphorylation

Phosphorylation by several protein kinases is known to alter TCF/LEFs protein properties, disrupting or enhancing specific protein-protein interactions. The Nemo-like kinase (Nlk) phosphorylates human Tcf4 on Thr178 and Thr189, and human Lef1 on Thr155 and Ser166, inhibiting their DNA binding ability. On the other hand, the Traf2 and Nck-interacting kinase (TNIK) interacts with both ß-catenin and Tcf4 and, by phosphorylating the latter, enhances the ß-catenin/Tcf4 complex transcriptional activity (Gao et al. 2014).

CK2 increases the affinity of Lef1 for ß-catenin by phosphorylating Ser42 and Ser62 of human Lef1. However, phosphorylation by CK1∂ on Ser40 of murine Lef1 has the opposite outcome, disrupting ß-catenin/Lef1 interaction. Furthermore, Gsk3 phosphorylates Tcf3 and inhibits its binding with ß-catenin, while CK1e enhances it (Gao et al. 2014).

A well-characterized mechanism regulates the phosphorylation of Xenopus Lef1, Tcf3 and Tcf4 by the homeodomain interacting protein kinase 2 (HIPK2), causing TCF/LEFs to dissociate from target promoters

containing WRE. Of note, Xenopus Tcf1 does not contain HIPK2 target sites and provides an elegant mechanisms for Wnt/ß-catenin to remove repressor transcriptional complexes and assemble Tcf1-containing transcriptional activator complexes (Gao et al. 2014).

SUMOylation and acetylation

TCF/LEFs can function differently also depending on their nuclear and sub-nuclear localization depending by SUMOylation. The small ubiquitin-related modifier (SUMO) modification resembles ubiquitin conjugation but uses a distinct enzymatic machinery. It has been demonstrated that SUMOylation of Lef1 and Tcf4 alter their subnuclear localization, forcing them into compartments called promyelocytic leukemia (PML) nuclear bodies.

SUMOylation of Lef1 targets its ß-catenin binding domain and inhibits its transcriptional activation function, while SUMOylated Tcf4, in its groucho/TLE binding domain, has increased transcriptional potential (Hoppler et al. 2007)

Acetylation of Drosophila TCF on lysine 25 by CREB-binding protein decreases its affinity for Armadillo (ß-catenin ortholog in Drosophila). In C. elegans, instead, acetylation of Pop1 (TCF/LEFs ortholog) by CBP/p300 is required for its nuclear localization and biological activity.

Furthermore, human Tcf4E2 is acetylated at lysine 150 by CBP relieving its transcriptional repressor, probably by altering the conformation of the Tcf4E2/DNA complex (Gao et al. 2014).

3.4 TCF/LEFs regulation of biological processes

The divergent roles of TCF/LEFs are starting to be elucidated in many biological processes in which a Wnt/ß-catenin role has been previously

recognized, from embryo development and cancer initiation, to adult stem cell maintenance and proliferation.

3.4.1 Embryo development

In Xenopus, Wnt signalling normally induces the dorsal side in the early embryo; this phenotype has been extensively used to study canonical Wnt pathway and its components. For instance, overexpression of Wnt ligands or ß-catenin on the opposite ventral side leads to the induction of ectopic dorsal development.

Tcf3 represses dorsal axis formation where Wnt is not activated (ventral side) but its ectopic expression leads to ventralization also on the dorsal side (Brannon et al. 1999). On the contrary, endogenous Tcf1 is required for normal dorsal axis development and shares an overlapping function with Lef1, whose ectopic overexpression induces, contrary to Tcf3, dorsalization also in the ventral side depending on the presence of the central alternative exon (Molenaar et al. 1998). These results suggest that TCF/LEFs are functionally different, with Tcf3 acting mainly as a repressor, and Tcf1/Lef1 acting as transcriptional activators of Wnt targets.

Furthermore, in *Xenopus* embryo both Tcf1 and Tcf3 regulate mesoderm induction but, while Tcf1 is strictly required, only partial defects are observed upon Tcf3 depletion. During fertilisation, maternal Tcf1 is mainly needed for the assembly of transcriptional activating complexes while Tcf3 represses target genes. Maternal Tcf4 at this stage has partially overlapping functions with Tcf1.. Tcf4 is also required for normal midbrain-hindbrain development; rescue experiments proved that different isoforms of Tcf4 (with or without LVPQ and SxxSS motifs) play different, crucial roles, in the process (Hoppler et al. 2007).

3.4.2 Intestinal stem cells and colorectal cancer

Wnt signalling plays a key role in maintaining stem cell homeostasis in intestinal crypts, a process that is often misregulated in colon cancers, mainly caused by Wnt pathway aberrant activity.

Tcf4 knock-out mice lack the intestinal proliferative compartment (Korinek et al. 1998, Hoppler et al. 2007); and Tcf4 is required to maintain proliferating cells in the crypt of healthy colon (Korinek et al. 1998) but it is also responsible for maintaining stemness in colorectal cancer cells. Tcf1 plays a tumour suppressor role in the intestine (Tcf1 knock-out induces intestinal neoplasms in colorectal cancer). In this context, the predominant isoform of Tcf1 is truncated (ΔN-Tcf1) lacking the ß-catenin binding domain and therefore acting as a dominant negative Wnt target transcriptional repressor. Thus, the tissue homeostasis results from a balance between Tcf4 (which activates Wnt target genes and promotes proliferation and stemness) and ΔN-Tcf1 (which represses target genes and inhibits proliferation, promoting terminal differentiation) (Figure 11).

Of note, Lef1 is absent from healthy colon but is selectively expressed in colon cancer cells.

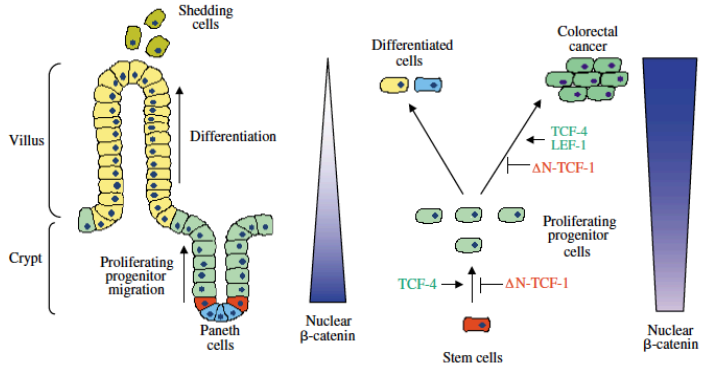

Figure 11 – Model of Tcf4 and ΔN-Tcf1 balance in healthy colon homeostasis and colon cancer cells. From Hoppler et al. 2007.

3.4.3 Skin and hair development

Multipotent adult stem cells are responsible for skin and hair grow, giving rise to epidermis, sebaceous glands, outer-root and inner-root sheath, and hair, while self-renewing to maintain stem cells in the niche.

Lef1 is expressed in the lineage that gives rise to the inner-root sheath and the hair, while Tcf3 is expressed in the stem cells and the lineage that produces the outer-root sheath.

Lef1 is essential for hair development and knock-out mice show reduced hair follicles, while the role of Tcf3 in skin development remains elusive, as Tcf3 knock-out mice die from axial and germ layer defects early in development (Merrill et al. 2004). Overexpression of Lef1 promotes hair follicle differentiation while overexpression of Tcf3 expands stem cell niche and interferes with differentiation. Once again, similarly to dorsal development in Xenopus, the functional differences between TCF/LEFs arise from LVPQ and SxxSS motifs (present in Tcf3 and absent in Lef1). Of note, overexpression of Tcf3 or ΔNTcf3 phenocopies each other. Overexpression of ΔNLef1, although being a repressive isoform, represses hair development but fails to repress epidermal differentiation, while promotes differentiation of sebaceous gland like-cells (Merrill et al. 2001), phenocopying the spontaneous mutations in Lef1 that, as previously discussed, promote sebaceous cell carcinoma (Takeda et al. 2006).

3.4.4 Immune system

TCF/LEFs were first identified and isolated from the immune system. T-cell factor 1 (Tcf1) isoforms are expressed at various stages during thymus development (Van de Wetering et al. 1996), and Lymphyoid enhancer factor 1 (Lef1) is expressed in developing T cells in the thymus and developing B cells in the bone marrow (Travis et al. 1991). The

function of Tcf1 and Lef1 is largely redundant in immune system development as double knockout mice have severe defects in T cell maturations. However, mutations in Tcf1 have more severe defects than the deletion of Lef1, suggesting that several Tcf1 isoforms possess functions that cannot be phenocopied by Lef1.

As discussed previously, both Tcf1 and Lef1 can encode for shorter ΔN isoforms lacking the ß-catenin binding domain. ΔN isoforms expression is carefully regulated and, as the T cells mature, there is a substantial increase of ΔN isoforms; upon T-cell stimulation, the expression of ΔN isoforms is again down-regulated (Hoppler et al. 2007).

The molecular mechanisms that allow the cells to selectively express full-length or ΔN isoforms remain elusive; surprisingly, both Lef1 and ΔN-Lef1 contain WRE in their proximal promoter but ΔN-Lef1 is selectively inhibited (Li et al. 2006), while only full-length isoforms of Tcf1 and Tcf4 containing the E-tails (with CRARF and WCXXCRRKKKCIRY motifs, together called C-clamp) are able to activate full-length Lef1 transcript (Atcha et al. 2003). Although there is not yet a nuclear magnetic resonance (NMR) or crystal structure of the C-clamp, experiments show that it has specific DNA-binding activities. The C-clamp carries specificity for a secondary, GC-rich sequence called a "Helper site" (Cadigan et al. 2012); as for intestine homeostasis, regulation of the balance between full-length and ΔN isoforms of TCF/LEFs is probably an important mechanism through which the balance between proliferation and apoptosis is maintained.

CHAPTER 4 – Embryonic stem cells and somatic cell reprogramming

4.1 The chase for pluripotency

Pluripotency is defined as the capacity of a cell to differentiate into all three germ layers and virtually into every cell type of the body. The chase for pluripotency, to understand its characteristics and properties, started with the study of naturally occurring, aggressive and "strange" tumors: teratocarcinomas.

Teratocarcinomas are tumours containing multiple tissue types, including fully differentiated structures such as teeth and hairs and their nature resumes an abnormal developmental process (Martello et al. 2014). In adult mice, testicular teratocarcinomas can sporadically form; cells from this tumours are able to be maintained continuously by serial transplantations, giving rise to other teratocarcinomas in recipient mice (Stevens et al. 1954).

In 1970, cells isolated from teratocarcinomas were named embryonic carcinoma (ECs) cells and were shown to be able to self-renew and propagate *in vitro*, while retaining the potential to differentiate into different cell types when injected *in vivo*. ECs were co-cultured with feeder layers of mitotically inactivated fibroblasts to improve their viability (Kahan et al. 1970) and, when allowed to form aggregates, formed structures termed embryoid bodies (Martin et al. 1975). Moreover, some clones from ECs cultured cell lines were able to produce mouse blastocyst chimeras. Despite their cancerous origin and their abnormal karyotypes, ECs helped scientist to shed light on the pluripotency concept but more had to come.

The major breakthrough came in 1981, when Evans and Kaufman were for the first time able to isolate embryonic stem cells (mESCs) from a developing mouse blastocyst (Evans et al. 1981). mESCs were similar to ECs but lacked genomic aberrations such as aneuploidy (often found in ECs), and mutations (generated in ECs through tumoriginenesis). Furthermore, ESCs were way more capable than ECs of generating chimeric mice with germline competence.

About ten years later, in 1992, it was shown that under appropriate culturing conditions, primordial germ cells (PGCs) from the mouse embryo could convert into proliferative stem cells (Matsui et al. 1992) with properties similar to mESCs (including pluripotency), thus closing the gap and suggesting that ECs from teratocarcinomas might originate from induced conversion of developing germ cells into PGCs *in vivo* (Leitch et al. 2013).

More recently epiblast stem cells (EpiSCs) were isolated from post-implantation mouse embryos (E5.5 – E.8). Although capable of multineage differentiation *in vitro*, EpiSCs do not contribute to chimera formation, thus represent a more developmentally advanced pluripotent state (Brons et al. 2007, Tesar et al. 2007); in culture, they require bFGF and Activin A signalling pathway to maintain self-renewal.

Of note, it has to be highlighted that pluripotent stem cells existence *in vivo* is limited to very specific stages, and progressively altered and then restricted during development (Figure 12).

All in all it appears that pluripotency, rather than being a specific property maintained by defined culture conditions or molecular signatures, can emerge from a broad spectrum of molecular states, which reflect the development *in vivo*.

Depending on the cell source, pluripotency can be "captured" in culture by providing (or neutralizing) environmental stimuli, which artificially

prolong, virtually indefinitely, both self-renewal and unrestricted differentiation potential.

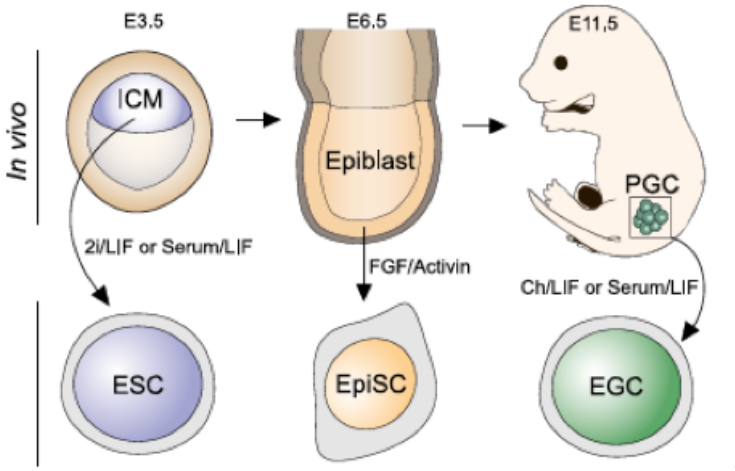

Figure 12 – Pluripotent stem cells can be isolated at different stages during mouse embryo development. Adpated from Hackett and Surani 2014.

4.2 Embryonic stem cells

During mouse embryogenesis (Figure 13), the zygote, a totipotent cell (capable of generating all germ layers and extra-embryonic tissues), divides to give rise to the morula (8-cells stage, mouse developmental stage E2.5).

Each one of the cells of the morula, called blastomeres, still retains totipotency as the original zygote. At E3.5 the blastomeres of the morula have further divided and specialized, and give rise to a structure called blastocyst, characterized by an inner cell mass (ICM) that retains pluripotency.

At E4.5, the ICM further specifies into Epiblast (which is still pluripotent) and Ipoblast (or primitive endoderm) which is committed to generate later on embryonic visceral endoderm (Davidson et al. 2015).

As previously discussed, mouse Embryonic Stem Cells (mESCs) were first isolated from a developing blastocyst in 1981 by Evans and Kaufman (Evans et al. 1981) and triggered the interest of the scientific community for their potential therapeutics application in regenerative medicine.

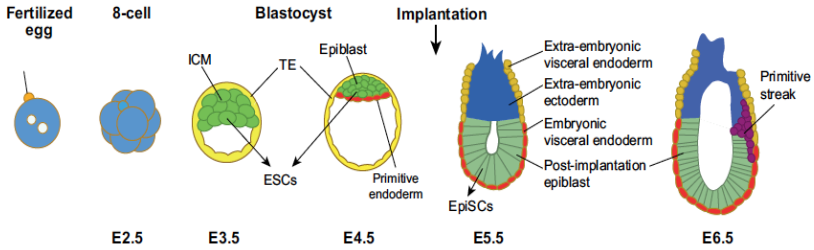

Figure 13 - Early events in mouse embryogenesis. Embryonic stem cells can be isolated from the inner cell mass of the pre-implantation blastocyst at E3.5-4.5. From Davidson et al. 2015.

mESCs can be expanded indefinitely *in vitro* under the appropriate culturing conditions conserving normal karyotypes (Evans et al. 1981). Standard culture conditions rely on foetal bovine serum (FBS) complemented media on feeder cells (usually irradiated mouse embryonic fibroblasts), or on gelatin-coated plates in medium containing FBS and leukaemia inhibitory factor (LIF) (Smith et al. 1988). mESCs show a remarkably fast (11-13 hours long) cell-cycle with little or undetectable G1 phase (White et al. 2005) and, similarly to cancerous cells, express telomerase which prevents telomeres shortening during cell division (Huang et al. 2014).

When allowed, mESCs undergoes differentiation and can *in vitro* recapitulate early phases of the developing embryo forming embryoid bodies. They can contribute to the formation of a chimeric mouse when injected into a developing blastocysts (blastocyst complementation and

chimera formation assay), which, depending on the pluripotency state of injected mESCs, can contribute to germline (Martello et al. 2014).
Remarkably, mESCs, when injected subcutaneously into immune deficient recipient mice, unleash their differentiation potential in a disordered way giving rise to teratomas containing structures from the three germ layers, similarly to ECs.

4.3 Naïve and primed pluripotency *in vitro*

Pluripotency and self-renewal of mESCs can be maintained *in vitro* indefinitely, by continuously providing extrinsic molecular inputs (Figure 14a).
One of these essential factors is leukemya inhibitory factor (LIF) which, acting through the gp130/LIF-R cell-surface receptor complex (Yoshida et al. 1994), activates the transcription factor STAT3. Consistently, mESCs can be cultured in absence of feeders in foetal bovine serum supplemented with LIF (Smith et al. 1988). STAT3 overexpression is able to support LIF-independent self-renewal while its depletion abolishes mESCs self-renewal even in presence of LIF (Niwa 2007).
The mechanism through which STAT3 acts principally relies on the regulation of several pluripotency promoting factors such as Klf4 and Gbx2 (Hall et al. 2009, Niwa et al. 2009, Tai et al. 2013), while its most likely important target is Tcfp2l1 which, as STAT3, is able to support LIF-independent self-renewal (Niwa et al. 2009).
Foetal bovine serum, in addition, sustains self-renewal principally by providing BMP4, which in turn activates the SMAD signalling pathway and Id (inhibitor of differentiation) genes. Accordingly, forced expression of Id genes or BMP4 treatment can substitute for serum requirements (Ying et al. 2003).

While pluripotency is certainly sustained in Serum/LIF conditions at cellular population levels, the activation of conflicting signalling pathways also promotes a significant degree of spontaneous differentiation, reflected by morphological, transcriptional and functional heterogeneity between cells. Hence, mESCs cultured in Serum/LIF exists in at least two different states: a "naive-state" population globally comparable to preimplantation epiblast, and a more developmentally advanced "primed" state characterized by a more marked expression of differentiation and lineage-associated genes (Hackett et al. 2014). In addition, further subpopulations might exist in Serum/LIF culture, such as trophoectoderm or primitive endoderm primed cells, contributing to transcriptional heterogeneity at population level. Interestingly, these two (or more) subpopulations can interchange their identity in culture (Abranches et al. 2013), suggesting a metastable equilibrium between the two states (Hackett et al. 2014).

Beside BMP4, which positively reinforce pluripotency through the activation of Id genes, foetal bovine serum also provides signals, with a batch-to-batch variability, that destabilize the pluripotency network, contributing to metastability and often challenging reproducibility of the experiments due to the unknown and variable composition of each lot.

To overcome this problem, FGF/ERK signalling, whose activity strongly influences exit from pluripotency, was explored as a mean to suppress mESCs spontaneous differentiation. Accordingly, Fgf4-/- or ERK2-/- mESCs are severely impaired in their differentiation potential toward both neural and meso-endodermal lineages (Kunath et al. 2007). Mechanistically, Fgf4 activates ERK2, which in turn phosphorylates Klf2 (a pluripotency factor) targeting it for proteasomal degradation (Yeo et al. 2014). Thus, the use of PD, a potent MEK inhibitor that prevents ERK1/2 activation downstream of Fgf4 signalling, was used succesfully in mESCs

culture, promoting both long term self-renewal and colony formation in a defined media (Ying et al. 2008).

While PD is able to suppress differentiation in absence of serum, it requires LIF to maintain viable mESCs. On the other hand, Chiron, a small molecule inhibitor of Gsk3, the key regulatory kinase for the Wnt/ß-catenin pathway, enhances self-renewal of mESCs in absence of BMP4/Serum or LIF (Schifferli et al. 1983). Combination of both PD and Chiron, leading to the simultaneous inhibition of Gsk3 and MEK kinases, has been proposed for mESC culture: the resulting so called 2-inhibitors culture media ("2i") can be used for mESC maintenance with no further requirement of either BMP4/Serum or LIF (Figure 14b) (Hackett et al. 2014).

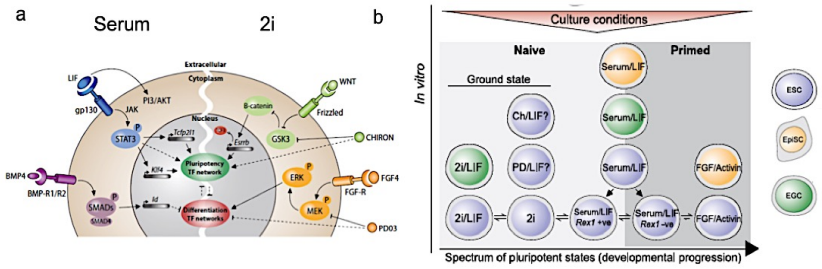

Figure 14 - a) Signalling pathways involved in mESCs pluripotency maintainance in both Serul/Lif (left) and 2iLif (right) culture media. b) Pluripotent cells exhibit different pluripotency spectra depending on the isolation and the culturing conditions. Adapted from Hackett and Surani 2014.

2i/LIF cultures have been reported to enable mESCs to contrast differentiation stimuli present in serum/LIF medium, thereby resulting into homogenous expression of pluripotency genes, spherical and uniform clone morphology and global DNA hypomethylation, ultimately enabling homogenous ground state pluripotency maintenance (Ying et al. 2008,

Nichols et al. 2009, Marks et al. 2012, Leitch et al. 2013, Kumar et al. 2014, Singer et al. 2014).

Recently, more insights into the foundations of ground state mESCs have been gained using population (Marks et al. 2012) and single cell (Kumar et al. 2014, Kolodziejczyk et al. 2015) high-throughput RNA sequencing (RNA-seq), indicating that coupled transcriptional and post-translational feedback loops among signaling pathways triggered by PD, Chiron and LIF might synergistically reinforce the self-renewing ground state (Dunn et al. 2014). The stability of such mechanisms in prolonged 2i/LIF cultures has, however, not been systematically assessed so far, although some evidence of mESC karyotypic and epigenetic instability, given prolonged exposure of cells to Gsk3 inhibition, has been reported (Tighe et al. 2007, Hassani et al. 2014).

Since 2i/Lif is gradually substituting Serum/Lif culturing condition as the golden-standard mESCs propagation medium, we performed experiments aimed at characterizing prolonged 2i/Lif culture conditions and results of this work are reported in CHAPTER 7.

4.4 The Wnt/ß-catenin pathway in pluripotency

The role of the Wnt/ß-catenin pathway in sustaining mESC self-renewal has been extensively studied in the past years (Wray et al. 2012). mESCs cultured in presence of Wnt ligands or Gsk3 inhibitors (such as BIO) (Sato et al. 2004), showed reduced differentiation and increased self-renewal properties (Ying et al. 2008, ten Berge et al. 2011).

Accordingly genetic ablation of key Wnt pathway negative regulators such as APC or Gsk3α and Gsk3ß (Doble et al. 2007) showed similar phenotypes (Wray et al. 2012). From a general point of view it has been considered that Wnt signalling promotes mESCs self-renewal.

Additionally Tcf3, a TCF/LEFs factor with repressive activity, has been found to co-occupy binding sites together with Nanog, Oct4 and Sox2 across the genome and Tcf3 knock-out cells exibit an enhanced self-renewal capability (Pereira et al. 2006, Cole et al. 2008). Tcf3 repression is relieved when nuclear ß-catenin accumulates in response to Wnt signalling although through an unclear mechanisms in mESCs (Wray et al. 2012).

Wnt3a conditioned media has been shown to activate also, through an unknown mechanisms, the JAK-STAT pathway (downstream of LIF signalling) (Ogawa et al. 2006). On the other hand small molecules Gsk3 inhibitors could trigger not characterised off-target effects and partial interfere with the MEK/ERK pathway in addition to ß-catenin stabilization (Zhen et al. 2007).

Various ß-catenin knock-out models in mESCs have been published so far leading to slightly different if not completely opposite results (Anton et al. 2007, Wagner et al. 2010, Lyashenko et al. 2011, Wray et al. 2011).

Two groups reports that ß-catenin loss causes a decrease in Nanog and Oct4 expression (Wagner et al. 2010) or forces mESCs into an EpiSCs-like state (in which self-renewal is maintained under Activin and FGF2) (Anton et al. 2007). More recently two independent groups generated ß-catenin knock-out mESCs from two different conditional knock-out alleles showing that ß-catenin knock-out mESCs, while cultured in presence of LIF, do not show any self-renewal defect (Lyashenko et al. 2011, Wray et al. 2011).

Differences in the phenotypes among alternative ß-catenin knock-out models have been attributed to the initial pluripotency state of the parental cell line and it has been proposed that, for fully pluripotent mESCs cells (able to form chimeras when injected into a developing blastocyst) ß-catenin is dispensable for self-renewal (Lyashenko et al. 2011).

However ß-catenin knock-out mESCs do not show any transcriptional response to Gsk3 inhibition with respect to canonical Wnt target genes (assessed either through the conventional TOP-flash assay or by measuring the mRNA levels of canonical Wnt targets) (Lyashenko et al. 2011, Wray et al. 2011) together with a strong impairment of the differentiation potential.

Surprisingly ΔC-ß-catenin isoforms lacking the C-terminal transactivation domain (hence transcriptionally inactive) can rescue both differentiation potential and self-renewal defects in absence of serum and LIF (Lyashenko et al. 2011, Wray et al. 2011) demonstrating that canonical Wnt-targets activation in response to Gsk3 inhibition plays little or no role in maintaining mESCs self-renewal.

Even if not transcriptionally active, ΔC-ßcatenin isoforms can still relieve Tcf3 mediated repression upon Wnt treatment or Gsk3 inhibition, and Tcf3 loss is epistatic to ß-catenin loss as demonstrated by Wray et al. (Wray et al. 2011) leading to the conclusion that Tcf3 de-repression is the key mechanisms through which ß-catenin (wild-type or ΔC) exerts its positive effects on mESC self-renewal.

On the other hand it has also been proposed that ß-catenin knock-out self-renewal and differentiation phenotypes are mainly mediated by cell-adhesion defects due to ß-catenin loss (Lyashenko et al. 2011).

ß-catenin knock-out cells under Serum+Lif condition are largely compensated for cell-adhesion defects by plakoglobin upregulation. Accordingly when plakoglobin is silenced in ß-catenin knock-out cells, self-renewal is rapidly lost and cells are not able to retain pluripotency, thus demonstrating that cell-adhesion is fundamental for self-renewal of mESCs (Lyashenko et al. 2011).

The differentiation defects are explained in Lyashenko et al. with the observation that, during embryoid bodies formation, ß-catenin is upregulated in wild-type cells while plakoglobin is downregulated.

Therefore ß-catenin knock-out cells exhibits cell-adhesion defects due to the physiological decrease in plakoglobin expression as the differentiation progresses. Since ΔC-ß-catenin can compensate for both phenotypes, the authors conclude that membrane ß-catenin functions are required for self-renewal of mESCs while TCF/LEFs dependent transcriptional activity is not (Lyashenko et al. 2011).

However it has to be noted that, at least in Wray et al. paper (Wray et al. 2011) some of the canonical Wnt targets are weakly activated in response to Gsk3 inhibition in presence of a ΔC-ßcatenin, as previously reported (Hsu et al. 1998), which may indicate that this isoform is not completely transcriptionally silent. Furthermore different canonical target genes show a different response to ΔC-ßcatenin mediated transactivation as well as the TOP-flash reporter assay casting the unresolved doubt that a basal activation of the Wnt target genes (or other ß-catenin transcriptional targets) could be sufficient for the observed phenotypes rescue.

Additionally ChIP-seq analysis of ß-catenin binding sites in mESCs revealed enrichment at about 9000 loci, of which roughly the half overlaps with Tcf3 and the Nanog/Oct4/Sox2 (NES) complex (Zhang et al. 2013) reinforcing Wray et al. observations about ß-catenin mediated Tcf3 de-repression (Wray et al. 2011) but also suggesting additional roles for ß-catenin mediated gene regulation (possibly dependent on other TCF/LEFs or other cofactors). It remains unclear why, since ß-catenin and Tcf3 co-occupy many target genes under Serum+Lif condition, ß-catenin loss does not produce extensive Tcf3 mediated repression producing a collapse of the core circuitry of pluripotency and which is the function of ß-catenin at other DNA binding loci, given that no significant genome-wide transcriptional changes are produced upon ß-catenin loss have been observed (Lyashenko et al. 2011).

To further complicate the landscape, the ß-catenin knock-out models produced from conditional knock-out alleles (Lyashenko et al. 2011,

Wray et al. 2011) result in the production of N-terminally truncated (ΔN) isoforms which have been overlooked in both papers although identified previously (De Vries et al. 2004) and more recently partially characterized in pre-implantation mouse embryo development (Messerschmidt et al. 2016). However to date a complete knock-out of ß-catenin in mESCs is missing and it is unknown whether ΔN-ß-catenin isoforms produced in previously characterized ß-catenin knock-out models can partially compensate or interfere with wild-type ß-catenin loss.

4.5 Somatic cell reprogramming

During development, pluripotency is gradually lost with the appearance of terminally differentiated and specialized cells. Conrad Waddington's famous theory, therefore depicted embryonic development as a ball rolling downhill to its final differentiated state in what is known an "epigenetic landscape" (Figure 15) (Waddington 1957). Waddington's theory implies that the developmental process is phisiologically unidirectional and terminally differentiated cells cannot reacquire pluripotency.

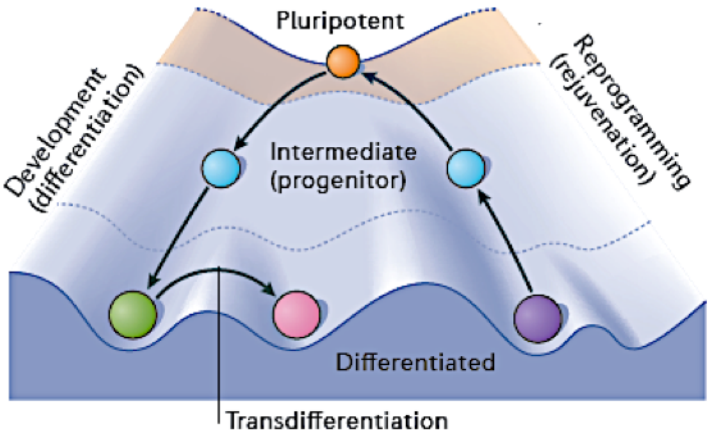

Figure 15 – Waddington's epigenetic landscape, adapted from Takahashi and Yamanaka 2016.

However experiments in 1962 by John Gurdon, demonstrated that in frogs, nuclei of somatic cells could be reprogrammed back to pluripotency when transferred into an enucleated oocyte. This technique, called somatic cell nuclei transfer, (SCNT)(Gurdon et al. 1958) succesfully generated an embryo genetically identical (a "clone") to the donor of the somatic cell, providing the first evidence that terminally differentiated cells could be rejuvenated by opportune experimental manipulation. To date several other group reproduced Gurdon's experiments in sheep and mice, expanding the applications beyond frogs (Wilmut et al. 1997)

In 1983, through a different approach, it was first reported that differentiated cells (fibroblasts, T lympocytes and others) could reacquire pluripotency upon cell-fusion with mouse embryonic stem cells leading to epigenetic changes and re-expression of pluripotency associated genes (Tada et al. 2001).

On the other hand, pioneering experiments demonstrated that it was possible to change cell-identity of terminally differentiated cells upon experimental manipulation.

For instance overexpression of the MyoD gene in cultured fibroblasts was found to be sufficient to induce muscle cells formation (Davis et al. 1987, Graf 2011). The concept of “transdifferentiation”, intended as a the controlled cell-indentity switch of a terminally differentiated cells into a different cell type, was soon confirmed in a variety of cellular systems leading to the identification of transcription factors to be used alone or in combination as “cocktails” to induce a precise cellular fate in target cells (Graf 2011).

All together pioneering reprogramming experiments provided the proof-of-principle concept of "cell-rejuvenation" and suggested the existence of or more reprogrammers factors that, similarly to transdifferentiation

approaches, would have been capable of erasing cell memory, triggering acquiring of pluripotency.

The scientific evidences so far created fertile soil for Yamanaka's pioneering experiment devoted to identify a transcription factors cocktail able to induce somatic cell reprogramming. Yamanaka's group carefully selected a set of 24 potential reprogrammers candidates expressed in mouse embryonic stem cells (embryonic cells associated transcripts – ECATs). Transduction of all the 24 candidates was able to reprogram mouse embryonic fibroblasts to ES-like cells. However when individually depleted from the transduction cocktail, only four factors proved to be strictly required to generate ES-like cells (Takahashi et al. 2006).

The identified set of four transcription factors, now called Yamanaka's factors, contained the octamer-binding protein 3/4 (OCT3/4), Krüppel-like factor 4 (Klf4), sex-determining region-Y box 2 (SOX2) and MYC, a well-known proto-oncogene (Yamanaka et al. 2010, Takahashi et al. 2016). Reprogrammed cells were strikingly similar to mouse embryonic stem cells at morphological, transcriptional, metabolic and epigenetic level and were named induced pluripotent stem cells (iPSCs) (Takahashi et al. 2006).

Soon after Yamanaka's group achieved somatic cell reprogramming of human cells with the same transcription factors cocktail (Takahashi et al. 2007), while a second group obtained human iPSCs by using Oct4/Sox2/Lin-28a and Nanog (Yu et al. 2007) opening iPSCs application to drug discovery, human disease modelling and regenerative medicine (Avior et al. 2016). For their landmark discoveries in somatic cell reprogramming Yamanaka and Gurdon were awarded with the Nobel prize in Medicine in 2012.

4.6 Elite, stochastic and deterministic reprogramming models.

Multiple cell types have been succesfully reprogrammed to iPSCs to date using Yamanaka's protocol, and the reprogramming process has been extensively studied to unravel the precise cascade of events that unlock pluripotency. However ten years after Yamanaka's paper the mechanism of OSKM-mediated reprogramming is not fully understood (Takahashi et al. 2016).

In particular the efficiency of OSKM-mediated reprogramming is remarkably low and several models have been proposed along the years to explain how reprogramming occurs upon OKSM delivery. One possibility is that, amongst somatic cell, only rare subpopulations retain the ability to be successfully reprogrammed upon OSKM transduction constituting an "elite" category of cells (for instance adult stem cells). (Takahashi et al. 2016). However lineage-tracing studies and clonal analysis demonstrated that iPSCs can be generated by terminally differentiated cells while single cell analysis on reprogramming cells showed that the majority of OSKM-transduced somatic cells embarks, but never complete, the reprogramming process (Kim et al. 2015).

During somatic cell conversion to iPSCs a sequential cascade of events must occur for succesffull generation of reprogrammed, ES-like, cells. Since the existence of "elite" cells is not supported by data, and assuming that OSKM transduction can, in principle, lead to the reprogramming of all transduced somatic cells, the precise cascade of events leading to iPSCs generation can follow a stochastic or deterministic way, depending on the ability of transduced cells to respond synchronously or not to OSKM-induced changes (Takahashi et al. 2016). The stochastic model seems more fitted to explain the observed reprogramming dynamics.

Indeed necessity to remove roadblocks to reprogramming (such as epigenetic, metabolic and cell-cycle progression barriers), transduction efficiency, stoychyiometry and expression levels of OSKM concur to lower the efficiency of the OSKM-mediated reprogramming, resulting in a stochastic acquisition of pluripotency.

However a closer look at the reprogramming process revealed that at early phase OSKM induce chromatin remodelling, subsequently silencing somatic genes and activating early-pluripotency markers (Soufi et al. 2012). This process is again largely stochastic and inefficient mainly due to incomplete epigenetic changes in the somatic cells. However in late reprogramming stages, the cascade of events leading to fully pluripotent iPSCs seems much more preditctable and close to the deterministic model (Kim et al. 2015). Thus reprogramming seems to be a dual step process with an early stochastic phase, eventually generating partially reprogrammed cells that, in a second wave can be more predictably converted to fully reprogrammed iPSCs (Takahashi et al. 2016).

More recently it has been shown that genetic ablation of Mbd3 (a component of the Mbd3/NurD nucleosome modelling and deacetylation complex) was able, together with OSKM, to robustly induce fast and efficient (about 100%) reprogramming in a variety of somatic cells (Rais et al. 2013) and pulse of C/EBPα overexpression (Di Stefano et al. 2014) along with OSKM factors, were able to reprogram murine B cells with unprecedented efficiency (close to 100%). These evidences shows that the early stochastic reprogramming phase can be suppressed by different experimental manipulations strengthening OSKM-early effects. In the future, the study of deterministic reprogramming models established so far will allow for a precise temporal description of the cascade of events leading to iPSCs generation, elucidating many of the molecular mechanisms underlying OSKM action and cell-memory erasure and hopefully leading to the development of high quality and safer iPSCs.

4.7 Roadblocks to somatic cell reprogramming

The precise mechanisms by which OSKM triggers iPSCs generation is not yet fully understood, however many molecular processes concurring to enhancement or inhibition of reprogramming efficiency have been identified.

Epigenetic modifiers have been also tested for their ability to enhance OSKM-mediated reprogramming. In particular modulation of enzymes such as WDR5, EZH2, SETDB1, SUV39H1 and DOT1 has been shown to negatively or positively influence the reprogramming efficiency (Takahashi et al. 2016). A similar effect can be achieved by treating reprogramming cells with vitamin C, which promotes the activity of JHDM1A and JHDM1B hystone demethylase, contributing to open chromatin formation (Esteban et al. 2010, Wang et al. 2011, Takahashi et al. 2016).

Cells undergoing reprogramming inhibit somatic cell genes expression and undergo extensive epigenetic and metabolic changes (from oxidative phosphorylation to a glycolysis based metabolism).

Epithelial-to-mesenchymal transition (EMT) is a developmental process by which epithelial cells change their identity by a series of controlled cell-cell and cell-matrix interaction switch, acquiring mesenchymal characteristics by changing cell-adhesion molecules (loosing E-cadherin expression) and upregulating EMT-specific transcription factors such as Snai1 (Li et al. 2010, Samavarchi-Tehrani et al. 2010). Fibroblasts display mesenchymal characteristics (they are a product of EMT) hence, for successfull reprogramming, they must acquire a mensenchymal fate, undergoing the opposite of EMT, or mesenchymal-to-epithelial transition (MET). In particular Sox2/Oct4 suppresses the EMT mediator Snai1, c-Myc downregulates Tgfß1 and Tgfß receptor 2 and Klf4 induces E-cadherin expression, globally enhancing MET transition (Li et al. 2010).

Furthermore, while E-cadherin is strictly required for somatic cell reprogramming, inhibition of EMT and enhancement of MET further improve the reprogramming efficiency demonstrating that MET is crucial for fibroblast conversion to iPSCs (Li et al. 2010).

Another crucial point in somatic cell conversion to iPSCs is the acquisition of self-renewal properties and the capacity to proliferate indefinitely. Myc is a well-known oncogene able to promote cell proliferation and it is not surprising that regulation of cell cycle affects the reprogramming efficiency and it has been shown that fast proliferating cells are more prone to successfully generate iPSCs upon OSKM transduction(Roccio et al. 2013, Zunder et al. 2015). For instance depletion of cell cycle regulators such as p53, CIP1, Ink4a/ARF ameliorates the efficiency of somatic cell reprogramming together with OSKM transduction (Banito et al. 2009, Kawamura et al. 2009, Li et al. 2009, Utikal et al. 2009). Accordingly over-expression of cell-cycle enhancers such as CyclinD1 has a similar outcome and concur to enhance reprogramming efficiency (Edel et al. 2010).

4.8 The Wnt/ß-catenin pathway during reprogramming

Among the original 24 ECATs selected by Yamanaka's group, ß-catenin transcript was already present as a potential "reprogrammer" for the accumulating evidences of Wnt/ß-catenin positive effects on mESCs self-renewal and pluripotency maintenance. However ß-catenin overexpression, in its active form, was dispensable for

iPSCs generation but subsequent experiments demonstrated that the Wnt/ß-catenin role plays a key "helper" role during somatic cell reprogramming.

It is known that constant Wnt3a treatment can enhance somatic cell reprogramming of mouse embryonic fibroblast transduced with Oct4, Sox2 and Klf4 in absence of c-Myc (Marson et al. 2008), suggesting that Wnt/ß-catenin pathway is able to partially substitute for the mitotic stimuli alternatively provided by c-Myc overexpression.

Previous work from our lab demonstrated that activation of the Wnt/ß-catenin pathway in mESCs, enhances their capability to reprogram somatic cells upon cell-fusion. However any perturbation of the Wnt pathway activity that fell below or above the optimum levels resulted in an impaired reprogramming efficiency (Lluis et al. 2008). Moreover genetic ablation of Tcf3, a downstream inhibitor of Wnt activity, enhances reprogramming efficiency and dynamics in either direct or cell-fusion mediated reprogramming experiments mainly by inducing epigenetic modifications (increase in H3 Acetylation and decrease in H3K9me3) (Lluis et al. 2011).

Finally reprogramming of mouse embryonic fibroblast is severely compromised in absence of endogenous ß-catenin and stimulation of the Wnt/ß-catenin pathway during the late phase of the reprogramming process strongly enhances the pre-iPSCs to iPSCs conversion rate (Marucci et al. 2014).

To date, however neither the temporal requirement or the mechanisms through which Wnt/ß-catenin exerts modulation of somatic cell reprogramming efficiency was addressed. For this reason we tried to unravel the role of Wnt/ß-catenin pathway during somatic cell reprogramming (presented in the Results section of the thesis) and reached conclusion similar to Catherine Plath's group (Ho et al. 2013) about a biphasic requirement for Wnt pathway activity during reprogramming, extending the results with a mechanisms by which Wnt/ß-catenin controls senescence and MET through Tcf1.

AIMS

The Wnt/ß-catenin signalling is crucial for self-renewal and pluripotency maintenance of mouse embryonic stem cells, and plays a key role during somatic cell reprogramming. However a complete mechanistic insight on how Wnt/ß-catenin regulates both processes is lacking. Therefore my work mainly focused on two aims, summarised below:

I

Dissect the mechanisms by which Wnt/ß-catenin controls somatic cell reprogramming at early at late stages of the reprogramming process.

(Please see Pag. 66 for a detailed introduction)

II

Characterize the impact of ß-catenin loss in mouse embryonic stem cells, using a de novo generated knock-out models to overcome the incomplete ß-catenin loss of previously published ß-catenin knock-out models in mESCs.

(Please see Pag. 56 for a detailed introduction)

III

Assess pluripotency grade of mESCs in prolonged 2i/Lif culture conditions.

(Please see Pag. 53 for a detailed introduction)

PART II – RESULTS

CHAPTER 5 – Temporal perturbation of the Wnt signalling pathway in the control of somatic cell reprogramming is modulated by TCF1.

The results presented in CHAPTER 5 have been published as part of the work

"Temporal perturbation of the Wnt signaling pathway in the control of cell reprogramming is modulated by TCF1"

(Aulicino et al. 2014)

Francesco Aulicino,[1,2,4] Ilda Theka,[1,2,4] Luigi Ombrato,[1,2] Frederic Lluis,[1,2,5,*] and Maria Pia Cosma[1,2,3,5,*]
[1]Centre for Genomic Regulation (CRG), Dr. Aiguader 88, 08003 Barcelona, Spain
[2]Universitat Pompeu Fabra (UPF), 08003 Barcelona, Spain
[3]Institucio´ Catalana de Recerca i Estudis Avanc ̧ats (ICREA), Pg. Lluis Companys 23, 08010 Barcelona, Spain
[4]These authors contributed equally to this work
[5]These authors contributed equally to this work

5.1 Silencing of Tcf1 does not affect pluripotency and differentiation potential of mESCs

In mESCs, Tcf3 and Tcf1 are the most expressed TCF/LEF family members (data not shown). As previously discussed, while Tcf3 mostly represses pluripotency genes, little is known about the role of Tcf1 in pluripotency.

To assess the role of Tcf1 in regulating mESC pluripotency and differentiation potential, we transduced mESCs with a control short hairpin (shScr), and two different constructs harbouring short-hairpin against Tcf1 (shTcf1-A and shTcf1-B) and hygromycin resistance gene

(pLKO Hygro). Efficient knock-down of Tcf1 was confirmed by qRT-PCR and western blot (Figure 16a and b). Morphology and pluripotency markers expression levels remained unaffected upon Tcf1 silencing (Figure 16).

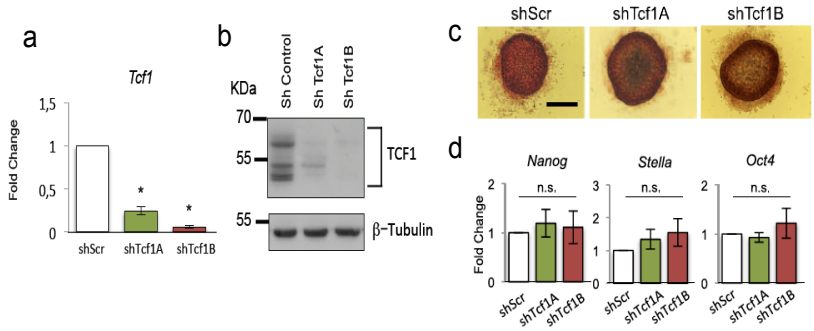

Figure 16 – Tcf1 silencing does not affect pluripotency marker expression. Efficient Tcf1 downregulation was achieved using both shTcf1A (70%) and shTcf1B (over 90%) constructs and confirmed through qRT-PCR (a) and western blot (b). Morphology and alkaline phosphatase staining are unaffected by Tcf1 knock-down (c) as well as the mRNA expression of the pluripotency markers Nanog, Stella and Oct4 (d) assessed through qRT-PCR.

Cells were then transduced with a synthetic TCF/LEFs responsive reporter. The 7TGP construct harbour seven repetitions of the WRE, controlling the expression of enhanced GFP (eGFP) and a constitutive cassette for Puromycin selection (Fuerer et al. 2010).

shSCR, shTcf1A and shTcf1B were transduced with the 7TGP reporter and selected with Puromycin for one week. Puromycin selection was withdrawn and cells were treated with 1 and 3 uM BIO (a small molecule Gsk3 inhibitor) for 24 hours and fluorescence measured through flow cytometry. As expected, Tcf1 depletion impaired, but not abrogated, mESCs capability to activate TCF/LEFs dependent transcription in response to Gsk3 inhibition (Figure 17). The residual reporter activation in shTcf1A and shTcf1B cells might be due to basal Lef1 expression, Tcf3 derepression or incomplete Tcf1 depletion.

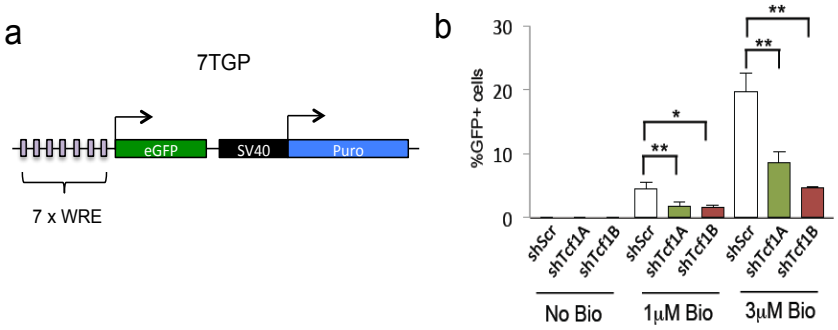

Figure 17 – Tcf1 silencing impairs mESCs response to Wnt pathway activation. shSCR, shTcf1A and shTcf1B mESCs were transduced with the 7TGP lentiviral TCF/LEFs synthetic reporter (a). Percentage of eGFP+ cells measured through flow cytometry in response to 24hrs BIO treatment at 1 or 3uM (b). Error bars represents standard deviation (n=4), asterisks represents statistical significance for T-test analysis (*=p<0,05, **=p<0,01).

Embryoid bodies (EBs) aggregation was used to assess the *in vitro* differentiation potential of mESCs depleted for Tcf1 and expression levels of pluripotency and lineage markers were analysed at various time-points through qRT-PCR.

Tcf1 depletion did not impair mESC capability to differentiate *in vitro* upon EBs aggregation and LIF withdrawal. Morphology of shTcf1A EBs was indistinguishable from EBs derived from control transduced cells (Figure 18-a), and pluripotency marker genes, such as Oct4, Nanog, and Rex1, decreased with the same efficiency and kinetics in both the ESCs-shScr and ESCs-shTcf1A derived EBs.

Furthermore, the mesoderm markers Brachyury and Flk1, the ectoderm markers Fgf5 and Pax6, and the endoderm markers Gata4 and Foxa2 were expressed with the expected timing at 3, 5, 7, and 9 days in ESCs-shScr, ESCs-shTcf1A derived EBs (Figure 18-b) and ESCs-shTcf1B (data not shown)

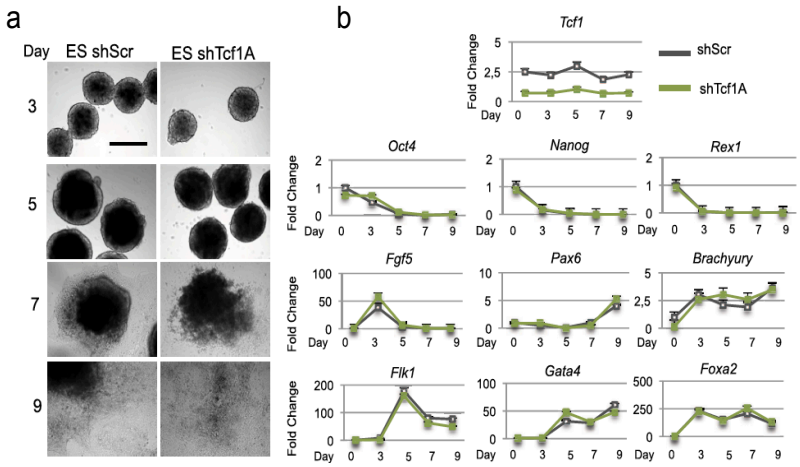

Figure 18 - Embryoid bodies aggregation experiment from shSCR and shTcf1A mESCs. (a) Morphology of EBs at 3, 5, 7 and 9 days of differentiation. Scalebar = 400 uM. (b) qRT-PCR of pluripotency and differentiation markers during EBs formation. One exemplificative experiment is shown out of three independent replicates. Pluripotency (Oct4, Nanog, Rex1), Ectoderm (Fgf5, Pax6), Mesoderm (Brachyury, Flk1), Endoderm (Gata4, Foxa2) markers showed similar expression dynamics in control and Tcf1 knockdown cells.

.

5.2 Continuous Tcf1 Silencing Impairs Reprogramming of MEFs to Pluripotency

Previous work from our and other laboratories demonstrated that Wnt/ß-catenin pathway activation enhances either cell-fusion mediated reprogramming (Lluis et al. 2008), or direct somatic cell reprogramming in absence of Myc overexpression (Marson et al. 2008). Upon Wnt signalling stimulation Tcf3, which mainly acts as a transcriptional repressor (Cole et al. 2008), is reduced, leading to activation of Wnt target genes, possibly through a different sets of TCF/LEFs factors. Indeed, depletion of Tcf3 in mESCs ameliorates self-renewal and stemness maintenance (Pereira et al. 2006, Yi et al. 2008). Accordingly, Tcf3KO

mESCs show an increased reprogramming potential upon cell-fusion with somatic cells, and Tcf3 knockdown increases reprogramming efficiency of neural stem cells to pluripotency (Lluis et al. 2011).

To date, little is known about the role of other TCF/LEF factors during somatic cell reprogramming and we sought to focus on Tcf1 function for its potential role in counteracting Tcf3-mediated target repression as demonstrated in mESCs for a subset of genes (Yi et al. 2011).

To study the role of Tcf1 in somatic cell reprogramming, we took advantage of a transgenic mouse model in which Yamanaka's four factors (Oct4, Klf4, Sox2 and c-Myc, OKSM) have been inserted in single copy in the Col1a1 locus, under the control of a TET responsive element, while the TET transactivator is ubiquitously expressed from the Rosa26 locus (Carey et al. 2010). The four factors are therefore homogenously expressed upon Doxycycline treatment, allowing for the reprogramming of a variety of primary cell cultures with reproducible reprogramming dynamics and efficiencies.

We isolated mouse embryonic fibroblasts with inducible OKSM (henceforth called MEF4F), and transduced them with shSCR, shTcf1A or shßcat. After transduction, MEF4F were selected for 72 hrs with hygromycin in order to deplete untransduced cells, then trypsinized and replated at equal numbers. Effective downregulation of Tcf1 and ß-catenin upon shTcf1-A or shß-cat, respectively, was assessed at protein and mRNA levels (Figure 19b and c).

Cells were then cultured for 12-14 days in presence of 2 µg/ml Doxycycline. In order to assess the reactivation of the endogenous pluripotency network, at day 12-14 Doxycycline was removed and cells were kept in culture for 4 additional days to ensure iPSC self-renewal in absence of exogenous OKSM expression. Finally, cells were stained for Nanog expression to identify reprogrammed iPSC colonies by immunofluorescence (Figure 19a). The number of NANOG+ colonies was

strongly reduced with either Tcf1 or ß-Catenin silencing, with respect to the control (Figure 19d). Furthermore, the few colonies that were formed after Tcf1 silencing were very small and with little NANOG expression (Figure 19e). In contrast, shScr-derived iPSCs formed with high efficiency, were positive to alkaline phosphatase (AP), expressed stem cell markers (such as SSEA-1, NANOG, OCT4, SOX2, Sall1, and Rex1) (Figure 19f)., and differentiated into all three germ layers (Figure 19g). These data show that continuous silencing of ß-catenin or Tcf1 for the whole process (16 days) impairs reprogramming efficiency.

Figure 19 - a) Experimental scheme for iPSC generation. MEF4F were infected with lentiviral vectors carrying shScr, shTcf1A,and sh-ß-cat. Infected cells were selected with hygromycin for 3 days. Doxycycline was applied from additional 12 days, to activate expression of Oct4, Klf4, Sox2, and c-Myc.
Then doxycycline was removed, and cells were allowed to grow for 4 days. At day 16, immunostaining against NANOG was performed, to count the number of reprogrammed clones. b) Western-blot of Tcf1 and ßcatenin on protein extracts of MEF4F transduced with shSCR, shTcf1A or shß-catenin after Hygromycin selection in absence of Doxycycline treatment. Tubulin was used as loading control. c) qRT-PCR of Tcf1 and ßcatenin on shSCR, shTcf1A or sh-ß-cat transduced MEF4F after Hygromycin selection, in absence of Doxycycline treatment. ΔCt were calculated on GAPDH mRNA level. d) Number of NANOG-positive (NANOG+) clones obtained upon shSCR, shTcf1 or sh-ß-cat transduction in MEF4F (n = 4 independent experiments) and e) representative immunofluorescence of Nanog+ clones derived from shSCR or shTcf1-A transduced MEF4F. f) Bright field (BF), Alkaline phosphatase staining (AP) and immunofluorescence of Nanog, Oct4, SSEA-1 and Sox2 on iPSCs derived from shSCR transduced MEF4F (scalebar = 200 μm). g) Immunofluorescence for MAP2 (Ectoderm), GATA-4 (Mesoderm) and Albumin (Endoderm) on embryoid bodies derived from shSCR iPSCs (Scalebar = 200 μm) . All pooled data are represented as means ± SD. The asterisks indicate statistical significance by t test analysis (* $p < 0.05$; ** $p < 0.01$).

Figure 19

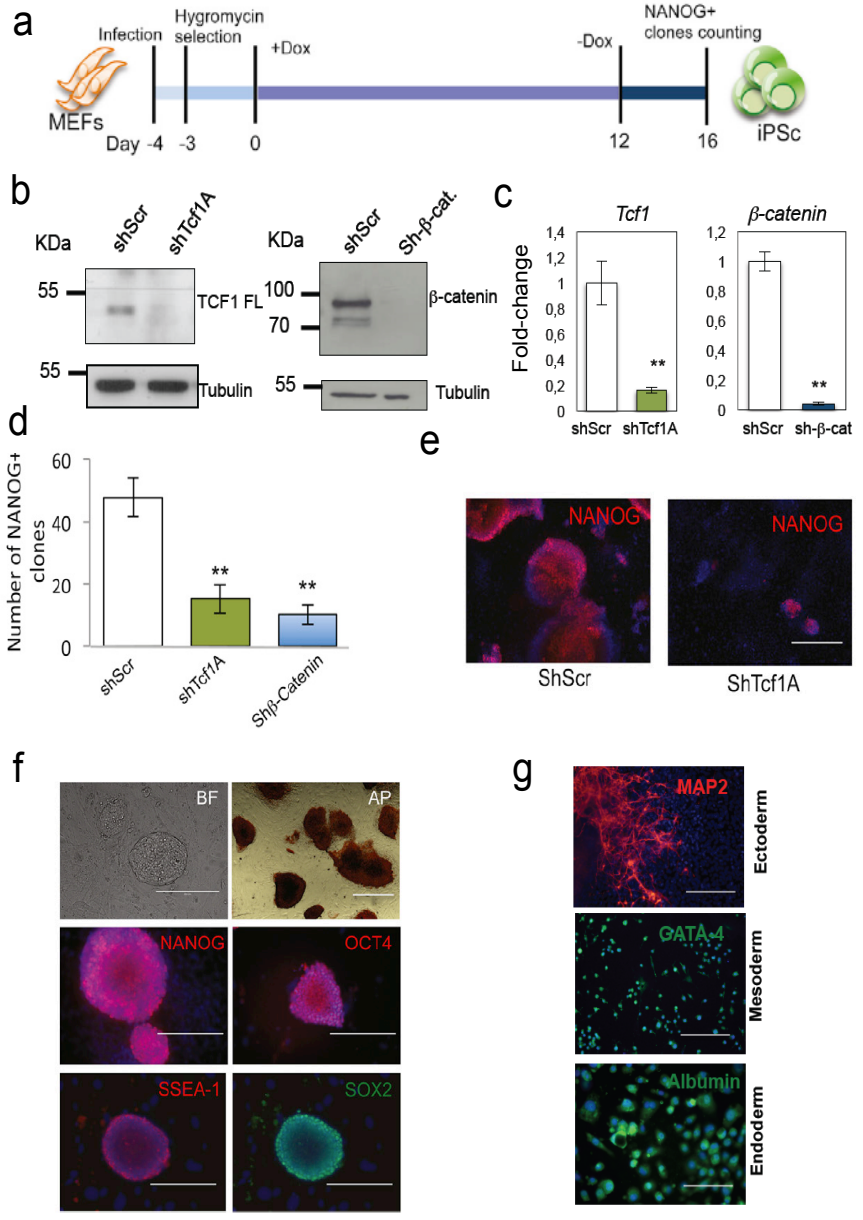
a
Infection
Hygromycin selection
+Dox
-Dox
NANOG+ clones counting
MEFs
iPSc
Day -4 -3 0 12 16
b
KDa
shScr
shTcf1A
55
TCF1 FL
Tubulin
Sh-β-cat.
100
70
β-catenin
c
Tcf1
β-catenin
Fold-change
shScr
shTcf1A
sh-β-cat
d
Number of NANOG+ clones
shScr
shTcf1A
Shβ-Catenin
e
NANOG
ShScr
ShTcf1A
f
BF
AP
NANOG
OCT4
SSEA-1
SOX2
g
MAP2
Ectoderm
GATA-4
Mesoderm
Albumin
Endoderm

5.2.1 Fully reprogrammed cells can be selected early from THY1 negative MEFs.

As we found that Tcf1 expression was dispensable for pluripotency maintenance but necessary for MEF reprogramming to pluripotency, we hypothesized that Tcf1 might have a role at the onset of the reprogramming process.

In order to dissect the mechanism through which Tcf1 controls reprogramming of MEF to pluripotency, we followed THY1 loss as an early marker of reprogramming. THY1 protein is a membrane marker of MEF and its expression is lost during early reprogramming phases (Brambrink et al. 2008, Stadtfeld et al. 2008, Polo et al. 2012), as only THY1 negative cells are successfully undergoing reprogramming (Polo et al. 2012). We therefore analysed gene expression profile of $THY1^{+}$ and $THY1^{-}$ cells FACS-sorted at 3, 6 and 9 days after Doxycycline addition (OKSM expression) (Figure 20a).

Enrichment of *Thy1* expression in sorted cells was confirmed by qRT-PCR (Figure 20d). As cells undergoing reprogramming embark into mesenchymal-to-epithelial transition (MET) (Samavarchi-Tehrani et al. 2010, Esteban et al. 2012), we also checked $THY1^{+}$ and negative cells for the expression of epidermal (*Epcam* and *Cdh1*) and mesenchymal (*Snai1*, *Slug* and *Vimentin*) markers (ten Berge et al. 2008) by qRT-PCR. As previously shown (Polo et al. 2012), we observed *Cdh1* and *Epcam* upregulation and *Snai1*, *Slug* and *Vimentin* downregulation in $THY1^{-}$ cells, while $THY1^{+}$ cells maintained a mesenchymal phenotype (Figure 20e). In addition, the senescence-associated genes *p21*, *p16*, and *p19*, which have been shown to be a barrier for MEFs reprogramming into iPSCs (Li et al. 2009), were down-regulated in $THY1^{-}$ cells (Figure 20e).

Finally we confirmed that, after sorting, only $THY1^{-}$ cells were able to generate fully reprogrammed iPSC colonies (Figure 20b).

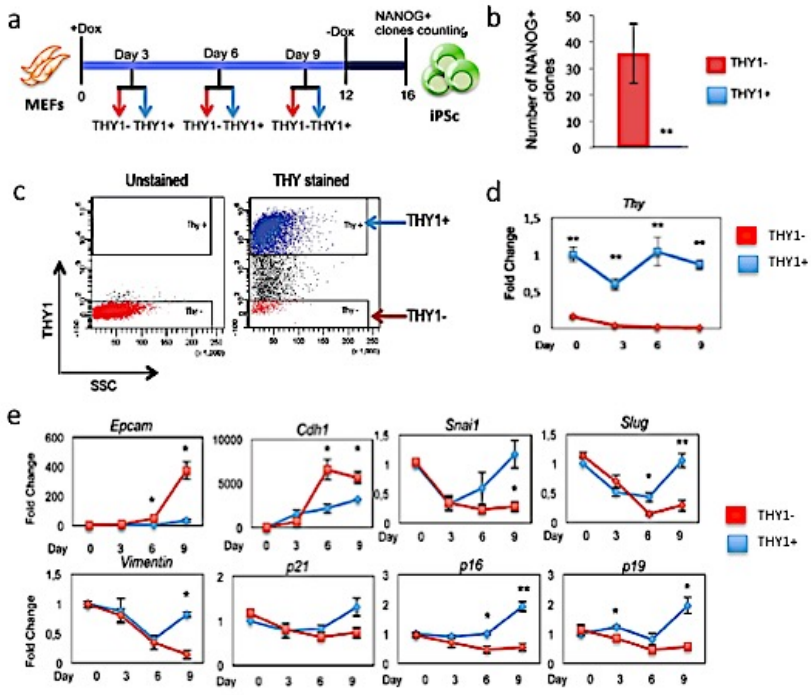

Figure 20 – a) Experimental scheme for the isolation of $THY1^+$ and $THY1^-$ cells during reprgramming of MEF4F, cells were stained for THY1 and FACS-sorted at 3, 6 or 9 of Doxycycline treatment. b) Nanog+ colonies generated by $THY1^+$ (blue) and $THY1^-$ (red) FACS-sorted at 6 days od Doxycycline treatment, replated in equal number and treated with Doxycyline for additional 10 days (n=3 independent experiments). c) FACS profile of unstained (left) and THY1 stained (right) MEF4F at 6 days of Doxycyline treatment. $THY1^+$ cells are showed in red and $THY1^-$ in blue. d) *Thy1* expression in $THY1^+$ and $THY1^-$ FACS-sorted cells. (n=3 independent experiments) measured by qRT-PCR. E) qRT-PCR showing the expression of epithelial (Epcam, Cdh1), mesenchymal (Snai1, Slug, Vimentin) and senescence (p21, p16, p19) markers in $THY1^+$ or $THY1^-$ cells (n=3 independent experiments).
All pooled data are represented as means ± SD. The asterisks indicate statistical significance by t test analysis (* $p < 0.05$; ** $p < 0.01$).

5.2.2 Wnt activity is reduced at early stages in cells undergoing reprogramming

In order to dissect the mechanism through which Tcf1 controls reprogramming of MEF4F to pluripotency, we analysed activity of the Wnt/ß-catenin pathway and expression of its downstream effectors during reprogramming in $THY1^+$ and $THY1^-$ populations.

Tcf3 mRNA level remained almost constant at all time points of the reprogramming process in THY1- cells (Figure 21a), while it increased between 6 and 9 days after Doxycycline treatment in $THY1^+$ cells (not undergoing reprogramming). This finding is in line with previous work from our lab, confirming that the cells that successfully undergo reprogramming maintain low levels of Tcf3 (Lluis et al. 2011). In contrast, Tcf1 expression levels increased progressively from 0 to 6 days in both $THY1^+$ and $THY1^-$ cells, to decrease again at 9 days post Doxycycline treatment (Figure 21a).

In addition, we found that expression of the Wnt/ß-catenin targets *CyclinD1*, *Axin2* was increased in the $THY1^+$ cells with respect to the $THY1^-$ cells, with a peak at 6 days (Figure 21a), indicating that Wnt activity is much higher in the $THY1^+$ cells, which do not undergo reprogramming.

Accordingly, ß-catenin protein levels were enriched in THY^+ cells (Figure 21c), and active ß-catenin (detected with an antibody raised against the unphosphorylated target residues of Gsk3) was enriched in nuclear extracts of THY^+, confirming that Wnt activity was higher in cells that were not undergoing reprogramming at day 6 post Doxycycline treatment (Figure 21d).

While the knock-down experiments showed a clear dependency of reprogramming efficiency on Tcf1 (Figure 19), at this point we were unable to clearly identify any significant change in *Tcf1* expression in

cells unergoing reprogramming (THY^-) versus the non-reprogrammed population (THY^+).

Since Tcf1 has several protein isoforms, including a full-length (FL) and a N-terminally truncated protein (ΔN) with different functions (Reya et al. 2005), we hypothesized that, despite similar Tcf1 RNA levels in $THY1^+$ and THY^- cells, different TCF1 protein isoforms could be expressed dissimilarly in the two populations. Of note, ΔNTCF1 isoforms, lacking the ß-catenin binding domain, were shown to work as constitutive Wnt-targets repressors (Roose et al. 1999, Waterman 2004). We therefore performed an explorative Western-blot on total protein extracts of unsorted MEF4F at 6 days of Doxycycline treatment using an a-FLTCF1 (antibody raised against the N-terminal portion of Tcf1) and a pan a-TCF1 antibody (raised against the central portion of the protein). While ΔNTcf1 isoforms, highly expressed in thymocytes, were not detected during the reprogramming process and in mESCs, FLTCF1 greatly increased at 6 days after doxycycline addition (Figure 21b). FLTCF1 was also equally expressed in THY+ and THY- cells at day 6 post Doxycycline treatment (Figure 21c). In addition, we confirmed that, also in mESCs, only FLTCF1 isoforms are expressed (Figure 21b). We therefore excluded the expression of N-terminally truncated and constitutively repressive TCF1 isoforms during the reprogramming process and in mESCs.

These data pointed out that, although Tcf1 mRNA and protein isoforms were similarly expressed in THY1+ and THY1- cells at day 6 post Doxycycline treatment, the activation of Wnt signalling was different in the two populations. In particular, THY1- negative cells showed lower Wnt signalling activity with respect to THY1+ cells (not undergoing reprogramming).

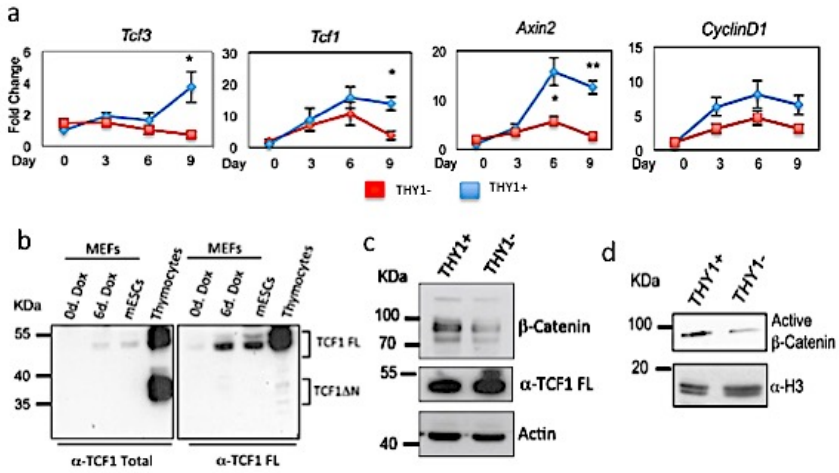

Figure 21 – a) qRT-PCR of TCF/LEFs factors (Tcf3 and Tcf1) or Wnt targets (Axin2 and CyclinD1) on THY1+ (blue) and THY- (red) sorted at 0, 3, 6 and 9 days post Doxycyline treatment (n=3 independent experiments, means ± SD are plotted, the asterisks indicate statistical significance by Student's t test analysis (* $p < 0.05$; ** $p < 0.01$). b) Western blot using a pan-Tcf1 antibody (a-TCF1 total, left panel) or a a-full-length TCF1 (a-TCF1 FL, right panel) on total protein extracts of MEF4F at 0 or 6 days of Doxycycline treatment, mouse embryonic stem cells (mESCs) and Thymocytes. c) Western blot of ß-catenin and FLTCF1 in total protein extracts of MEF4F at day 6 post Doxycyline treatment isolated for the presence or the absence of THY1, Actin was used as loading control. d) Western blot against the unphosphorylated form of ßcatenin in nuclear protein extracts of THY1+ and THY1- MEF4F sorted at 6 days post Doxycycline treatment, Histone-3 (H3) was used as a nuclear loading control.

5.2.3 Tcf1 acts as a repressor of mesenchymal and senescence genes in absence of nuclear ß-catenin in MEF4F.

It is known that Tcf1, similarly to other TCF/LEFs, can act as a transcriptional repressor in absence of nuclear ß-catenin by binding to corepressor factors of the Groucho-related family (Roose et al. 1998, Reya et al. 2003).

We therefore hypothesised that Tcf1 knock-down effect on reprogramming could be explained by taking into account the repressive Tcf1 activity in dependence of nuclear ß-catenin presence.

To investigate this hypothesis, we overexpressed FLTcf1 (the isoform which increases during reprogramming) and ΔNTcf1 as control in MEF4F in absence of Doxycycline. As expected *Axin2* was drastically downregulated upon both isoforms' overexpression, confirming that, in absence of Wnt-activation, Tcf1 isoforms repress Wnt-targets genes regardless to their ability to bind (FLTcf1) or not (ΔNTcf1) ß-catenin (Figure 22a). However, the repressive activity of Tcf1 was converted into an activation of the Wnt-pahtway when ß-catenin was exogenously activated using Chiron (a Gsk3 inhibitor) or Wnt3a in MEF4F infected with FLTcf1 (Figure 22b).

Furthermore, we observed that the mesenchymal genes *Vimentin*, *Slug* and *Snai1* were downregulated by the overexpression of both isoforms of Tcf1, as well as the senescence genes *p21*, *p19* and *p16* (Figure 22a). In contrast, senescence genes and Snai1 did not change in their expression when the Wnt pathway was activated in shTcf1A-MEF4F (Figure 22c).

Finally, to determine whether TCF1 directly regulates MET and senescence genes, we performed chromatin immunoprecipitation (ChIP) assay in MEF4F, which demonstrated binding of TCF1 to Snai1, p21, and Axin2 promoters (Figure 22d).

We next investigated whether the overexpression of Tcf1, contrary to its knock-down, could improve the reprogramming process.

We transduced MEF4F with either empty vector (EV) or FLTcf1 constructs, and stained the cells for THY1 expression at 6 days post Doxycycline treatment. FLTcf1 transduced MEF4F showed an increased percentage of $THY1^-$ cells compared to empty vector (Figure 23a). Also, $THY1^-$ cells from the FLTc1 transduced MEF4F showed a further downregulation of *Axin2*, and of the mesenchymal marker *Vimentin*,

Snai1 and *Slug* and the senescence markers p19 and p21 when compared to THY1$^-$ cells from MEF4F transduced with the empty vector (Figure 23b).

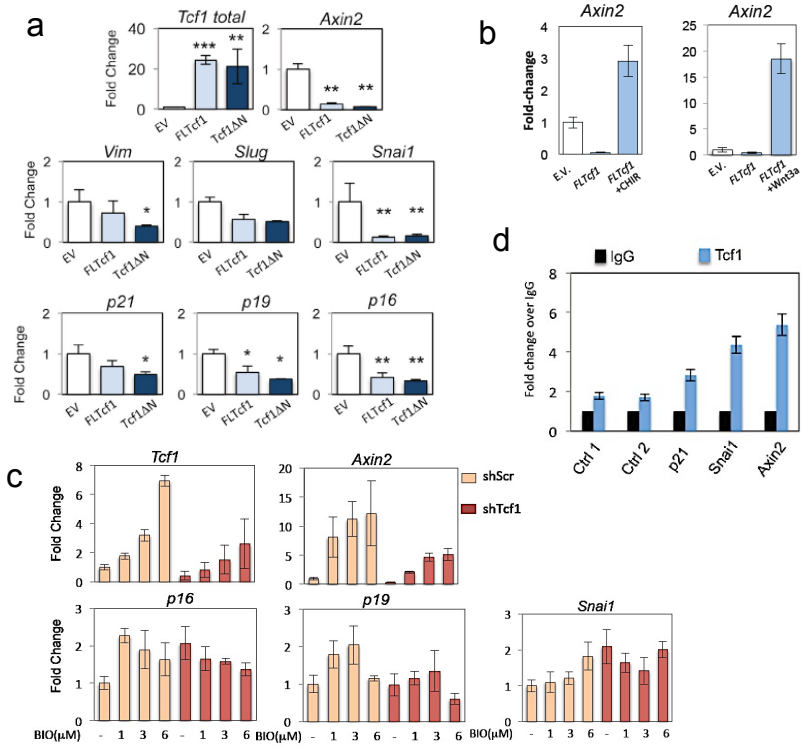

Figure 22 – a) qRT-PCR of Tcf1 (oligos common to exogenous and endogenous isoforms), Axin2, Snai1, Vimentin (Vim), Slug, p21, p19 and p16 on total RNA extracts from MEF4F transduced with empty vector (EV), FLTcf1 or ΔNTcf1 constructs (average of three independent experiment is plotted, error bars represents ST.DEV, the asterisks indicate statistical significance by t test analysis (* $p < 0.05$; ** $p < 0.01$). b) qRT-PCR of Axin2 levels on total RNA extracts of MEF4F transduced with either empty vector (EV) or FLTcf1 in response to Chiron 3 uM (left panel) or Wnt3a (right panel) treatment for 24 hours. (n=2 independent experiments). c) qRT-PCR expression analysis of four-factor MEFs infected with shScr or shTcf1 and treated for 12h with increasing concentrations of Chiron as indicated (N.T.:Non-Treated); (n=2 independent experiments). d) Quantitative ChIP assay of the TCF1 targets Axin2, Snai1, and p21 in the four-factor MEFs. ChIP was performed using rabbit immunoglobulin G or a specific antibody against TCF1 (n = 2 independent experiments).

Since Tcf1 increased at day 6 post Doxycycline treatment, we assessed if Tcf1 was required at this time point in THY1$^-$ cells to be successfully reprogrammed. To this end, we transduced MEF4F with shSCR or shTcf1A. After Hygromycin selection, cells were counted and replated equally. Doxycycline was added until day 6 and THY1$^-$ cells were FACS sorted and replated for reprogramming. As expected, we found a reduction of NANOG+ colonies from shTcf1A transduced THY1$^-$ cells with respect to shSCR (Figure 23c). Accordingly, mRNA levels of the epithelial markers *Cdh1* and *Epcam* were downregulated in THY1- cells transduced with shTcf1, while *Snai1*, *p21* and *p16* expression was upregulated (Figure 23d).

This showed that the repressive activity of Tcf1 towards mesenchymal and senescence related genes is required at early stages to enhance the reprogramming process.

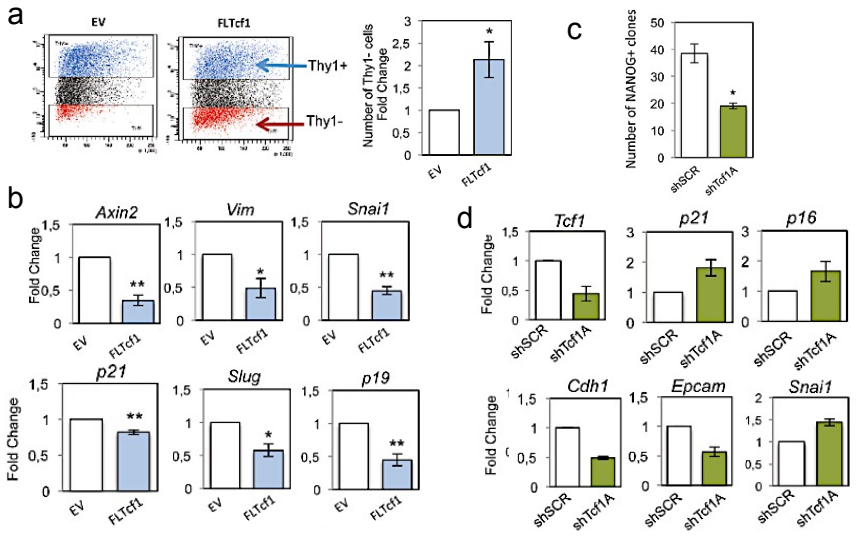

Figure 23 - a) MEF4F were infected with lentivirus overexpressing FLTcf1 or with an empty vector (EV) and selected with hygromycin. Six days after doxycycline induction, cells were analyzed by THY1 expression by FACS (n = 3 independent experiments, error bars represents ST.DEV, the asterisks indicate statistical significance by t test analysis (* $p < 0.05$;). b) qRT-PCR on total of Axin2, Vim, Snai1, p21, Slug and p19 on total RNA extracts of EV (white) or FLTcf1 (blue) transduced MEF4F, sorted at 6 days of Doxycyline treatment for the absence of THY1 ($THY1^-$ cells), (n = 3 independent experiments, error bars represents ST.DEV, the asterisks indicate statistical significance by t test analysis (* $p < 0.05$; ** $p<0.01$). c) Number of NANOG+ colonies proceeding from THY1- cells sorted at 6 days of Doxycyline treatment frome either shSCR (white) or shTcf1A (green) transduced MEF4F. After sorting cells were plated at equal numbers and Doxycyline was added for additional 10 days and finally removed for 4 days before immunostaining (n=3 independent experiments, error bars represents ST.DEV, the asterisks indicate statistical significance by t test analysis (* $p < 0.05$; ** $p<0.01$)). d) qRT-PCR on total RNA extracts of $THY1^-$ sorted after six days of Doxycyline treatment from shSCR (white) or shTcf1A (green) transduced MEF4F (n=2 independent experiments).

5.3 Wnt-"OFF" state is an early reprogramming marker

To further monitor whether Wnt ''off'' cells in early reprogramming phases embark upon efficient reprogramming, we infected four-factor MEFs with a lentivirus carrying the 7xTcf-eGFP reporter (7TGC) for TCF/ß-catenin activity and mCherry under the constitutive SV40 promoter (Fuerer et al. 2010). MEF4F were transduced with 7TGC construct, Doxycycline was applied and mCherry+ cells were sorted at day 6 for different eGFP fluorescence levels (isolated into four fractions ranging from GFP- to GFP+ cells, and having different levels of Wnt pathway activation (Figure 24a). Axin2 mRNA levels were measured in the four population as a control for the sorting strategy, confirming a correlation between eGFP expression and Wnt pathway activation level (Figure 24b).

We then inspected the transcriptional profile of MEF4F undergoing reprogramming 6 days after Doxycycline treatment based on their maximum of minimum Wnt activity respectively P5 and P9 populations.

7TGC transduced MEF4F were treated with Doxycycline for 6 days and then FACS-sorted in two populations for their eGFP expression (GFP+ and GFP- cells, Figure 24c). As expected, the expression of Wnt target genes (*Axin2*, *CyclinD1* and *BMP4*) was downregulated in GFP- vs GFP+ cells, as well as the expression of the mesenchymal marker genes *Vimentin*, *Slug* and *Snai1* and the senescence markers p19 and p16. Accordingly, epithelial marker genes such as *Cdh1* and *Epcam* were upregulated, as well as pluripotency markers. Furthermore, the expression of Thy1 was downregulated, confirming a correlation between Thy1 loss and the Wnt "OFF" state (Figure 24d).

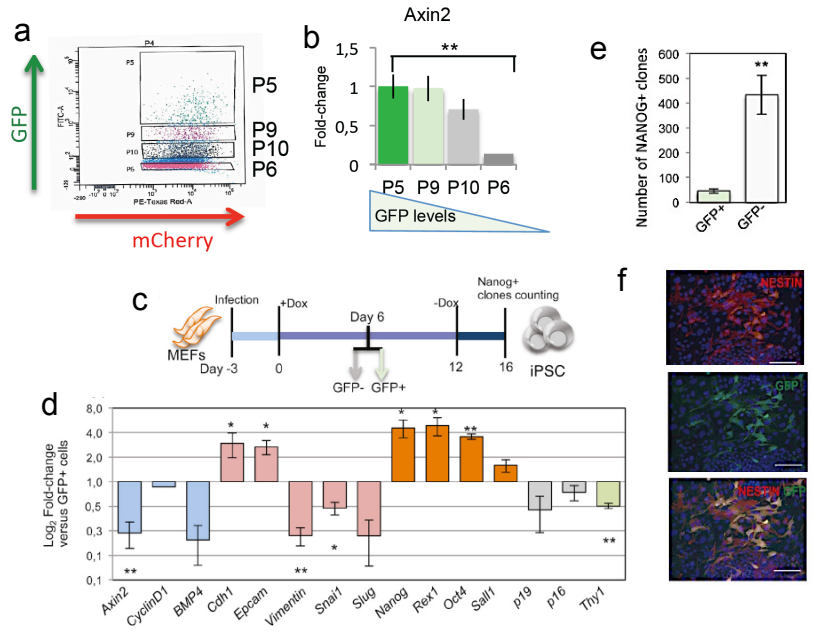

Figure 24- a) MEF4F transduced with 7TGC were treated with Doxycyline for 6 days. Cells positive for mCherry expression were sorted by different levels of eGFP expression (P5, P9, P10 and P6) at 6 days after doxycycline induction. qRT-PCR of Axin2 expression is shown; (n= independent experiments, error bars represents ST.DEV, the asterisks indicate statistical significance by t test analysis (* $p < 0.05$; ** $p<0.01$)). b) qRT-PCR on total RNA extract from 7TGC transduced MEF4F at 6 days of Doxycyline treatment FACS sorted by different levels of eGFP (P5=High, P9=intermediate, P10=low, P6=negative), n= 3 independent experiments error bars represents ST.DEV, the asterisks indicate statistical significance by t test analysis (* $p < 0.05$; ** $p<0.01$)). c) MEF4F were transduced with lentiviruses carrying 7TGP reporter.. d) GFP+ and GFP cells were sorted 6 after Doxycycline treatment and analyzed by qRT-PCR for Wnt (blue), MET/EMT (pink) and Pluripotency markers (Orange). Thy1 expression was also analysed (n = 3 independent experiments, bars are average of 3 independent experiments represented as Log2FC of GFP- cells versus GFP+ cells, error bars represent ST.DEV, asterisc indicate statistical significance by t test analysis (* $p < 0.05$; ** $p<0.01$). e) GFP+ and GFP- cells sorted at day 6 after Doxycycline treatment were replated in equal numbers and cultured for additional 12, days in presence of Doxycycline. NANOG+ colonies were analyzed at day 16 (n=3 independent experiments, error bars represent ST.DEV, asterisc indicate statistical significance by t test analysis (* $p < 0.05$; ** $p<0.01$). f) GFP+ cells FACS-sorted at day 6 were analyzed by immunofluorescence for the expression of Nestin. Scale bars, 100 mm

Finally, GFP+ and GFP- cells sorted at day 6 were replated at equal number and allowed to form iPSCs colonies (Figure 24e); as expected from their transcriptional profile, GFP- cells with a low Wnt activity produced iPSCs more efficiently than GFP+ cells. Also, GFP+ showed expression of Nestin, a neural precursor marker, suggesting that they were more differentiated or transdifferentiating into different cell types rather than reprogrammed back to pluripotency (Figure 24f).

All together, these results clearly indicate that, during the initial steps of the reprogramming process (up to 6 days after Doxycycline induction in our system), the Wnt ‘‘off’’ state is a robust and early marker of reprogramming.

5.4 Temporal perturbation of the Wnt pathway controls somatic cell reprogramming

Since our experiments suggested that Wnt “OFF” state could be considered an early marker of reprogramming, we asked wether its perturbation at defined time-points could substantially alter the reprogramming efficiency.

In order to inhibit the Wnt pathway during the reprogramming process, we used IWP2, a small-molecule inhibitor of Wnts’ secretion (ten Berge et al. 2011) (see section for details 2.8.2).

We treated MEF4F with IWP2 and Doxycycline for six days and analysed the gene expression profile of the whole population of cells. While Axin2 was downregulated (confirming the succesfull Wnt activity inhibition by IWP2), *Tcf1* was decreased and *Tcf3* upregulated. Pluripotency genes were instead slightly upregulated in IWP2 treated cells with respect to control (vehicle treated cells).

Next, we wanted to assess the effect of Wnt pathway perturbations during reprogramming by either inhibiting or activating the pathway using Wnt3a at specific time-points.

The number of iPSCs, NANOG+ colonies was strongly increased when IWP2 was applied for the first 3 or 6 days of the reprogramming process, demonstrating that Wnt inhibition in the early phases is beneficial for the reprogramming process. However, when cells where treated with IWP2 from day 6 to 12 or for the whole reprogramming process (12 days), iPSC colony number strongly decreased with respect to the control (Figure 25c).

Accordingly, treatment with Wnt3a at early time point (Days 0-4), or for the whole reprogramming process strongly decreased the number of iPSC colonies; in contrast, Wnt3a treatment at late stages (Days 8-12) resulted into a slight increase in the reprogramming efficiency (Figure 25c).

Finally, inhibition of the pathway at early stages and activation at late stages (IWP2 Days 0-4, Wnt3a Days 8-12) further ameliorated reprogramming efficiency, while the opposite (Wnt3a Days 0-4, IWP2 Days 8-12) almost yielded no reprogrammed clones (Figure 25c).

All together this data pointed for a time-dependent role for Wnt/ß-catenin during the reprogramming process, in which inhibition at early stages should be followed by activation in late stages to successfully achieve somatic cell reprogramming.

In addition, the silencing of p21 after IWP2 treatment for 6 days did not result in an increase of reprogramming, further confirming that p21 is an important effector of the Wnt pathway inhibition in the reprogramming process (Figure 25f-g).

We reasoned that, as for Wnt pathway, also Tcf1 knock-down effect could have radically changed if temporally controlled, instead of being constitutive as in previous experiments. To test this hypothesis we transiently transfected shTcf1-A construct into MEF4F and treated cells

with Doxycycline without any Hygromycin selection treatment, in this way Tcf1 knock-down was lost within 6 days (Figure 25d). We found that, whereas the constant inhibition of Tcf1 resulted in a decreased number of NANOG+ colonies (Figure 25c), Tcf1 transient inhibition resulted in increased reprogramming efficiency (Figure 25e).

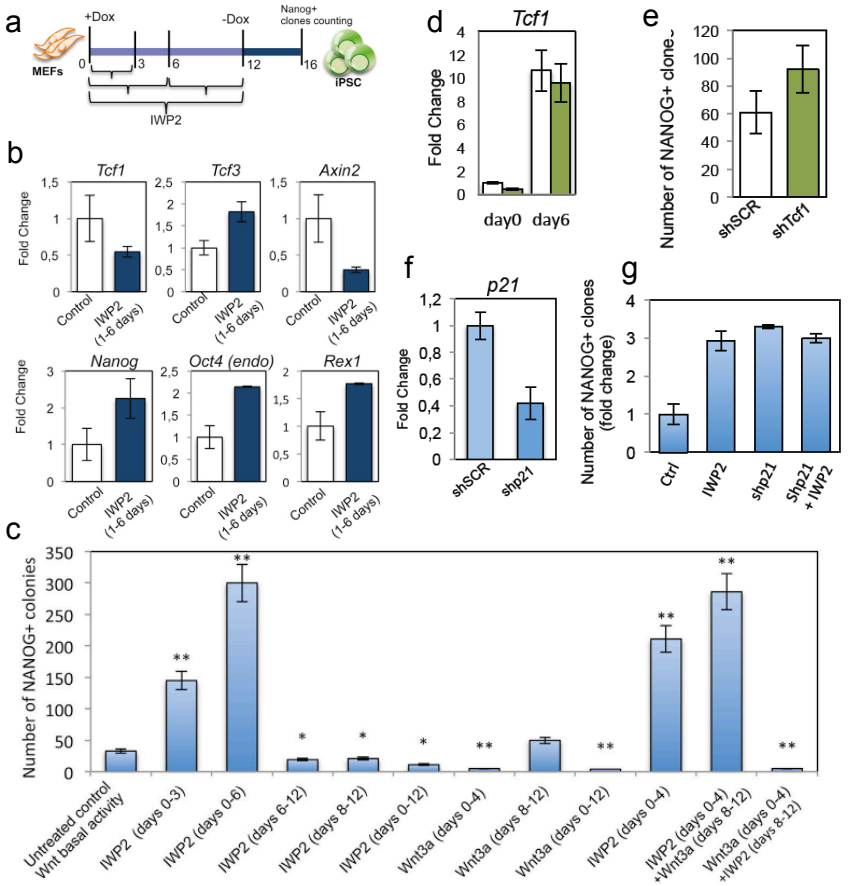

Figure 25 a) Schematic representation of IWP2 temporal treatment during a reprogramming experiment. b) qRT-PCR on total RNA extract of 2uM IWP2 or Vehicle treated MEF4F at 6 days of Doxycyline treatment. c) Number of NANOG+ colonies emerged from 2uM IWP2 and 100 ng/ml Wnt3a treatment for the indicated time windows. Doxycyline was added for 12 days and then removed for additional 4 days before NANOG immunostaining. d) qRT-PCR on total RNA extracts of MEF4F transiently transfected with either shSCR or shTcf1A constructs. Day0 = 48 hours after transfection, Day 6= 48 hours after transfection + 6 days of Doxycyline treatment. (n=2 independent experiments). e) Number of NANOG positive (NANOG+) clones obtained according to experimental procedure indicated in (d) (n=2 independent experiments)). f) qRT-PCR of *p21* on total RNA extracts of MEF4F transduced with either shSCR or sh-p21 (n=2 independent experiments). g) MEF4F were transduced with either shSCR or sh-p21. Doxycyline was applied for 12 days with or without 2 uM IWP2 treatment at early stage (Days 0-6). Immunostaining against Nanog was performed, to count the number of reprogrammed clones. (n=2 independent experiments).

CHAPTER 6 – Characterization of a new ß-catenin knock-out model in mESCs

6.1 ß-catenin knock-out models produce N-terminally truncated isoforms.

ß-catenin mRNA has 15 exons, with ORF spanning from exon 2 to exon 15 (Figure 26a). Current ß-catenin knock-out models relies on CRE-mediated excision of a DNA fragment flanked by two LoxP sites encompassing exons 2-6 (*Ctnnb1*^{tm2Kem}) (Brault et al. 2001) or 3-6 (*Ctnnb1*^{tm4Wbm}) (Huelsken et al. 2000). Three groups have independently studied both alleles to elucidate ß-catenin role in mESCs, reaching comparable conclusions (Lyashenko et al. 2011, Wray et al. 2011, Raggioli et al. 2014).

We noticed that currently available ß-catenin knock-out alleles are flawed by the production of N-terminally truncated (ΔN) proteins generated by alternative splicing (*Ctnnb1*^{tm4Wbm}) (Figure 26b) or from a secondary ATG within a Kozak consensus sequence downstream of the excised region (*Ctnnb1*^{tm2Kem}) (Figure 26c) (De Vries et al. 2004, Messerschmidt et al. 2016). With regard to the *Ctnnb1*^{tm2Kem} allele, the generation of a ΔN-ßcatenin isoform from a secondary ATG within a Kozak consensus sequence in Exon VII (downstream the excision site) was already identified and partially characterized in 2004 by Knowles group (De Vries et al. 2004). The truncated protein from *Ctnnb1*^{tm2Kem} molecular weight is ≈52 KDa, contains armadillo repeats 6-12, thus retaining the entire binding sites for many ß-catenin interactors such as CREPB/p300 and BRG1as well as a portion of the binding sites for APC, E-cadherin and

TCF/LEFs and it was detected in the pronuclei of zygotes and 2-cell stage mouse embryos lacking E-cadherin (De Vries et al. 2004).

More recently Knowles group further investigated the effect of ß-catenin ablation in the developing mouse embryos. The authors proved that, likewise to *Ctnnb1*^{tm4Kem}, also *Ctnnb1*^{tm4Wbm} produces a ΔN-isoform of about 48 KDa, possibly emerging from splice junction of Exons 1 and 8 upon Exons 3-6 excision.

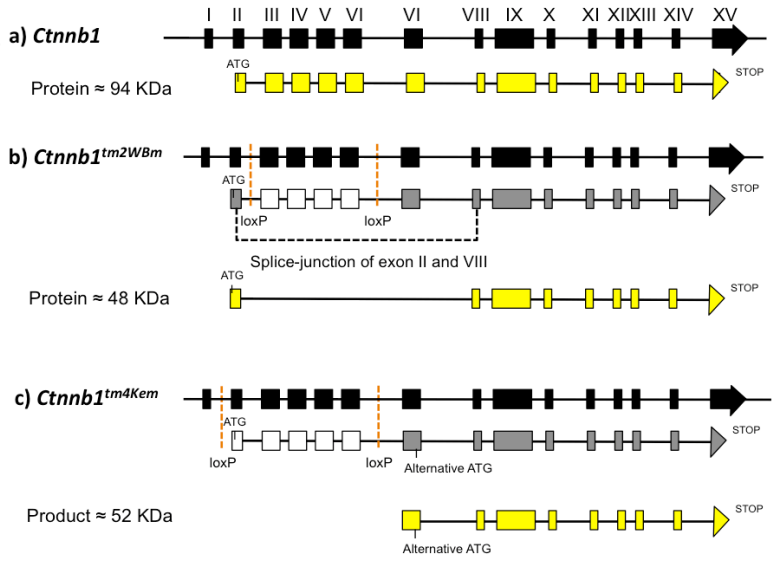

Figure 26 – Schematic representation of ß-catenin inducible KOalleles. Squares represents exons numbered from TSS (I-XV). Gray represents mRNA, white excised exons and yellow represent ORFs. LoxP sites are indicated by dashed red lines. a) Wild-type ß-catenin locus (Ctnnb1) produces a 94 KDa protein. b) *Ctnnb1*^{tm4Wbm} allele produces a 48 KDa protein, possibly emerging from splice junction of exons I-VIII upon exons III-VI deletion. b) *Ctnnb1*^{tm2Kem} produces a 52 KDa protein from a secondary ATG within a Kozak sequence in exon VII, downstream the excised exons II-VI.

To address the flaws in both designs, the authors generated a third knock-out model that, by inducible excision of the C-terminal exons, results in a complete loss of ß-catenin (Messerschmidt et al. 2016), showing that the ΔN-ßcatenin isoform substitutes, albeit incompletely probably due to its low expression level, the intact ß-catenin during preimplantation development (Messerschmidt et al. 2016).

Remarkably, despite already published evidences that ΔN-ßcatenin isoforms were generated from both *Ctnnb1*^{tm2WBm} and *Ctnnb1*^{tm4Kem} alleles, the authors of the papers where these knock-out alleles were described (Lyashenko et al. 2011, Wray et al. 2011, Raggioli et al. 2014) did not mention possible caveats. Actually all the western-blot independently reported in the papers by the three groups showed no signs of truncated ß-catenin isoforms upon CRE-mediated recombination and excision of exons 2-3 or 3-6. This could be explained either by technical issues (use of antibodies recognizing N-terminal/C-terminal portions of ß-catenin, western-blot membranes cut and hybridized separately, usage of a-ß-catenin and loading control antibodies simultaneously) or simply because it might be that truncated isoforms are after all not expressed in mESCs.

We therefore checked for the expression of ΔN-ßcatenin isoforms in mESCs lines bearing the *Ctnnb1*^{tm4Kem} or the *Ctnnb1*^{tm2WBm} alleles kindly provided by Kemler's group. SR18 cells (*Ctnnb1*^{tm4Kem}) (Raggioli et al. 2014) and NLC1 cells (*Ctnnb1*^{tm2WBm}, Kemler's group, unpublished) stably carry a CRE-ERt2 construct, which allow for fast and robust ß-catenin deletion upon treatment with 4'-HydroxyTamoxifen (4OHT) and CRE-mediated recombination upon its nuclear translocation (Raggioli et al. 2014). Furthermore SR18 cells are heterozygous for ß-catenin allele, already harbouring only one copy (fl/del), while NLC1 cells had two floxed alleles (fl/fl).

NLC1 and SR18 cells were treated with 4OHT for 72 hours and ß-catenin expression was analysed by western-blot using an antibody

against the C-terminal portion of ß-catenin. We found, as previously reported by Raggioli et al. (Raggioli et al. 2014), that wild-type ß-catenin allele (94 KDa) was homogeneously deleted in SR18 cells and we confirmed the robustness of CRE-ERt2 also in NLC1 cells (Figure 27a).

However upon CRE-mediated recombination ΔN-ßcatenin isoforms appeared in both knock-out models with the expected molecular weights, confirming the incomplete knock-out in both cell lines. NLC1 (*Ctnnb1*^{tm2WBm}) expressed a 48 KDa protein and SR18 (*Ctnnb1*^{tm4Kem}) expressed a 52 KDa protein. Remarkably 52 KDa protein was already detectable in heterozygous SR18 (fl/del) and its expression increased when the remaining ß-catenin allele was excised (del/del) (Figure 27a).

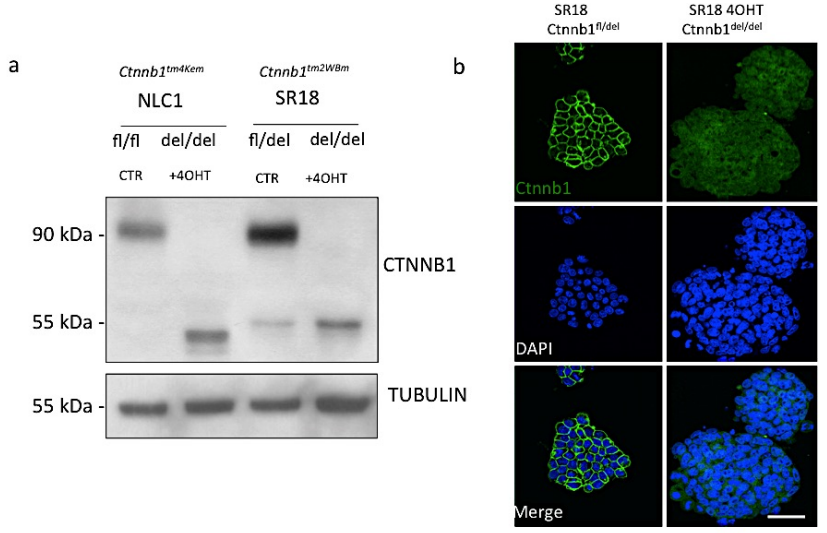

Figure 27 Currently available ß-catenin knock-out models in mESCs result in the expression of N-terminally truncated isoforms. a) Western blot performed on total protein extracts of NLC1 and SR18 cells treated with 4OHT for 72hrs. An antibody raised against the C-terminal portion of ß-catenin was used. Tubulin was used as a loading control after stripping. ΔN-ßcatenin isoforms were readily detected upon CRE-mediated recombination of 48 KDa (NLC1 del/del) and 52 KDa (SR18 fl/del and del/del). b) Immunofluorescence using an antibody raised against the C-terminal portion of ß-catenin on SR18 control cells and SR18 treated with 4OHT. Immunostaining reveal incomplete ß-catenin deletion. Furthemore ΔN-ßcatenin mislocalized in nuclei and cytoplasm and was not detected at the cell membrane.

In addition we performed immunofluorescence experiments using an antibody against the C-terminal portion of ß-catenin in $SR18^{fl/del}$ and $SR18^{del/del}$. Immunofluorescence confirmed the partial deletion of ß-catenin. ΔN-ßcatenin isoforms have a partial conservation of the E-cadherin binding domain, as suggested by de Vries et al. 2004 (De Vries et al. 2004). However ΔN-ßcatenin did not localize at the cell membrane while it accumulated rather homogeneously in both nuclear and cytoplasmic compartments suggesting its failure to interact with E-cadherin.

To confirm that the detected ΔN-ßcatenin isoforms were produced from the recombined Ctnnb1 locus, we designed three different short hairpin constructs targeting different regions of ß-catenin mRNA, and subcloned them into pLKO Hygro for lentiviral-mediated shRNA delivery. shß1 and shß3 targeted respectively the CDS downstream the deletion and the 3'UTR while shß2 targeted the CDS on exon V, between the loxP sites (Figure 28a).

Female mESCs fl/fl and del/del harbouring the $Ctnnb1^{tm2WBm}$ allele were kindly provided by Hartmann's group (Lyashenko et al. 2011). mESCs fl/fl and del/del were transduced with pLKO shß1, shß2, shß3 and a control hairpin and selected with Hygromycin for 1 week. Total protein extracts were analysed for western blot using an antibody against the C-terminal region of ß-catenin. The three constructs were able to downregulate ß-catenin protein expression in fl/fl cells as compared to the control hairpin (Figure 28b, right) however only shß1 and shß3, targeting regions downstream the loxP sites could downregulate the ΔN-ßcatenin isoform (Figure 28b, right) while shß2, targeting the exonV in the floxed region, did not alter its expression.

This demonstrates that ΔN-ßcatenin isoforms are generated from incomplete ß-catenin knock –out, excluding the possibility of technical artefacts due to unspecific antibody staining.

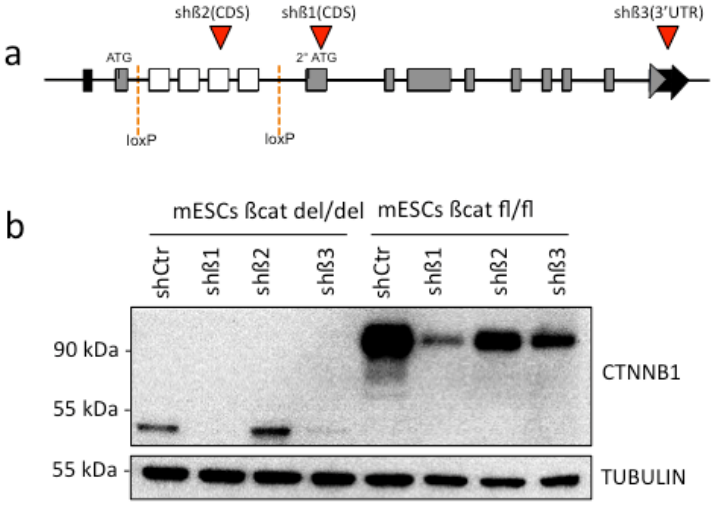

Figure 28 - ΔN-ßcatenin isoforms are produced from mRNA of Ctnnb1 locus. a) Three short-hairpin targeting different regions of ß-catenin mRNA (red triangles). Shß1 and shß2, respectively targeting two regions downstream of the floxed site, and shß2 targeting a region within the loxP sites. b) Western blot using anti C-terminal ßcatenin antibody on protein extract of female mESCs (Ctnnb1tm2WBm fl/fl or Ctnnb1tm2WBm del/del) cells transduced with lentiviral vectors (pLKO Hygro) carrying shß1, shß2, shß3 or a control short hairpin (shCtr). Short hairpins efficiently downregulate ß-catenin expression in mESCs ßcat fl/fl cells (94 KDa protein), while in mESCs ßcatenin del/del cells only shß1 and shß3 were able to downregulate the ΔNßcatenin isoform (48 KDa).

Since ΔN-ßcatenin isoforms have not be described as physiologically relevant neither characterized, it is still unknown if these N-terminally truncated ß-catenin isoforms can partially rescue or interfere some of the wild-type ß-catenin functions.

Remarkably, while ß-catenin del/del blastocysts development is interrupted at the gastrulation stage (E7.5, in which the role of Wnt/ß-catenin pathway has been extensively studied), heterozygous blastocysts (ßcat fl/del) from either KO models develop into phenotypically normal and fertile mice (De Vries et al. 2004, Lyashenko et al. 2011, Messerschmidt et al. 2016). In light of the incomplete ß-catenin excision it can be speculated that, since ßcat fl/del mice are phenotypically normal, ΔN-ß-catenin isoforms (which coexist together with the wild-type in heterozygous mice) do not interfere with normal embryo development. On the other hand, evidences for ΔN-ß-catenin functions are suggested from the work of Messerschmidt et al. (Messerschmidt et al. 2016) since a complete ß-catenin knock-out model showed more pronounced defects in pre-implantation embryo development with respect to knock-out models in which ΔN-ß-catenin isoforms are generated.

6.2 CRISPR/Cas9-based ß-catenin KO strategies: trial-and-error

Since the presence of ΔN-ß-catenin isoforms has not been taken into account when assessing the impact of ß-catenin deletion in mESCs (Lyashenko et al. 2011, Wray et al. 2011, Raggioli et al. 2014), we sought to generate an alternative, novel knock-out model, taking advantage of CRISPR/Cas9 technology. Briefly RNA-guided Cas9 nucleases from the microbial clustered regularly interspaced short palindromic repeats (CRISPR) adaptive immune system has been re-engineered for genome

editing in mammalian cells by simply specifying a 20-nt targeting sequence within its guide RNA (Ran et al. 2013).

Single-guide RNA (sgRNA) and Cas9 can be easily delivered in a single vector such as px459-Puro, which in addition allows for selection of efficiently transfected cells. Cas9 is then guided by the sgRNA on the targeted DNA region and exerts a nuclease activity which is ultimately repaired either through non-homologous end-joining (NHEJ) or homologous directed repair (HDR), offering a fast and robust platform for generating either knock-out or knock-in model (Ran et al. 2013).

In the majority of the cases Cas9-induced double strand break is repaired through NHEJ that induces small insertion/deletion (indel) producing thereby a frame-shift in the open reading frame, which results in a protein knock-out (Ran et al. 2013).

Since neither alternative splicing of exon I and VIII or truncated protein products deriving from the secondary ATG in exon VII are physiologically produced from wild-type *Ctnnb1* alleles, we figured out that these isoforms are only produced when the genomic Ctnnb1 locus is rearranged and the promoter, upon excision of the floxed exons, is joined to downstream regions.

Therefore we designed a single sgRNA to target a region immediately downstream of ß-catenin ATG in order to obtain a frame-shift in the ORF that would have led to complete ß-catenin knock-out without massive locus rearrangement and promoter shifting (Figure 29a). However, despite the efficiency of the sgRNA (validated by T7 assay described in (Ran et al. 2013)), we failed to identify any decrease in ß-catenin protein levels at pool levels and by immunofluorescence (data not shown).

We therefore sought to simultaneously use two sgRNA respectively targeting exon II and exon III, in order to induce a defined microdeletion (Figure 29b). Since desired deletion produces a shorter amplicon in PCR of the Ctnnb1 locus from genomic DNA, the success of this approach was

readily detectable. We successfully isolated homozygous clones for the microdeletion but, once again, ß-catenin was detected by immunofluorescence with a C-terminal antibody in all analysed clones although western blot analysis on isolated clones revealed that protein levels and molecular weights of ß-catenin greatly varied among clones, producing truncated isoforms of about 70 KDa (data not shown).

Taken together these two approaches indicate that ß-catenin ORF (independently of the upstream deletion), can be recovered from the uppermost ATG after the deletion.

However, since our aim was to generate a complete knock-out of ß-catenin, we did not characterized further the nature of the truncated proteins generated by CRISPRs/Cas9 editing with either approaches. We designed a third knock-out strategy instead, trying to induce a large deletion spanning from either exon II-IX or exon III-IX, therefore removing the secondary ATG present in exon VII (Figure 29c).

Furthermore this approach should have avoided alternative splice-junctions of non-excised exons, since all the sgRNA used target regions inside coding exons (unlike previously described loxP strategies targeting intronic regions).

Genome editing efficiency was assessed at DNA and protein level in E14 mESCs cells transfected with pairwise combination of sgRNA+Cas9 constructs. sgRNA 1 (targeting exon II) and sgRNA 3 (targeting exon IX) showed the highest editing efficiency at DNA level (about 30% deletion in the pool) (Figure 29c) and successfully decreased the amount of wild-type ß-catenin protein (94 KDa) assessed by western blot (Figure 29c) but once again resulted in the production of a 40 KDa truncated protein (different from the 48 KDa and 52 KDa truncated protein described in (Messerschmidt et al. 2016)).

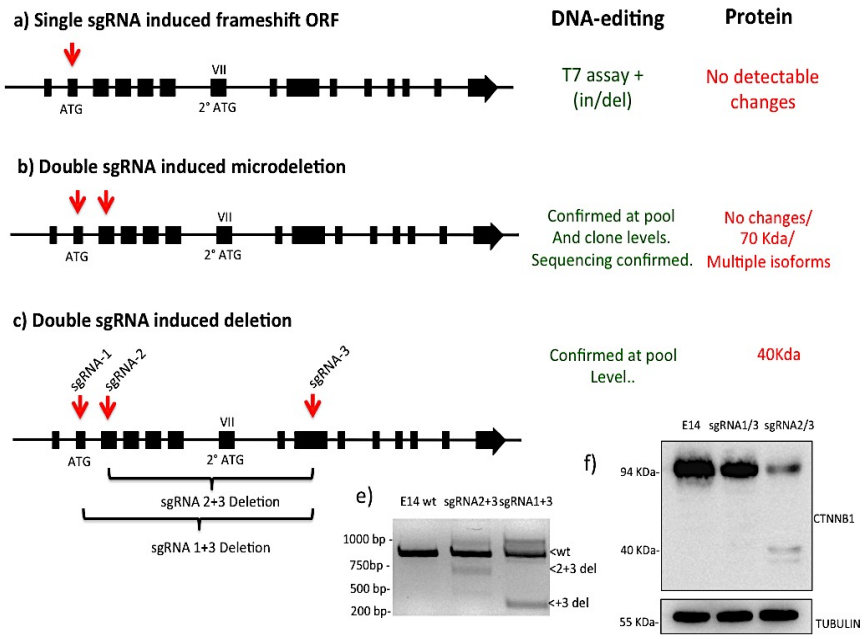

Figure 29 –CRISPR/Cas9-based ß-catenin knock-out results in the production of truncated isoforms. Exons are represented as black-boxes, red arrows indicate sgRNA target sites. a) A single sgRNA downstream the canonical ATG was used. The genome-editing efficiency at the target site was predicted through T7 assay in the whole cell population upon transfection and selection with px459-Cas9-Puro. No detectable changes in protein levels and molecular weight were detected through western-blot using a C-terminal ß-catenin antibody. b) Two sgRNA were used to induce a microdeletion between exon II and exon III, downstream the ATG. Homozygous clones for the microdeletion were isolated and sequenced. Western blot analysis revealed a variety of protein rearrangement (wt-like protein, 70 KDa protein, or multiple isoforms). c) Double sgRNA strategy to induce two different deletions (exon II-IX) or exon (III-IX). DNA editing efficiency of c) was evaluated through genomic DNA PCR e) and western blot on protein extracts f) (membrane was stripped and reprobed wit anti-TUBULIN as a loading control).

The latest approach provided more indirect information about the nature of ß-catenin truncated isoforms upon Ctnnb1 locus editing. In particular alternative splicing-junctions between exonII and the exons downstream the deletion are not possible in this approach (Figure 29c, the deletion encompass canonical splicing sites between exon II-III). The most

probable alternative is, as suggested from previous design strategies (Figure 29a and b), that truncated isoforms are produced from the uppermost ATG after the deletions (regardless the deletion type or length). More generally, if confirmed, this observation is particularly interesting for the current CRISPR/Cas9-based knock-out technology, suggesting that single sgRNA approaches, or induction of microdeletion, can result in the production of truncated isoforms rather than functional knock-outs and could be particularly misleading for those genes for which a complete and validated panel of antibodies is not available or for genes which are not expressed in the edited cell-lines (e.g. lineage marker genes in mESCs).

6.2 Whole ß-catenin deletion using CRISPR/Cas9

Given the experimentally frustrating outcomes of the CRISPR/Cas9 designs so far, we decided to completely delete Ctnnb1 coding region.
We therefore designed two additional sgRNAs, one targeting the intronic region upstream of exon II (sgRNA-4) and the other targeting exon XV (sgRNA-5) to be used in combination for a deletion of about 10 Kbp, removing all exons from II to XV (Figure 30a).
sgRNAs were sub-cloned into px459-Cas9-Puro and co-transfected in E14 mESCs. Cells were then selected with Puromycin for 72 hours. Pools were assayed for genome editing efficiency both at DNA and protein levels through PCR from genomic DNA and western blot on protein extracts respectively, revealing an average KO efficiency of about 50% with no detectable truncated proteins (data not shown).

Since no defects have been reported for cells only harbouring one copy of ß-catenin, we screened clones for the presence of homozygous deletion assayed by PCR on genomic DNA. Out of the screened clones,

Eß11, Eß15 and Eß47 displayed homozygous ß-catenin deletion at DNA level (Figure 30b).

Importantly western blot on protein extracts of Eß11, Eß15 and Eß47 using an anti C-terminal ß-catenin antibody confirmed the complete knock-out of the protein, with undetectable N-terminally truncated protein as expected (Figure 30c). The same result was confirmed through immunofluorescence using an anti C-terminal ß-catenin antibody and, unlike previous knock-out models (please see Figure 27f), no signal from possibly truncated isoforms was detected (Figure 30d).

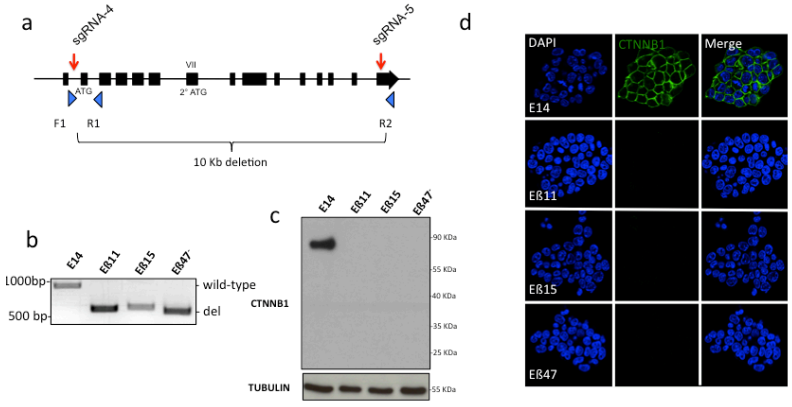

Figure 30- Complete ß-catenin knock-out using a double sgRNA approach. a) Schematic representation of the knock-out strategy: exons are represented by black boxes (not in scale), red arrows indicate sgRNAs target sites; blue triangles indicate primers and respective orientations used for PCR on genomic DNA. b) Genomic DNA PCR confirmed the deletion for Eß11, Eß15 and Eß47 clones. C) Western blot on total protein extract from Eß11, Eß15 and Eß47 clones and the parental cell line (E14) using an anti C-terminal ß-catenin antibody. Membrane was stripped and reprobed for Tubulin expression as loading control. d) Immunofluorescence on E14 parental cell line (top), Eß11, Eß15 and Eß47 using an anti C-terminal ß-catenin antibody (green channel).

In our hands whole-gene deletion proved to be much cleaner than previous designs in generating a complete protein knock-out. Importantly we deliver the first mouse embryonic stem cell lines (Eß11, Eß15 and Eß47) and a complete ß-catenin knock-out design strategy that can be easily adapted to other cell types.

Of note in the future a complete ß-catenin KO could also be obtained by establishing mESCs from C-terminal ß-catenin floxed mice recently produced by Messerschmidt et al. (Messerschmidt et al. 2016) upon CRE-mediated recombination.

6.3 ß-catenin knock-out cells do not exhibit major proliferation, cell-adhesion or pluripotency markers defects.

ß-catenin knock-out mESCs, hereafter named ßcatKO, displayed overall morphology comparable to wild-type cells as previously reported (Lyashenko et al. 2011, Wray et al. 2011) when plated at clonal density (see Figure 33c vehicle), however morphological defects (flat clones with dispersed cells, see Figure 33a vehicle) are evident when cells are seeded to obtain 40-50% confluence.

Also proliferation was not affected by ß-catenin depletion as Eß11, Eß15 and Eß47 displayed a normal proliferation rate (Figure 31a and b) doubling time of about 12 hours) and no significant difference in cell-cycle profile (Figure 31c).

ß-catenin interacts with E-cadherin and α-catenin at adherens junctions, contributing to mESCs dome-shaped colony morphology and tight cell-cell interaction. Absence of major morphological and cell-adhesion defects in ß-catenin knock-out models was attributed to γ-catenin

(plakoglobin) upregulation at protein level (Lyashenko et al. 2011, Wray et al. 2011).

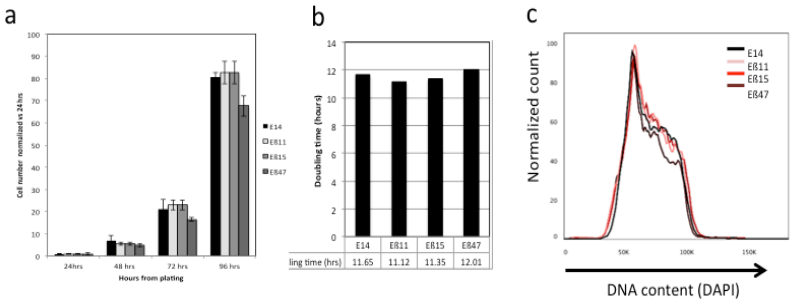

Figure 31 – ßcatenin KO cells display a normal cell cycle and proliferation rate. a) Growth curve over 4 days culture of E14, Eß11, Eß15 and Eß47. b) Doubling time derived from a) for wild-type and ßcatKO clones. c) Cell-cycle FACS profile on fixed cells. DAPI was used to stain DNA.

We therefore checked for cell-adhesion protein expression in Eß11, Eß15 and Eß47 ßcatKO clones. Plakoglobin was upregulated in all three clones as detected by immunofluorescence (Figure 32a) and western blot (Figure 32e), while no changes in protein levels or localization were detected for E-cadherin by immunofluorescence (Figure 32b) or extracellular E-cadherin staining assessed by FACS (Figure 32c), confirming previous findings that ß-catenin knock-out cell-adhesion defects are largely compensated by plakoglobin upregulation (Lyashenko et al. 2011, Wray et al. 2011).

Also, accordingly to previously published knock-out models, we did not detect any significant difference in Nanog and Oct4 protein levels under Serum+Lif culturing conditions with respect to the parental cell lines either by immunofluorescence (Figure 32d) or western blot (Figure 32e), confirming that, under Serum+Lif condition, ß-catenin it is not required for the core pluripotency network maintainance.

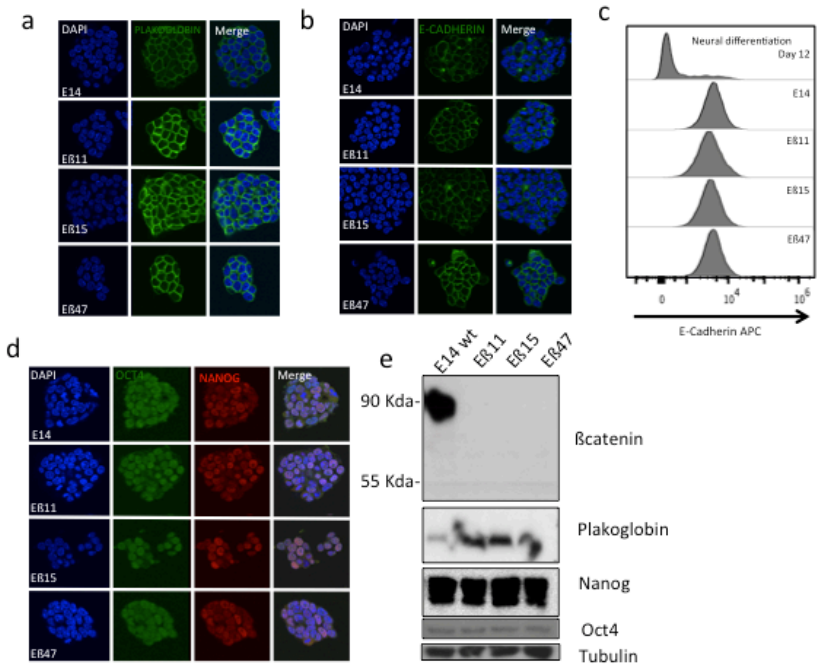

Figure 32 Plakoglobin compensates for ßcatenin absence in mESCs while pluripotency marker expression is unaffected under Serum+Lif condition. Immunofluorescence on E14 parental cell line (top), Eß11, Eß15 and Eß47 ßcatKO clones for plakoglobin (a) and E-cadherin (b). c) Extracellular staining of E-Cadherin on E14 cells during neuroectodermal differentiation day 12 (negative control), E14 Serum+Lif and Eß11, Eß15 and Eß47 ßcatKO clones. d) Immunofluorescence staining for Oct4 and Nanog in E14 parental cell lines Eß11, Eß15 and Eß47 ßcatKO clones. e) Western blot for ßcatenin (C-term antibody), Plakoglobin, Oct4 and Nanog on protein extracts of E14 parental cell lines Eß11, Eß15 and Eß47 ßcatKO clones. Tubulin was used as loading control.

6.4 ß-catenin knock-out cells do not respond to Gsk3 inhibition

As previously shown, Gsk3 inhibition enhances pluripotency of mESCs mainly through stabilization of ß-catenin (Wray et al. 2011). As a consequence of enhanced cell-cell interaction, mESCs acquires a round-shaped morphology when treated with Chiron 3 uM (a Gsk3 inhibitor) while, as expected, Gsk3 inhibition does not alter morphology of Eß11, Eß15 or Eß47 in which ß-catenin is absent (Figure 33a). Accordingly, parental cell lines strongly upregulates canonical Wnt targets such as *Axin2, Sp5* and *Cdx1* upon 72 hours Chiron 3uM treatment while Eß11, Eß15 and Eß47 did not show any significant canonical Wnt pathway activation (Figure 33b).

Interestingly Eß11, Eß15 and Eß47 showed lower AP intensity under serum+Lif condition with respect to the parental cell lines and while Chiron 3uM enhanced E14 AP staining in terms of intensity and homogeneity between clones, ßcatKO cells showed only a slight improvement (Figure 33c and d).

This weaker AP staining levels under Serum+Lif conditions (despite no changes in Nanog and Oct4 expression) could suggest that, as for cell adhesion defects, ß-catenin absence defects related to pluripotency (if any) could be compensated by still unknown mechanisms.

Transcriptional profile of Ctnnb1^{tm4Wbm} del/del cells was assessed by Lyashenko et al. (Lyashenko et al. 2011) through microarrays analysis revealing no differentially expressed genes with the exception of five genes (l7Rn6, H19, Rhox5 (up-regulated) and Trpv6, Daam1 (down-regulated)). However the ß-catenin KO cells used in Lyashenko et al. were female (therefore not directly comparable with E14 that we used which are male) and expressed the 48KDa N-terminally truncated ß-catenin isoform

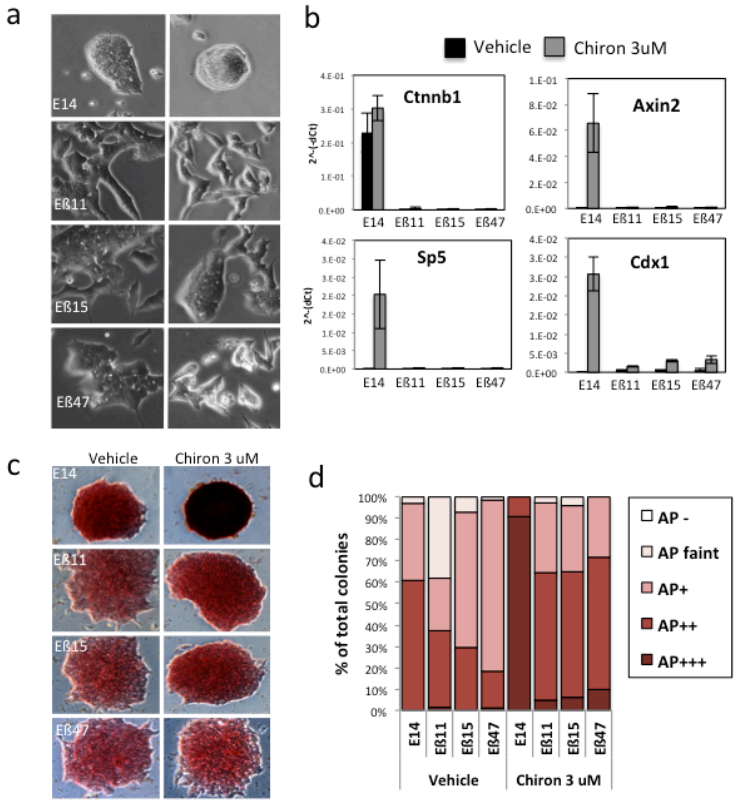

Figure 33 – Response to Gsk3 inhibition is impaired in ß-catenin KO clones. a) Phase contrast microscopy of parental and ßcaKO clones under serum+Lif condition, plated at 40-50 % confluence upon 72 hrs treatment with either vehicle (DMSO 0,3 ul/ml) or Chiron 3uM in Serum+Lif condition. b) qRT-PCR of parental and ßcatKO clones for the indicated markers upon 72 hrs treatment with either vehicle (DMSO 0,3 ul/ml) or Chiron 3uM in Serum+Lif condition. Alkaline phosphatase staining c) and quantification d) on E14, Eß11, Eß15 and Eß47 plated at clonal density (300 cells/well) and either vehicle (DMSO 0,3 ul/ml) or Chiron 3uM in Serum+Lif condition.

.

6.5 ß-catenin is indispensable for self-renewal of mESCs in serum-free media.

mESCs can be cultured in serum free media supplemented with Chiron (Gsk3 inhibitor), PD (MAPK inhibitor) and LIF (see pag. 53). While we confirmed that ß-catenin is not needed for self-renewal of mESCs under

Serum+Lif culture condition (Lyashenko et al. 2011, Wray et al. 2011) it has been reported that ß-catenin is indispensable for self-renewal and pluripotency maintenance of mESCs cultured in serum-free media.

In agreement with previous ß-catenin KO characterization (Wray et al. 2011) we found that ßcatKO clones showed impaired self-renewal under serum-free culturing media conditions. AP staining of cells seeded at clonal density showed morphology defects and a remarkable decrease of AP intensity in presence of PD+Lif, Chiron+Lif, PD+ Chiron without Lif , and 2iLif.

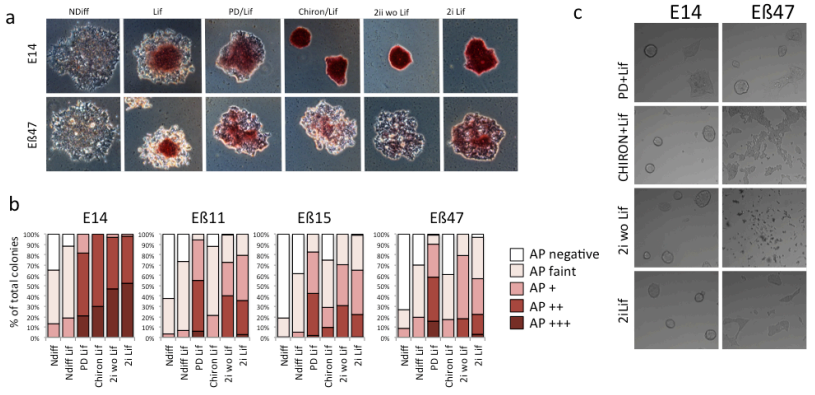

Figure 34 – a) AP staining of E14 parental cell lines and Eß47 ßcatKO clone in serum free culturing conditions. Cells were cultured in Serum+Lif and plated at clonal density (300 cells/well). 24 hours after plating Serum+Lif was replaced with indicated serum-free media and cells were cultured for additional 6 days before AP staining. b) Quantification of a). AP staining intensity categories are normalized on the total number of clones in each condition. c) Bright-field images of E14 parental cell line and Eß47 cultured for three passages in PD+Lif, Chiron+Lif, 2i without Lif and 2i+Lif.

In particular AP staining intensity strongly decreases with respect to wild-type cells, when ßcatKO were cultured in Chiron+Lif, once again indicating that Gsk3 inhibition enhancement of self-renewal is mainly mediated by ß-catenin (Figure 34a a-b). However, despite low AP staining intensity, ß-catKO cells can be expanded in 2iLif and PD+Lif. ßcatKO

can also be expanded under Chiron+Lif culturing condition although cells showed a different morphology. Finally, as previously reported (Lyashenko et al. 2011), self-renewal was severely impaired in ßcatKO cells cultured in 2i in absence of LIF in which colonies disaggregate and cells dies or exhibit a differentiation phenotype.

6.6 Rescue isoforms constructs

mESCs ßcatKO are defective in canonical Wnt signalling and show impaired self-renewal properties and an absolute requirement for Lif in serum-free culturing conditions. Importantly ΔN-isoforms, present but not characterized in previous knock-out models, are not sufficient to rescue these phenotypes (Lyashenko et al. 2011, Wray et al. 2011).

Since all three analysed clones for the assessed phenotypes are comparable, we chose to perform rescue experiments only with Eß47 ßcatKO clone. Rescue isoforms constructs have been generated de novo and subsequently sub-cloned into lentiviral vectors under the control of a constitutive EF1a promoter (pL-EF1a SV40-Puro, described in materials and methods), starting from a full-length ß-catenin cDNA cloned from total RNA of E14 wild-type cells.

We generated a ΔN-ßcatenin (putatively reproducing the N-terminally truncated isoform produced by the *Ctnnb1*^{tm4Kem} allele), a ΔC-ßcatenin (lacking the C-terminal transactivation domain and previously described in (Hsu et al. 1998)) and the wild-type ß-catenin (Figure 35a).

Eß47 clone was transduced with either empty vector (EV), ΔN-ßcatenin, ΔC-ßcatenin or wild-type ß-catenin and cells were selected for one week with Puromycin. Correct expression and localization of rescue-isoforms was assessed by co-immunofluorescence using either a N-terminal or C-terminal antibody against ß-catenin (Figure 35b).

As expected ΔN-ß-catenin was detected with an anti C-terminal antibody, ΔC-ß-catenin with the anti N-terminal and wild-type ß-catenin was detected with both.

Importantly ΔN-ßcatenin expression pattern (not detected at membrane level but distributed across cytoplasms and nuclei) was similar to ΔN-ßcatenin generated by CRE-mediated recombination of *Ctnnb1*^{tm4Kem} (Figure 27b), while ΔC-ßcatenin was mainly localized at the cell-membrane. Finally wild-type ß-catenin was correctly detected using both antibodies at cell-membrane with little or no cytoplasmic or nuclear signal as in the E14 parental cell-line (Figure 30b).

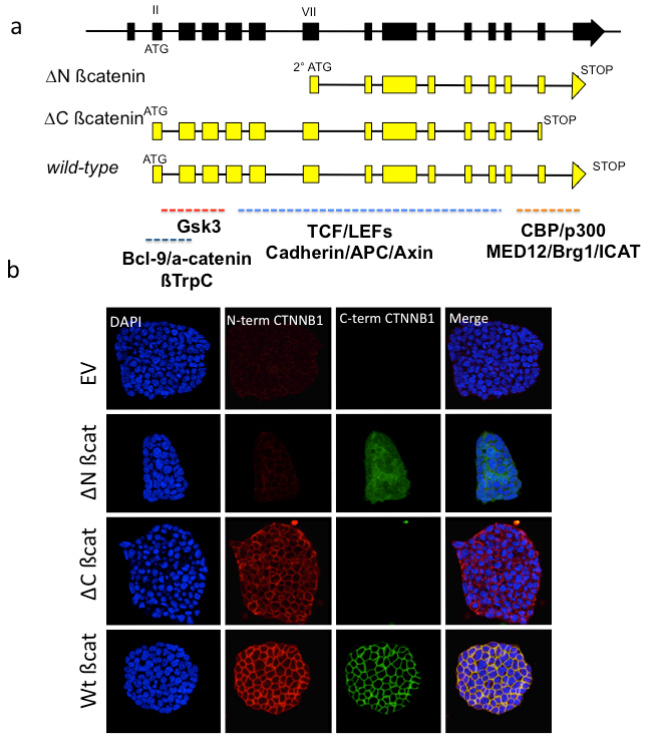

Figure 35 – a) Schematic representation of rescue isoforms cloned into pL-EF1a SV40 Puro (Yellow), introns are shown for clarity. b) Co-immunofluorescence with anti-N-term or anti-C-term ßcatenin antibodies on Eß47 cells transduced with either empty vector(EV), ΔN-ßcatenin, ΔC-ßcatenin or wild-type ß-catenin. Cells were selected with Puromycin for one week prior to immunofluorescence. Nuclei were counterstained with DAPI.

6.7 Self-renewal defects are rescued by either wild-type or ΔC-ßcatenin constructs.

Since Gsk3 inhibition only marginally ameliorates AP staining intensity of mESCs in absence of ß-catenin, we assess the potential of ΔN, ΔC or wild-type ß-catenin isoforms to rescue this phenotype.

To this purpose Eß47 transduced with either EV, ΔN, ΔC or wild-type ßcatenin were plated at clonal densitity and cultured in presence of DMSO 0,3 ul/ml or Chiron 3 uM for 6 days as carried out in the experiments included in (Figure 33c) .

EV or ΔN-ßcat transduced Eß47 cells did not show any significant change in AP-staining intensity with respect to un-transduced Eß47 cell lines, failing to recover the phenotype of parental E14 cultured in Chiron 3 uM (Figure 36a).

While either ΔC-ßcatenin or wild-type ßcatenin were equally able to restore AP staining intensity increase and morphological changes induced by Chiron 3 uM treatment to levels similar to the parental E14 cell line.

Similarly we reported that, although morphology of ßcatKO cells was overall unaffected when cells were plated at clonal density, major morphological defects could be observed when cells were plated at around 50% confluence (Figure 33a – Vehicle).

This phenotype was rescued by ΔC and wild-type ß-catenin but not by ΔN-ß-catenin isoform, confirming that previous knock-out models are comparable to a complete ß-catenin deletion with respect to morphology and self-renewal defects (Figure 36b).

We finally confirmed by qRT-PCR the canonical target genes *Axin2*, *Brachyury*, *Cdx1* and *Sp5*. As expected wild-type ß-catenin was fully able to activate canonical target genes although at levels much lower than the parental E14 line indicating that ß-catenin isoforms are not expressed at

endogenous levels comparable to wild-type cell lines, except for *Cdx1,* who was only slightly upregulated upon Eß47-EV basal level (Figure 36c).

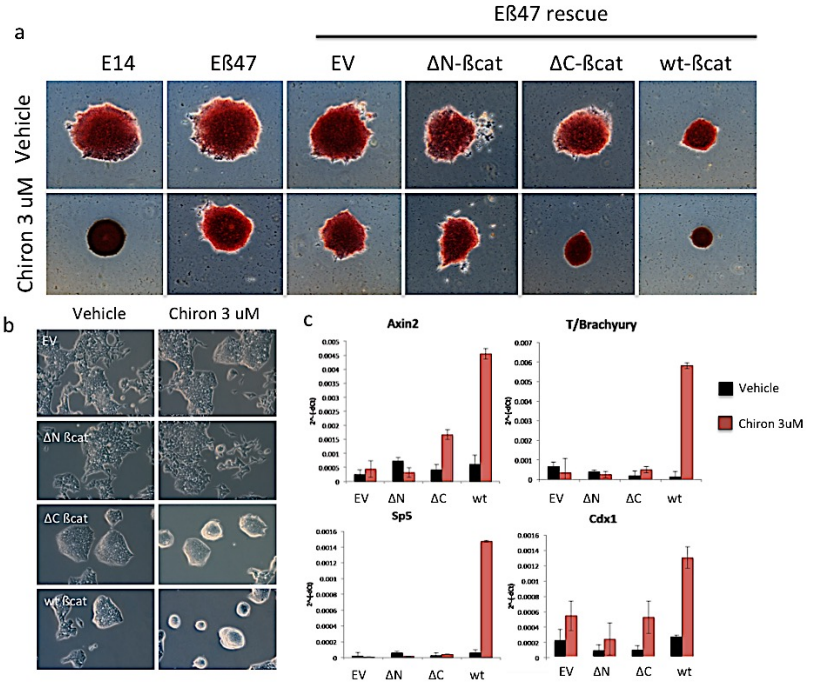

Figure 36 – ΔN-ßcatenin does not rescue ß-catenin KO for morphology defects and activation of canonical Wnt-target genes in response to Gsk3 inhibition. a) Alkaline phosphatase staining on E14 and Eß47 ßcat KO cells transduced with pL-EF1a SV40 Puro empty vector (EV) and ΔN, ΔC or wild-type ß-catenin. Cells were plated at clonal density (300 cells/well) and cultured for 6 days in presence of DMSO 0,3 ul/ml (Vehicle) or Chiron 3 uM. b) Eß47 transduced with EV, ΔN, ΔC or wild-type ßcatenin constructs and cultured for 72 hours with Vehicle or Chiron 3 uM. Cells were seeded at 40000 cells/well. c) qRT-PCR on canonical Wnt-targets in response to 72 hours Chiron 3 uM treatment in Eß47 cells transduced with EV, ΔN, ΔC or wild-type ßcatenin constructs.

ΔC-ßcatenin, although transcriptionally defective, showed residual activation canonical target genes *Axin2* and *Brachyury,* but not of *Sp5*. This could either indicate a residual transactivation activity or a Tcf3-

mediated de-repression of Wnt-targets as suggested by Wray et al .(Wray et al. 2011).

ΔN-ßcatenin however, as suggested by previous knock-out models expressing the truncated N-terminal isoforms, did not show any significant changes in canonical Wnt genes activation, essentially confirming previous findings (Lyashenko et al. 2011, Wray et al. 2011).

We then assess the capability of ß-catenin isoforms to rescue the self-renewal and AP staining defects of ßcatKO cells cultured in absence of serum. Eß47 transduced with with EV, ΔN, ΔC or wild-type ß-catenin were seeded at clonal density and cultured for one week in serum free media supplemented with combinations of PD, LIF and Chiron as in experiments included in (Figure 34a) then stained for alkaline phosphatase activity.

ΔN-ßcatenin transduced Eß47 cells did not show any significant difference in morphology and AP staining intensity in any of the culturing conditions, essentially proving to be not functional with respect to these phenotypes. On the contrary AP staining intensity and morphological defects of Eß47 ßcatKO cells was successfully achieved upon rescue with wild-type and ΔC-ßcatenin (Figure 37).

All together these results confirm that previous knock-out models, although incomplete, are functionally equivalent to a complete ß-catenin deletion with respect to the phenotypes analysed so far. Moreover, as previously found by other groups (Lyashenko et al. 2011, Wray et al. 2011), we confirm that wild-type and ΔC-ßcatenin isoform are functionally equivalent in rescuing morphological and self-renewal defects of ßcatKO cells.

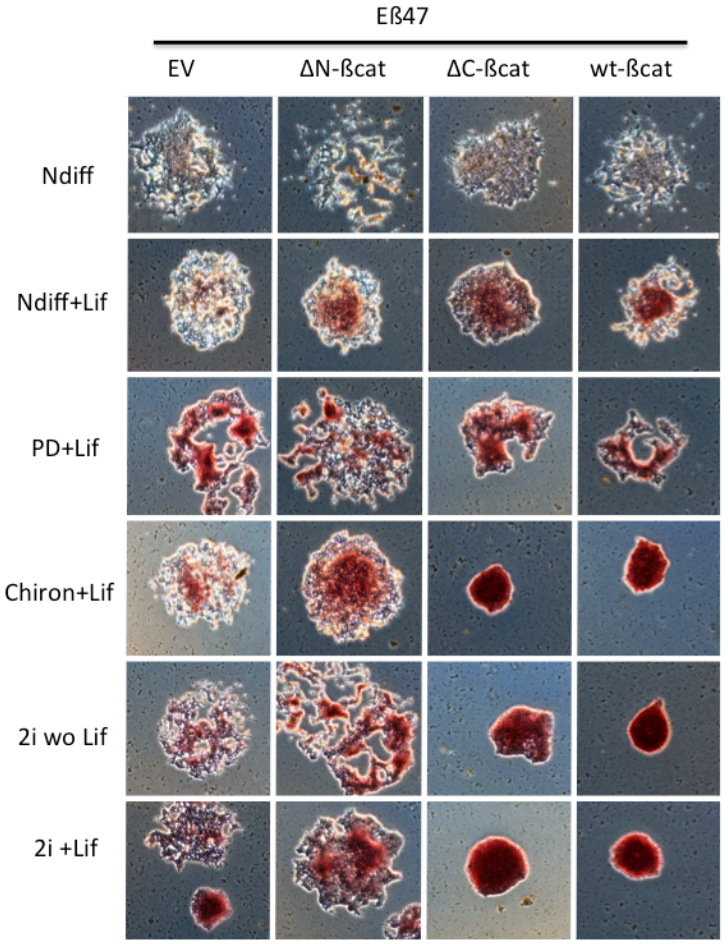

Figure 37 – AP staining of Eß47 ßcatKO cells transduced with empty vector (EV), ΔN, ΔC or wild-type ßcatenin constructs and cultured in serum free media with the indicated combinations of PD, Chiron and Lif. 2i wo Lif=PD+Chiron in absence of Lif. 2i+Lif =PD+Chiron+Lif. Cells were plated at clonal density (300 cells/well) and cultured in the indicated media for 6 days.

CHAPTER 7 – Prolonged culture of mouse embryonic stem cells in 2i/LIF medium promotes a lapsed ground state of pluripotency

The results presented in CHAPTER 7 are part of the submitted work:

"Prolonged culture of mouse embryonic stem cells in 2i/LIF medium promotes a lapsed ground state of pluripotency "

Elisa Pedone,[1,2,6] Francesco Aulicino,[1,2,6] Maria Aurelia Ricci,[1,2,3] Chris Douglas Robert Wyatt,[1,2] Melike Lakadamyali,[3] Manuel Irimia,[1,2] Lucia Marucci,[1,4,*,$], and Maria Pia Cosma[1,2,5,*,$]

1Centre for Genomic Regulation (CRG), The Barcelona Institute of Science and Technology, 08003 Barcelona, Spain
2Universitat Pompeu Fabra (UPF), Dr Aiguader 88, 08003 Barcelona, Spain
3ICFO-Institut de Ciencies Fotoniques, The Barcelona Institute of Science and Technology, 08860 Castelldefels (Barcelona), Spain
4Department of Engineering Mathematics, University of Bristol, Bristol BS8 1UB, UK
5ICREA, Pg. Lluís Companys 23, 08010 Barcelona, Spain
6Co-first author
$Co-last author
*Correspondence: lucia.marucci@bristol.ac.uk (L.M), pia.cosma@crg.es (M.P.C.)

7.1 Prolonged culture in 2i/Lif increases Nanog and Rex1 heterogeneity and promotes morphological changes.

To analyse the impact of prolonged 2i/LIF cultures on ground state pluripotency stability, we cultured wild-type mESCs (E14Tg2a) firstly in serum/LIF (henceforth called S mESCs), then in 2i/LIF up to 10 passages (henceforth called Low Passages (LP) mESCs) and for more than 13 passages (henceforth called High Passages (HP) mESCs). As previously reported (Chambers et al. 2007, Cahan et al. 2013), S mESCs showed heterogeneous protein levels of Nanog, which was either expressed at high or low levels from cell to cell, in correlation with β-catenin mosaic expression, consistently with our previous results (Marucci et al. 2014) (Figure 38a). Switch to 2i/LIF medium, LP clones acquired a rounded morphology and presented overall homogeneous expression of Nanog and nuclear accumulation of β-catenin (Figure 38b), characteristic of naïve pluripotency (Ying et al. 2008, Marks et al. 2012). Surprisingly, upon prolonged cultures, such features were impaired: HP mESCs showed mosaic Nanog expression patterns, cytoplasmic localisation of β-catenin, and flat morphology (Figure 38c). Remarkably, this phenotype could be reverted to a naïve-like one: HP mESCs cultured in serum/LIF (called HP/S mESCs) for 6-10 passages and then transferred back to 2i/LIF (called HP/S/2i mESCs, Figure 38d) for additional 6-10 passages re-acquired rounded morphology, homogenous expression of Nanog and nuclear accumulation of β-catenin, resembling LP ESCs (Figure 38e).

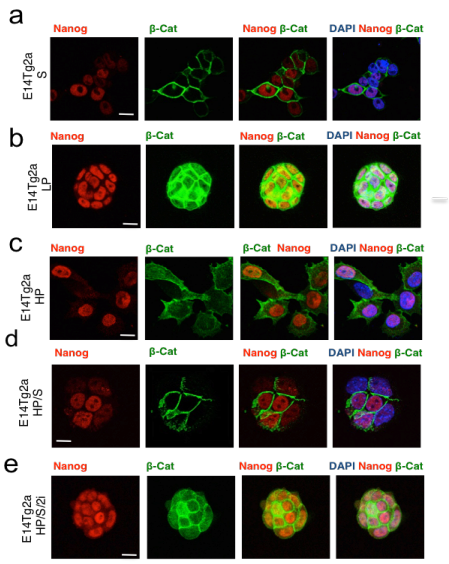

Figure 38 - (a-e) Immunofluorescences of β-catenin and Nanog in E14Tg2a cultured in Serum/LIF medium (a) or 2i/LIF medium for low (LP) (b) or high number of passages (HP) (c), HP switched to Serum/Lif (HP/S) (d) and HP/S switched again to 2i/Lif (e).

The switch between LP and HP state, and the rescued HP/S/2i phenotype were further confirmed using Rex1GFPd2 mESCs (Wray et al. 2011), in which GFPd2 is transcribed from the endogenous Rex1 promoter (Wang et al. 2006). As previously reported (Toyooka et al. 2008, Marks et al. 2012), in serum/LIF Rex1 expression was heterogeneous, with 60±6%, 9±1% and 31±5% cells showing high, medium and low GFP expression respectively, while LP and HP/S/2i cells were almost all GFP positive (Figure 39). Rex1 homogeneity was lost in HP cells, with mESCs showing a multistable Nanog, β-catenin and dGFP distribution, and flat morphology (Figure S1B-H). Interestingly, the peak of high and low GFP populations in HP were less separated than in S along the FITC-A axis (Figure 39), with a significantly higher percentage of cells expressing

medium GFP in HP (29±2.4%) than in S (9±1%), suggesting that HP cells have a pluripotency state different from S and LP mESCs.

All together these data indicate that prolonged culture of mESCs in 2i/LIF medium (HP cells) can induce an increase in Nanog and Rex1 heterogeneity and changes in the morphology of the clones, suggesting that mESCs can reach a novel state distinct from S and LP states, which we called "lapsed" ground state.

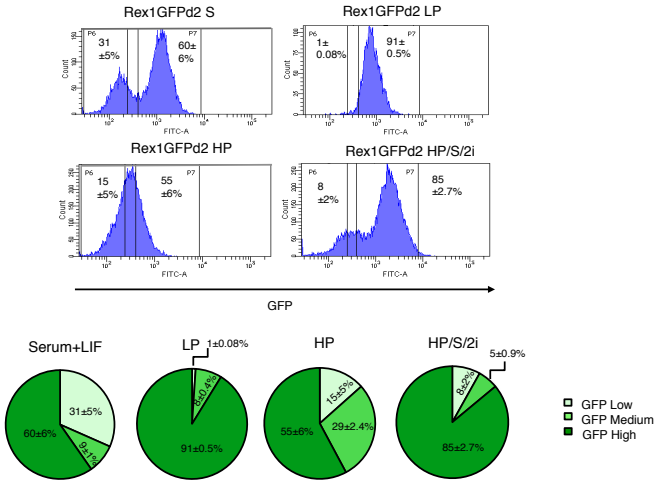

Figure 39 - GFP distribution and representative FACS profiles of S, LP, HP and HP/S/2i Rex1GFPd2 mESCs.

7.2 Prolonged culture in 2i/Lif promotes chromatin changes and differentiation potential biases.

These observations also suggest a loss of pluripotency in HP and HP/S mESCs; therefore, we investigated the structure of the chromatin fiber in mESCs cultured in the different conditions. We have recently reported that the chromatin fiber is formed by nucleosome clutches, which contain higher number of nucleosomes in mESCs cultured in serum/LIF versus 2i/LIF (Ricci et al. 2015). Low number and density of nucleosomes in

clutches is correlated with ground state pluripotency (Ricci et al. 2015). We therefore inspected chromatin fiber structure at nanoscale level in S, LP, HP and HP/S/2i mESCs using super resolution microscopy. Nucleosome numbers are directly related with the number of single molecule localizations ((Ricci et al. 2015) and Methods). We found that median number and density of localizations in the clutches of LP and HP/S/2i mESCs were lower than that found in HP mESCs, which instead had a median number of localizations, even higher than S mESCs, in both E14/TOP-dGFP (Figure 40) and Rex1GFPd2 mESCs (data noth shown). These data show that LP mESCs contain fewer nucleosomes per clutch and less dense clutches with respect to those of HP mESCs, indicating that LP mESCs have a higher pluripotency grade than HP mESCs.

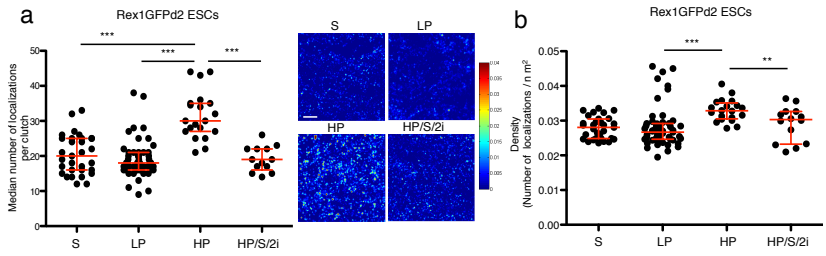

Figure 40 - (a) Dot plots showing the median number of H2B localizations per clutch in S (n=16), LP (n=44), HP (n=20) and HP/S/2i (n=18) E14Tg2a mESCs. (a, Inset) Density images showing regions of high (red) and low (blue) H2B density (number of H2B localizations per unit area) in S, LP, HP, and HP/S/2i E14Tg2a mESCs according to the color scale bar. (b) Dot plots showing the median density of H2B localizations per clutch in S (n=16), LP (n=44), HP (n=20) and HP/S/2i (n=18) E14Tg2a mESCs.

Due to the impaired pluripotency grade, we expected HP to show differentiation defects. We found that S mESCs, as previously reported (Marks et al. 2012), and HP mESCs were less prone to generate neural precursors (Sox1 expressing cells) than LP mESCs (Figure 41a). In

addition, when transferred into epiblast stem cell (EpiSC) culture conditions to investigate differentiation towards a primed pluripotency state (Guo et al. 2011), HP mESCs showed a faster increase of the EpiSC marker Fgf5 than S and LP mESCs (Figure 41b), suggesting a differentiation bias towards EpiSCs. .

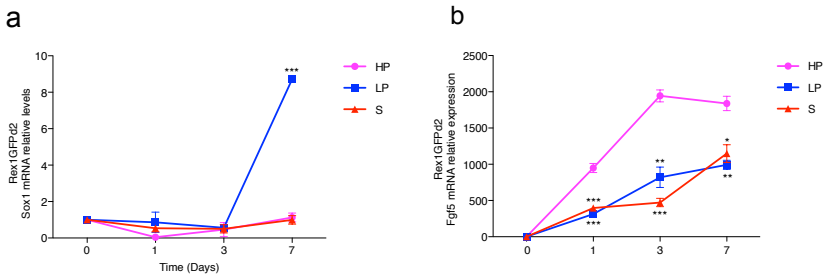

Figure 41 - (a) Monolayer neural differentiation of S, LP, HP and HP/S/2i E14Tg2a mESCs; Sox1 is measured by qPCR and plotted as fold change with respect to time zero. (b) Epiblast stem cells (EpiSC) differentiation of S, LP, HP and HP/S/2i E14Tg2a mESCs; Fgf5 is measured by qPCR and plotted as fold change with respect to time zero. Data are means ±SEM (n=4, G, H). p >0.1, *, p <0.05, **, p <0.01, ***, p <0.0001.

7.3 Transcriptome changes induced by prolonged 2i/Lif culture

To further characterize the molecular phenotype of mESCs cultured in the different conditions genome-wide, we analysed their transcriptome profiles by RNA-Seq. Unsupervised clustering (Figure 42a) showed that S and HP/S (which are both cultured in Serum/LIF) cluster together, while LP, HP/S/2i and HP (which are all cultured in 2i/LIF) form a distinct group. However, HP cells are notably different from LP and HP/S/2i cells, and appear separated in a Principal Component Analysis (PCA, Figure 42b). These data indicate that HP cells have a transcriptional signature that is different from both S and LP cells, while rescued conditions (HP/S and HP/S/2i) resemble S and LP states, respectively.

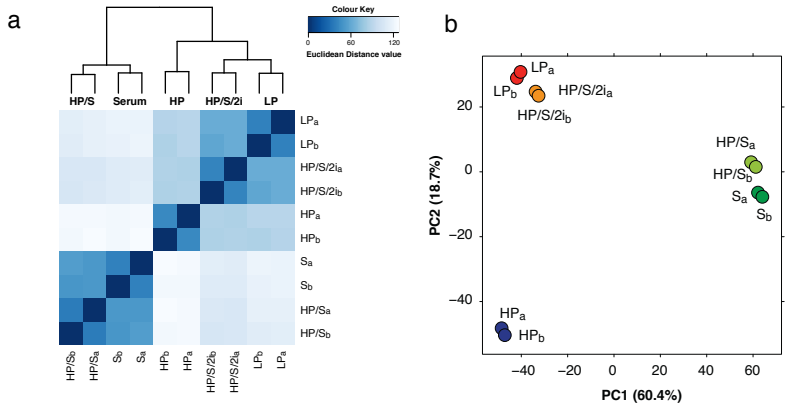

Figure 42 – (a) Heat-map and unsupervised hierarchical clustering of transcriptional profiles of E14Tg2a mESCs cultured in serum/LIF (S), 2i/LIF p<10 (LP), 2i/LIF p>13 (HP), HP cultured in serum (HP/S), HP rescued in 2i (HP/S/2i). (b) PCA of S, LP HP, HP/S and HP/S/2i samples, including replicates for each condition.

Consistent with these patterns, we found a high number of differentially expressed genes among the different conditions (Table 4; p value cut-off of 0.001, Fisher Exact test as implemented in EdgeR (Robinson et al. 2010). Interestingly, 1,944 genes were differentially expressed between HP and LP mESCs (fold change >1), 706 of which had a fold change >2, confirming that the transcriptional profile of HP mESCs is distinct from that of LP mESCs. In contrast, a lower number of genes changed comparing HP/S mESCs versus S mESCs or LP mESCs versus HP/S/2i mESCs (Figure 2B), suggesting that the naïve state (LP) and the serum state (S) could be, at least partially, rescued.

	Comparison					
	LP vs S	**HP vs LP**	**HP vs S**	**HP/S/2i vs S**	**HP/S vs S**	**HP/S/2i vs LP**
pval<0.001; FC>1	3277	1944	3421	2988	338	725
pval<0.001; FC>2	1594	706	1790	1483	103	211

Table 4 - Number of Differentially expressed genes in the different culture conditions (p value<0.001 and log2 fold change>1 or >2, as indicated).

Gene Ontology (GO) and KEGG pathway analyses of differentially expressed (DE) genes between LP and S mESCs (p value <0.001, fold change >1, Table 5 and Figure 43) produced similar results to those previously observed with RNA-sequencing data from short-term 2i/LIF cultures (Marks et al. 2012). Genes involved in development and metabolism-associated functions were significantly enriched in LP mESCs (see Table S1, Biological Process in all genes DE), confirming the different pluripotency phenotypes in the two media. Moreover, we found upregulation in S mESCs (Figure 43, LP<S) of focal adhesion and Rap1 signaling, consistent with the different morphology of mESC colonies cultured in serum/LIF (Price et al. 2004), and of the phosphatidylinositol 3-kinase (PI3K)/Akt signaling pathway, possibly due to the reported differences of the cell-cycle in 2i/LIF cultures (Marks et al. 2012, Kolodziejczyk et al. 2015), to which PI3K-Akt is coupled (Jirmanova et al. 2002). Genes belonging to the mitogen-activated protein kinase (MAPK) signalling pathway, which is associated with a cell state primed towards differentiation (Kunath et al. 2007), were also upregulated in S mESCs when compared to LP (Figure 43, LP<S), confirming previous observations (Marks et al. 2012). In contrast, metabolism-associated genes were increased in LP mESCs (Figure 43, LP>S) consistent with previous results (Marks et al. 2012). Interestingly, few metabolism-associated genes were also enriched in the HP vs S comparison (Figure 44, Table 6).

HP mESCs also included a substantial enrichment of specific signalling pathways associated to differentiation (Figure 44, Table 6), including the p53 signalling and other pathways associated to cancer, as well as the Hippo pathway, which were upregulated in HP compared to S (Figure 44, HP>S, Table 6). The differences between LP and HP mESCs became more evident when we compared DE genes between these two conditions (Figure 45, Table 7). Metabolism-associated genes were clearly downregulated in HP mESCs (Figure 45, HP<LP), while genes involved in differentiation and development were enriched among HP upregulated genes (Figure 45, HP>LP and Table 7), indicating that HP mESCs display a different state of pluripotency than LP. Interestingly, as in the HP vs S comparison, genes upregulated in HP (Figure 45, HP>LP) also showed enrichment for cancer-associated pathways and for genes involved in the Hippo pathway, a known regulator of stemness highly active in pluripotent epiblast cells and coupled to the Wnt/β-catenin, TGFβ, Notch and PI3K/Akt pathways (Mauviel et al. 2012). Indeed, Wnt pathway genes appeared significantly differentially expressed in HP compared to LP cells, as well as genes belonging to the TNF pathway, reported to be upregulated during mESC differentiation (Kim et al. 2008).

LP vs S

KEGG Pathway Terms	Count	PValue
Axon guidance	43	1,46E-08
Glutamatergic synapse	38	1,50E-07
PI3K-Akt signaling pathway	80	1,34E-06
Circadian entrainment	32	2,29E-06
Pathways in cancer	87	2,43E-06
ECM-receptor interaction	29	6,19E-06
Cholinergic synapse	34	7,66E-06
Focal adhesion	51	1,70E-05
Dilated cardiomyopathy	27	1,80E-05
Thyroid hormone synthesis	24	2,31E-05
Retrograde endocannabinoid signaling	30	2,53E-05
Leukocyte transendothelial migration	34	3,65E-05
Biological processes Terms	**Count**	**Pvalue**
single-organism developmental process	1084	9,43E-41
developmental process	1090	4,92E-40
anatomical structure development	997	3,54E-39
multicellular organismal development	950	1,00E-38
system development	854	2,37E-37
anatomical structure morphogenesis	575	2,28E-33
cellular developmental process	810	1,07E-31
cell differentiation	755	4,57E-28
regulation of multicellular organismal process	561	1,78E-25
regulation of developmental process	502	3,35E-24

Table 5 - Functional annotation analysis (KEGG pathway and top 10 significant biological processes) of the differentially expressed genes (p value<0.001, fold change>1) in the LP vs S comparison.

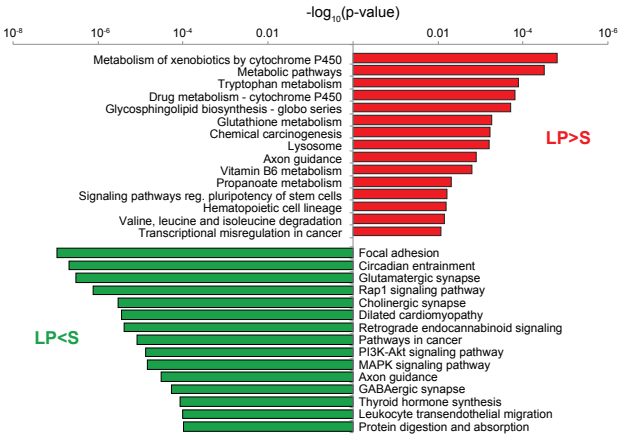

Figure 43 - Functional annotation analysis of the differentially expressed genes (adj p-value<0.001, fold change>1) between LP and S

HP vs S

KEGG Pathway Terms	Count	PValue
Axon guidance	44	1,19E-08
Glutamatergic synapse	39	1,09E-07
Signaling pathways regulating pluripotency of stem cells	44	1,09E-07
Pathways in cancer	90	1,40E-06
Ras signaling pathway	56	2,03E-05
Circadian entrainment	30	3,79E-05
Focal adhesion	51	4,09E-05
Glutathione metabolism	20	8,45E-05
Biological processes Termns	**Count**	**Pvalue**
single-organism developmental process	1118	7,11E-41
developmental process	1125	2,43E-40
anatomical structure development	1028	2,70E-39
anatomical structure morphogenesis	610	6,82E-39
cellular developmental process	853	2,51E-36
system development	867	4,08E-34
cell differentiation	798	6,65E-33
multicellular organismal development	954	1,48E-32
regulation of multicellular organismal process	577	2,42E-25

Table 6 - Functional annotation analysis (KEGG pathway and top 10 significant biological processes) of the differentially expressed genes (p value<0.001, fold change>1) in the HP vs S comparison.

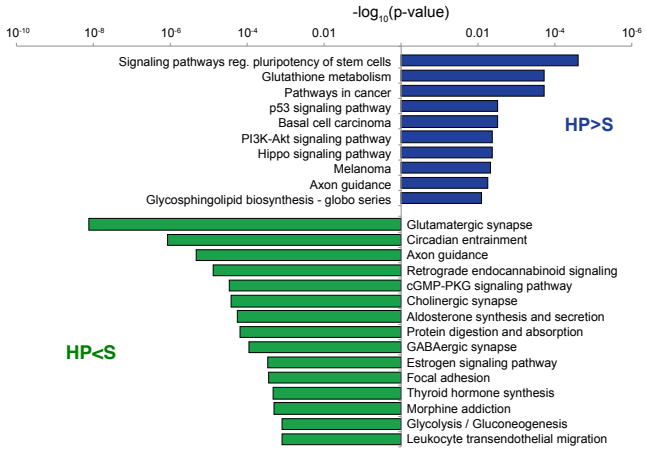

Figure 44 - Functional annotation analysis of the differentially expressed genes (adj p-value<0.001, fold change>1) between HP and S

HP vs LP - KEGG Pathway

KEGG Pathway Terms	Count	PValue
Proteoglycans in cancer	32	1,83E-04
TNF signaling pathway	21	2,27E-04
Wnt signaling pathway	24	4,93E-04
Focal adhesion	31	6,84E-04
Pathways in cancer	50	8,21E-04
Ras signaling pathway	33	8,71E-04
Glutathione metabolism	13	9,07E-04
PI3K-Akt signaling pathway	21	3,61E-03
Biological processes Terms	**Count**	**PValue**
single-organism developmental process	614	3,21E-17
developmental process	618	1,66E-16
anatomical structure development	564	3,33E-16
anatomical structure morphogenesis	323	1,76E-14
cellular developmental process	462	3,36E-14
cellular component morphogenesis	186	3,37E-14
multicellular organismal development	526	6,18E-14
movement of cell or subcellular component	218	2,03E-13
cell development	279	2,77E-13
system development	468	6,77E-13

Table 7 - Functional annotation analysis (KEGG pathway top 10 significant biological processes) of the differentially expressed genes (p value<0.001, fold change>1) in the HP vs LP comparison.

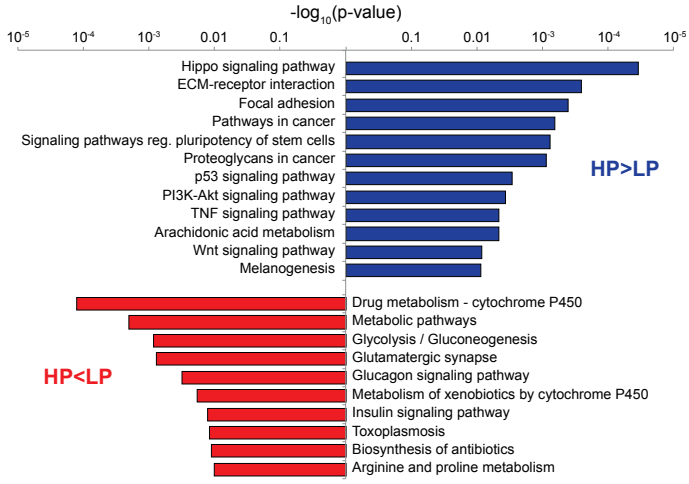

Figure 45 - Functional annotation analysis of the differentially expressed genes (adj p-value<0.001, fold change>1) between LP and S

7.4 Impairment of Wnt/ß-catenin activity

Given the enrichment for the Wnt pathway among DE genes in HP (Figure 45), the relevance of this pathway for pluripotency maintenance, somatic cell reprogramming and cell adhesion (Lluis et al. 2008, MacDonald et al. 2009, Wray et al. 2011, Ho et al. 2013, Aulicino et al. 2014, Marucci et al. 2014) and the fact that the Wnt pathway is activated by Chiron in 2i/LIF medium, we next investigated Wnt pathway activity in HP cells.

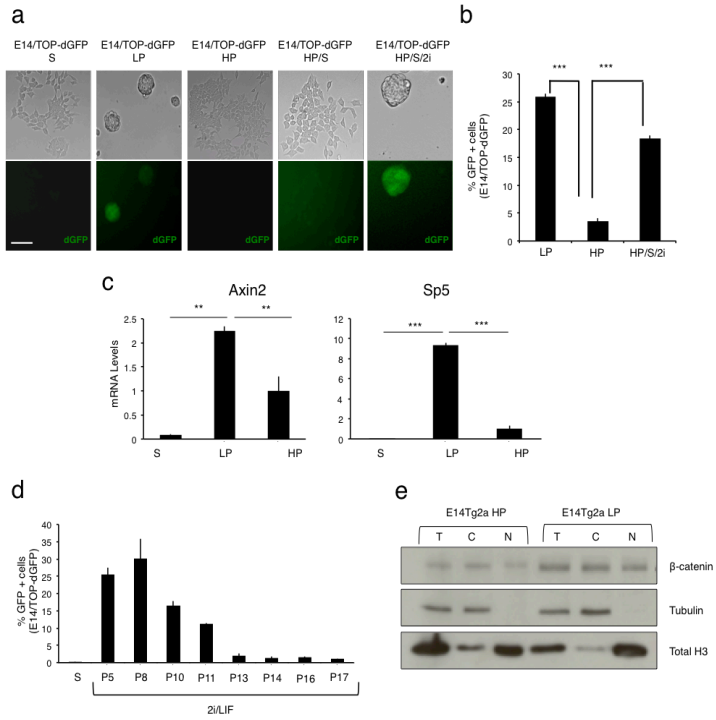

Figure 46 – (a) Microphotographs of S, LP, HP and HP/S/2i E14/TOP-dGFP mESCs. (b) percentage of GFP+ LP, HP and HP/S/2i E14/TOP-dGFP mESCs analysed by FACS; (c) qPCR of Wnt pathway targets (Axin2 and Sp5) in S, LP, and HP E14/TOP-dGFP mESCs; (d) Percentage of dGFP+ E14/TOP-dGFP grown in 2i/LIF analysed by FACS at the indicated passages. (F) Western blot of total β-Catenin in total, cytosolic and nuclear protein extracts from LP and HP E14Tg2a mESCs.

E14tg2a mESCs carrying a destabilised GFP (dGFP) under the control of a synthetic Wnt-responsive promoter (TOP-dGFP mESCs) (Biechele et al. 2008) showed activation of the reporter, and β-catenin target genes only in LP and HP/S/LP conditions (Figure 46a-d).

During passages, the initial GFP increase upon Chiron treatment (when passing from serum/LIF to 2i/LIF) was gradually lost, switching off from passage 10 onward in 2i/LIF (Figure 46d).

Consistently, β-catenin levels were higher in LP than in HP mESCs, both in the nuclear and cytosolic compartments (Figure 46e). These results confirm an association between ground state pluripotency stability and Wnt/β-catenin signalling function, whose misregulation might arise from feedback mechanisms triggered by continuous Gsk3 inhibition (Jho et al. 2002, Lustig et al. 2002, Niida et al. 2004, Rao et al. 2010).

7.5 Prolonged 2i/Lif culture promotes a lapsed ground state of pluripotency

Recently, it has been reported that the combined use of Gsk3 inhibitor and IWR1 – a tankyrase inhibitor that leads to β-catenin cytoplasmic retention with consequent impairment of its transcriptional functions – can maintain mouse Epiblast SCs (mEpiSCs) pluripotency (Kim et al. 2013). Given our observation of impaired β-catenin target gene activation in HP mESCs, we inquired whether these cells show transcriptomic similarities with mEpiSCs. Clustering analysis of our samples and 4 mEpiSC samples (Factor et al. 2014), based on the expression of the 100 genes most significantly differentially expressed in the LP vs HP comparison, showed that HP cells do not cluster together with mEpiSCs (Figure 47), indicating that they have a unique transcriptional profile, and are different from both ground and primed pluripotent cells. This observation is further supported by the distributions of relative expression values of the full set of DE

genes between HP and LP in the different culture conditions (Figure 48), including a nearly complete expression level rescue to LP in the HP/S/2i condition. Notably, HP/S/2i were more similar to LP than to HP (Figure 48), suggesting the partial rescue of the naïve state, however metabolism-associated genes were still higher in LP than in HP/S/2i (data not shown). Conversely, HP/S mESCs resulted comparable to the S mESCs since no enriched terms for HP/S > S or HP/S<S were found for $p<0.01$ (data not shown). Next, to further evaluate HP mESC distinct transcriptomic signature we performed Gene Set Enrichment Analysis (GSEA) (Subramanian et al. 2005) (Figure 49).

To identify genes that were specifically regulated in the HP condition, we compared HP to all the other samples (S, LP and the two rescued HP/S and HP/S/2i). Multiple genes appeared significantly varying in the HP condition (Figure 49a). For example, we found a positive enrichment for the p53 signalling pathway (NES= 1.65**,** N p value= 0.007**,** Figure 49b), consistent with the KEGG pathway results for HP>S and HP>LP (Figure 44, Figure 45, Table 6, Table 7). On the other hand, genes involved in "mismatch repair" were negatively enriched in HP cells (NES=-1.6, N p value=0.005), suggesting that the DNA repair machinery might be not fully functional in HP but partially rescued in the HP/S/2i condition (Figure 49c). Also in agreement with the KEGG pathway analysis, metabolism-associated genes showed a significant negative enrichment in HP cells versus all other conditions, with the Glycolysis and Gluconeogenesis pathway being the most significantly downregulated (Figure 49d, NES=-2, N p-value=0).

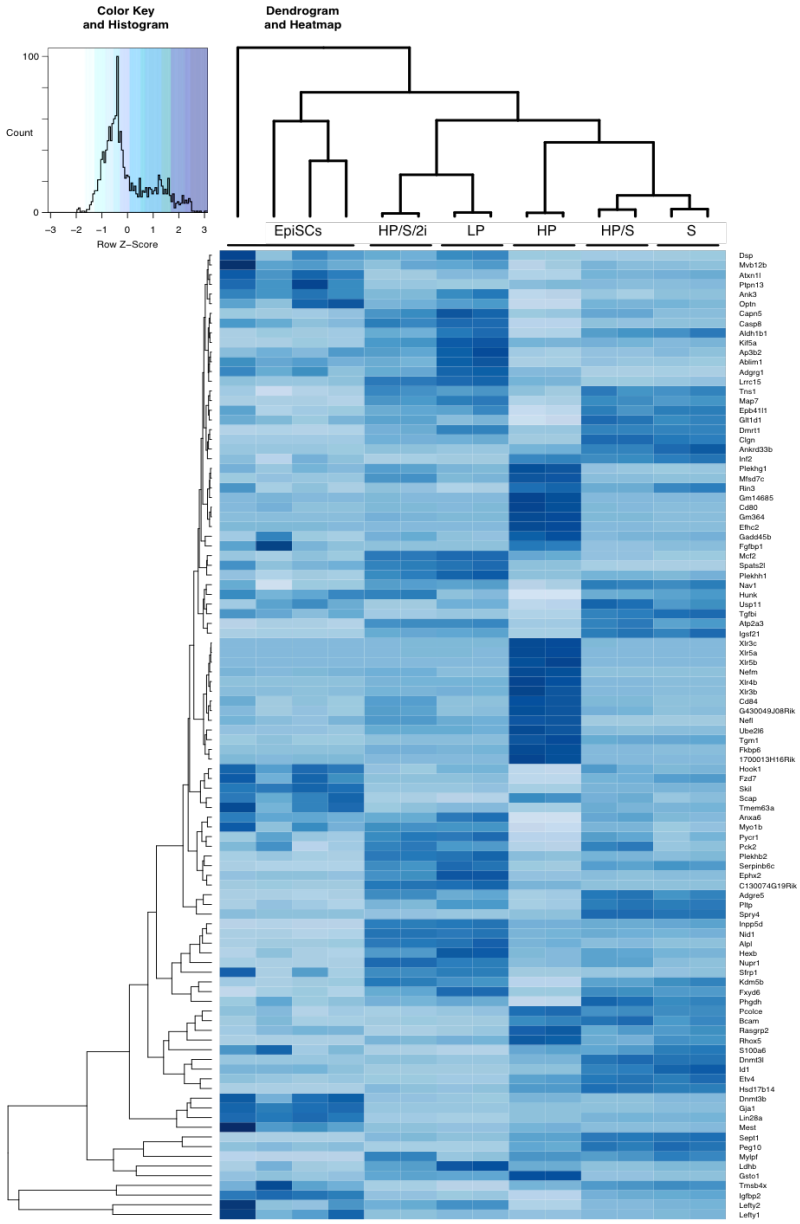

Figure 47 - Heat-map and hierarchical clustering of of S, LP, HP, HP/S, HP/S/2i mESCs, and EpiSCs, based on expression of the top 100 (ranked for minimal pvalue, fold change>1) DE genes between HP and LP.

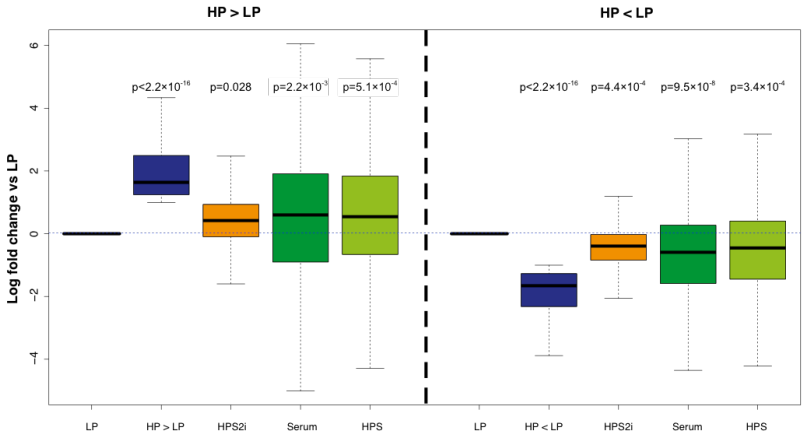

Figure 48 - Box plot showing distribution of the DE genes in HP vs LP (pvalue<0.001, fold change >1, HP>LP on the left, HP<LP on the right) in LP, HP, HP/S, HP/S/2i. Data are represented as log2 fold change vs LP and the p values were calculated using a wilcoxon test between conditions, corrected for multiple testing

Finally, we examined the expression of well-characterized pluripotency and lineage markers in HP cells compared to the other conditions. It has been reported that naïve mESCs, as compared to serum/LIF cultured cells, present, at population level, comparable expression of pluripotency genes, and reduced expression of lineage-associated markers, in particular mesoderm and ectoderm markers (Marks et al. 2012). We clustered the samples according to the expression of a comprehensive set of markers (Price et al. 2013) (Figure 50, log2 TPM plotted). While for pluripotency, mesoderm, primitive endoderm and trophoectoderm genes HP samples clustered with LP ones (Figure 50a-d, respectively), for both endoderm and ectoderm genes HP clustered separately from both S and LP mESCs (see clusters in Figure 50e and f), suggesting a bias of cells cultured for extended period in 2i/LIF towards the latter two lineages. As expected from the cluster analysis, genes such as *Gli3*, *Sp6* and *Gata3* (endoderm), and *Cdh1*, *Lefty1*, *Lefty2* and *Pax6* (ectoderm) were significantly

differentially expressed in HP versus LP (Figure 50e and f). Looking at pluripotency genes, *Sox2* showed a slight decrease in HP cells (Figure 50a). Interestingly, *Tcfcp2l1*, a key gene for the maintenance of self-renewal induced by all 2i/LIF components (LIF, CHIR, and PD) (Ye et al. 2013), was also slightly downregulated in HP mESCs (Figure 50a). This result suggests a possible impairment of the synergistic action of LIF, CHIR, and PD in maintaining naïve pluripotency in prolonged cultures in 2i/LIF medium.

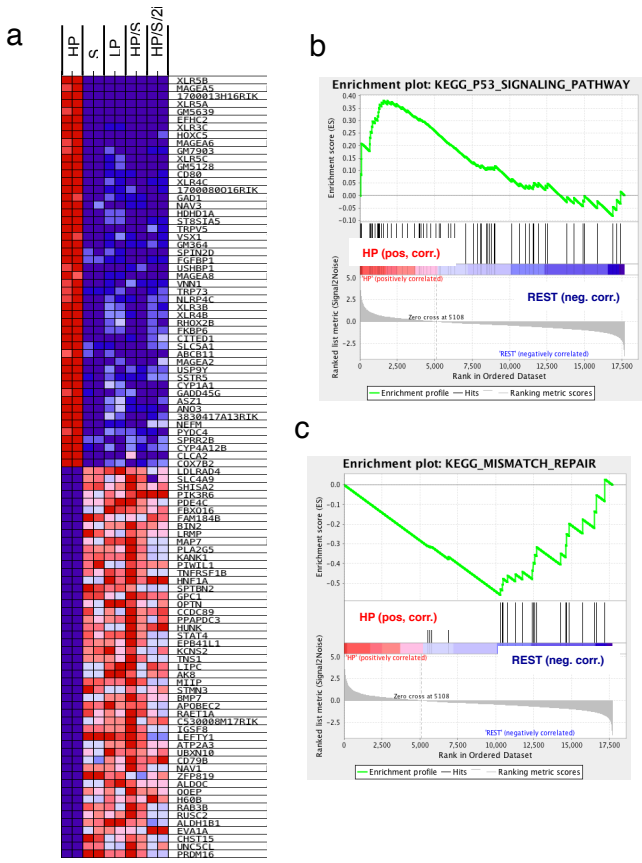

Figure 49 – (a) Heatmap representing the range of expression value of all genes uniquely enriched in the HP versus all other samples (S, LP, HP/S, HP/S/2i). (b-d) GSEA of genes uniquely enriched in HP culturing condition. GSEA plots of p53 signalling (b), mismatch repair (c) and glycolysis and gluconeogenesis (d) pathway enrichment in HP versus all other samples (indicated in the plots as "REST")

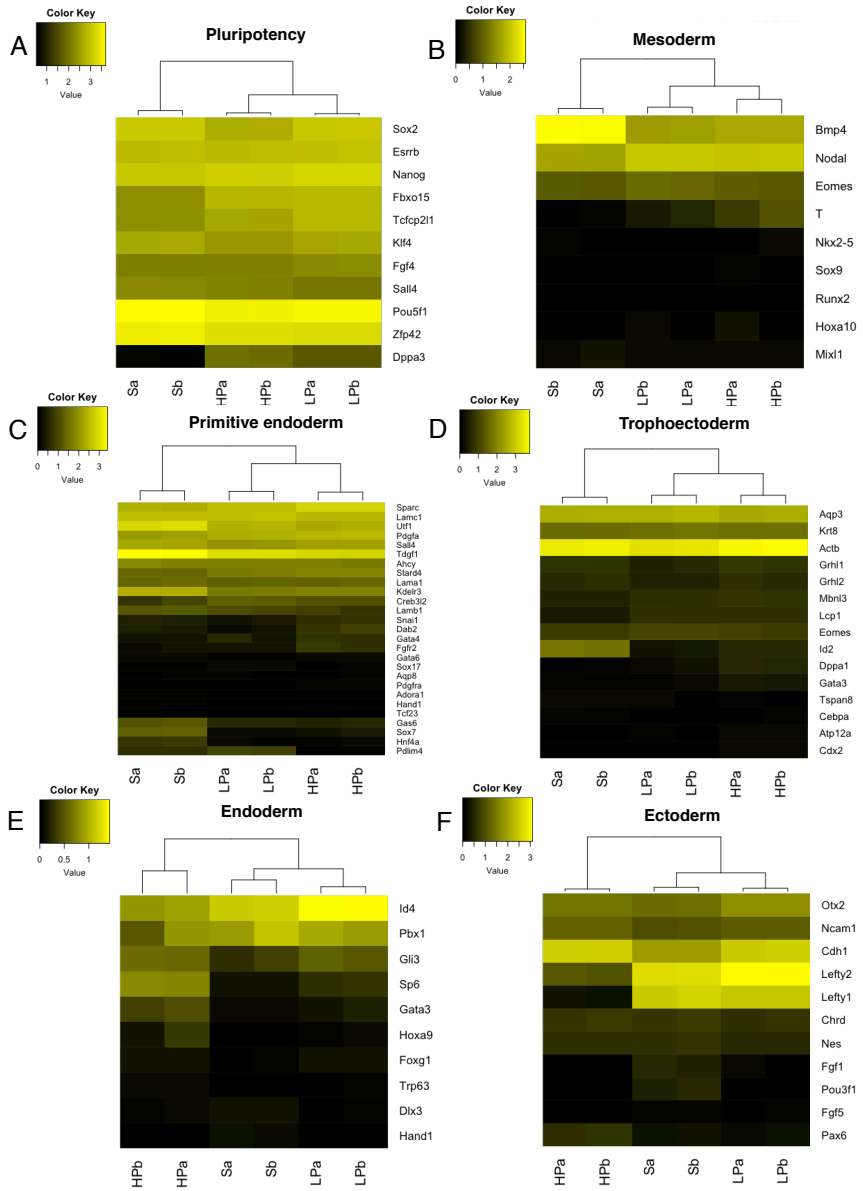

Figure 50 – (a-f) Heatmap showing log2 TPM of pluripotency (a), mesoderm (b), primitive endoderm (c), trophoectoderm (d), endoderm (e) and ectoderm (f) genes in S, LP and HP conditions (including replicates for each condition). Samples are clustered for gene expression in each set.

PART III – DISCUSSION

CHAPTER 8 – Temporal perturbation of the Wnt signalling pathway controls somatic cell reprogramming.

Wnt3a treatment can enhance somatic cell reprogramming of mouse embryonic fibroblast transduced with Oct4, Sox2 and Klf4 in absence of c-Myc (Marson et al. 2008).

Previous work from our lab demonstrated that activation of the Wnt/ß-catenin pathway in mESCs, enhances their capability to reprogram somatic cells upon cell-fusion (Lluis et al. 2008). Furthermore, Tcf3 depletion increases both cell-fusion mediated and direct reprogramming efficiencies by facilitating epigenetic barriers removal (Lluis et al. 2011).

Here we demonstrated that Wnt signalling is dynamically activated during somatic cell reprogramming in different cellular subpopulations. Wnt is not active at early stages and active at late stages in cells that are successfully undergoing reprogramming.

Similar conclusions, pointing out stage-specific requirements for Wnt/ß-catenin signalling and TCF/LEFs proteins during somatic cell reprogramming, have been drawn by Plath's group (Ho et al. 2013). Temporal perturbation of the Wnt pathway with either IWP2 or Wnt3a yielded similar results to our experiments, confirming a biphasic role for Wnt/ß-catenin pathway during reprogramming (Figure 51a-b). Of note, Ho and colleagues achieved knock-down of TCF/LEFs factors using siRNA transfection instead of constitutive viral vectors. This allowed the authors to efficiently test modular combination of TCF/LEFs factors depleted at specific time points and for a limited time due to the transient transfection.

The authors confirmed in the MEF cell population our results about Tcf1 temporal requirement, proving a partial overlap of Tcf1 and Lef1 functions (Figure 51c-d). Moreover, they extended their studies to other TCF/LEFs proteins, focusing on Tcf3 function in the regulation of reprogramming (Figure 51c-d).

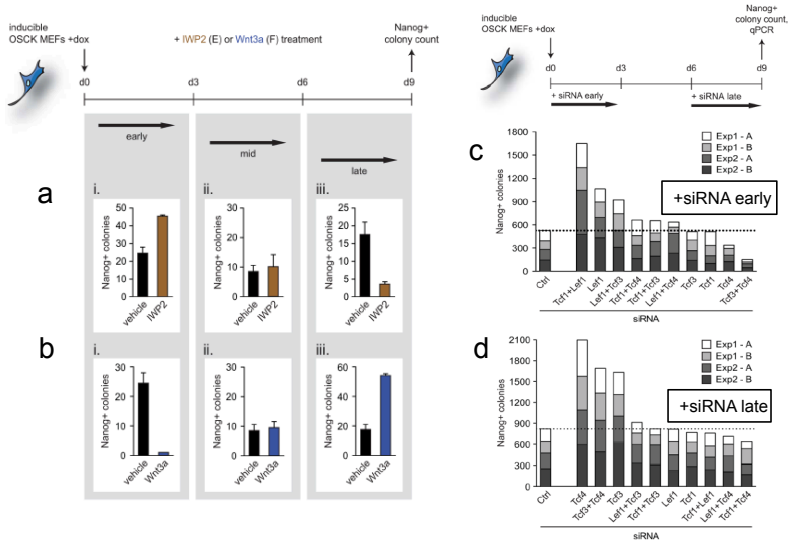

Figure 51 – Adapted from Ho et al. 2013. Nanog+ colonies obtained from MEF4F treated with IWP2 (a) or Wnt3a (b) at early, mid or late stage of reprogramming. c-d) Nanog+ colonies obtained from MEF4F transiently transfected with combination of siRNA against Tcf1, Lef1, Tcf3 or Tcf3 at early (c) or late (d) reprogramming stages.

Interestingly, from Ho et al. data it results that Tcf1 siRNA, either at early or late stages of the reprogramming process, significantly affects the reprogramming efficiency only when Lef1 is simultaneously down-regulated. It is possible, however, that Tcf1 transient down-regulation through siRNAs is not sufficient to trigger an efficient reprogramming phenotype. In contrast, the simultaneous siRNA of Lef1 (which in turns transcriptionally controls Tcf1) further downregulates Tcf1 levels.

The identification of the Wnt "OFF" state as an early reprogramming marker has several implications for iPSCs generation protocol

standardization. Reprogramming is a two step process characterised by an early "stochastic" phase followed by a more predictable "second-wave" with hierarchical activation genes crucial for successful reprogramming (Takahashi et al. 2016). However, further experimental perturbations can remarkably reduce or completely abrogate the stochastic phase, *de facto* leading to highly efficient, deterministic reprogramming (Rais et al. 2013, Di Stefano et al. 2014).

For OSKM-mediated reprogramming, early isolation and genome-wide characterization of Wnt-"OFF" cells could help clarify the sequential steps required to overcome the stochastic phase, providing clues to enhance iPSCs generation, and therefore extending previous findings (Polo et al. 2012, Zunder et al. 2015).

Many other signalling pathways have been suggested to regulate somatic cell reprogramming (for a detailed review please see (Hawkins et al. 2014)), whose activity can be efficiently regulated using small molecule activators/inhibitors. In particular, TGFß signalling pathway regulates EMT and it has been shown that its inhibition enhances somatic cell reprogramming by promoting MET and increasing Nanog expression (Maherali et al. 2009). It would be extremely interesting to investigate whether temporally controlled inhibition of TGFß signalling could further enhance iPSCs generation.

It remains difficult to date to extend our results to human somatic cell reprogramming where a homogeneous and efficient transgene delivery system cannot be established. However, it has been demonstrated in a OKS-reprogramming system that somatic cells from patients with a rare syndrome in which Wnts secretion is impaired cannot be reprogrammed back to pluripotency (Ross et al. 2014).

However, to date, it is unknown if temporal modulation of the Wnt pathway can be used to increase reprogramming efficiency of human somatic cells. If translated to human, temporal perturbation of Wnt/ß-

catenin signalling pathway could provide a mean to increase reprogramming efficiency. Such approach could be used to guide the cells stepwise into pluripotency helping them to overcome roadblocks such as cell-fate conversion and switch in cell-cycle (through Tcf1) and regulation of epigenetic markers (through Tcf3).

The role of Tcf1 in mESCs has been poorly characterized so far, although it has been demonstrated that, in medium lacking LIF, Tcf1 contributes to Wnt3a-mediated stimulation of pluripotency (Yi et al. 2011). We largely confirmed, by using different constitutive knockdown constructs, that Tcf1 depletion has no effect on pluripotency. In addition, we recently generated mESCs KO cell lines for Tcf1 with no defects in pluripotency maintainance (De Jaime-Soguero et al., unpublished data).

Here, we have demonstrated that Tcf1 is dispensable for pluripotency maintenance and differentiation potential of mESCs, while it is instead a regulator of the reprogramming process. Our results indicate that some transcription factors do not always control both somatic cell reprogramming and ESC self-renewal.

In addition to a temporally controlled role for Wnt/ß-catenin pathway during reprogramming, we have also characterized the activity of Tcf1 in $THY1^-$ cells. Here, in absence of nuclear ß-catenin, Tcf1 mainly acts as a repressor of the canonical Wnt pathway at the onset of the reprogramming process, by repressing mesenchymal genes and promoting MET transition. On the other hand, in THY^+ cells (characterized by a higher Wnt/ß-catenin activity and nuclear ß-catenin accumulation), Tcf1 acts as an activator on the same set of genes (Figure 52).

Of note, during the reprogramming process $THY1^+$ cells represent the majority of the total cell population, therefore the repressive activity of Tcf1 in the $THY1^-$ cells can only be studied by isolating them.

It is known that the Wnt/ß-catenin pathway plays a role in supporting epithelial-to-mesenchymal transition during development and embryoid bodies formation (ten Berge et al. 2008, Yao et al. 2011).

Here we showed that the role of Tcf1 during reprogramming is correlated with a repression of MET- and senescence-associated genes. Ho et al. (Ho et al. 2013) provided evidence that Tcf3 and Tcf4 effects at early reprogramming stage are mediated by their repressive role on Wnt/ß-catenin target genes, including Tcf1 and Lef1. However the authors speculated that Tcf3 and Tcf4 could trigger additional mechanisms.

Previous work from our lab showed that Tcf3 deletion increases AcH3 (Histone-3 acetylation) and decreases H3K9me3 (Histone-3 lysine-9 trimethylation), ultimately enhancing the reprogramming process by removing epigenetic barriers to the pluripotent state (Lluis et al. 2011). Tcf1 modulation instead affects somatic cell reprogramming efficiency by regulating distinct cellular processes (MET and senescence), suggesting that Tcf3 and Tcf1 act on distinct set of genes concurring to regulate different aspects of somatic cell transition to iPSCs.

MET transition during reprogramming has been extensively studied and it has been reported that Sox2, Oct4 and c-Myc are able to suppress Snai1 and TGFß-signalling whereas Klf4 has been shown to upregulate E-cadherin (Samavarchi-Tehrani et al. 2010). Here we found that Tcf1 is able to further regulate MET during reprogramming by repressing directly Vim, Slug and Snai1, which in turn represses E-cadherin expression as previously described (Batlle et al. 2000).

Somatic cell reprogramming is accompanied by profound changes in transcriptional profile, epigenetic landscape, cell-cycle shortening and other cellular processes. For mouse embryonic fibroblasts, down regulation of senescence genes and mesenchymal to epithelial transition must occur to obtain ES-like reprogrammed cells (Esteban et al. 2012, Mahmoudi et al. 2012).

In addition to MET genes, we found that Tcf1 also regulates senescence genes, contributing to two of the most important processes during the reprogramming of somatic cell to pluripotency. Proliferation and cell-cycle of terminally differentiated cells is tightly controlled, with a marked G1/S checkpoint regulated, among other proteins, by members of the INK/ARF family. On the other hand, mESCs show a fast doubling time (between 11-13 hours), apparently lacking a G1/S checkpoint and with little or no expression of cyclin-inhibitors such as $p16^{INK4a}$ or $p19^{ARF}$, similar to cancer cell lines. A short cell-cycle is thought to be a marker or pluripotency, as mESCs undergoing differentiation increase their doubling time and express INK/ARF proteins showing an higher percentage of cells blocked in G1 (Coronado et al. 2013, Pauklin et al. 2013).

Senescent or aged cells show instead a cell-cycle arrest due to $p16^{INK4a}$ induction. For this reason, amongst others, mouse embryonic fibroblasts can be reprogrammed back to pluripotency more efficiently than adult fibroblasts, and upon transduction with Yamanaka's factor, fast proliferating cells are more likely to be successfully reprogrammed (Roccio et al. 2013). Moreover mouse fibroblasts cannot be efficiently reprogrammed upon overexpression of $p19^{ARF}$ or $p16^{INK4a}$ due to their anti-proliferative effect, while p53 or p21 knock-down can accelerate reprogramming of both human and mouse fibroblasts (Li et al. 2009, Utikal et al. 2009).

Here we show that Tcf1 mediates a role in controlling senescence genes during reprogramming, mainly contributing to repress p21 and p19 in $THY1^{-}$ cells, hence indirectly promoting cell-cycle progression and proliferation in absence of nuclear ß-catenin.

Finally we cannot definitively conclude that Tcf1 role during reprogramming mainly acts through regulation of senescence associated genes or MET. Since the initial steps of reprogramming are rather noisy, it would be interesting to perturb Tcf1 levels during reprogramming and use

a single-cell sequencing approach to possibly identify additional targets of Tcf1 and fully elucidate the mechanisms through which it regulates this process.

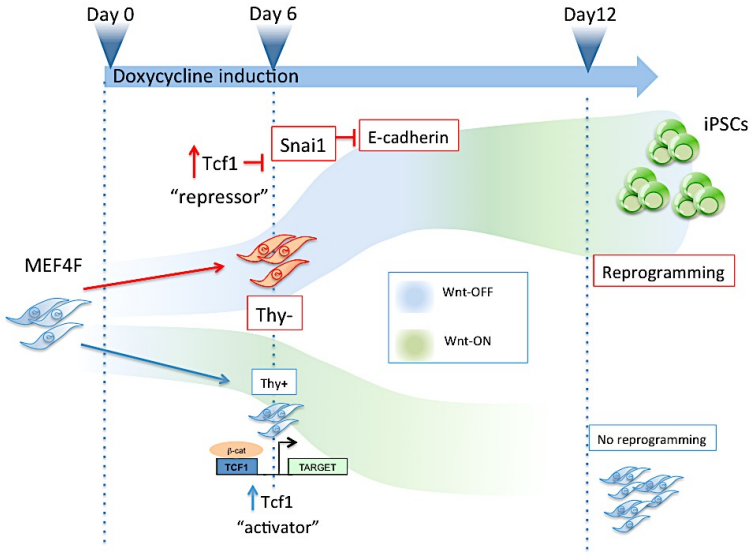

Figure 52 – Schematic representation of Tcf1 role during somatic cell reprogramming. Adapted from Aulicino et al. 2014. Tcf1 controls the expression of MET and senescence-associated genes in a ß-catenin dependent way. In THY1- cells undergoing reprogramming, Tcf1 behaves as a repressor, suppressing the expression of mesenchymal and senescence-associated genes and promoting MET. In THY1+ cells, Tcf1 behaves as a transcriptional activator of the same subset of genes lowering the reprogramming efficiency and favouring EMT and cell-cycle arrest.

Conclusions

- The Wnt-“OFF” is an early reprogramming marker.
- During early reprogramming phase, Tcf1 acts as a repressor of mesenchymal-to-epithelial and senescence-associated genes.
- Constitutive activation or inhibition of the Wnt pathway is detrimental for the reprogramming process.
- Temporal perturbation of the Wnt pathway enhances murine somatic cell reprogramming.

Future plans

- Evaluate the impact of temporal perturbation of additional signalling pathways involved in iPSCs generation.
- Extend our findings to human iPSCs generation

CHAPTER 9 – Characterization of a new ß-catenin knock-out model in mESCs

The role of Wnt/ß-catenin signalling pathway in mESCs has been extensively studied over the past years using either recombinant Wnt ligands or small-molecules activators/inhibitors of the Wnt pathway.

Activation of Wnt/ß-catenin signalling in mESCs has been reported to sinergistically acts with LIF to prevent differentiation and maintaining pluripotency (Hao et al. 2006, Ogawa et al. 2006).

Wnt ligands or active ß-catenin induction are unable to support self-renewal in absence of LIF, indicating an "helper" role for Wnt/ß-catenin pathway in supporting LIF signalling (Ogawa et al. 2006), while a small-molecule inhibitor of Gsk3 (BIO) has been reported to sustain mESCs also in absence of LIF on short term assays (Sato et al. 2004).

Although the main effect of Gsk3 inhibition in mESCs is mediated by Wnt/ß-catenin activation through ß-catenin stabilization, these findings may suggest that Gsk3 has additional functions in regulating pluripotency or, alternatively, that unknown side effects of Gsk3 inhibitor should be taken into account (Wray et al. 2012).

Genetic ablation of APC or Gsk3a/b, resulting in accumulation of unphoshorylated ß-catenin produced similar phenotypes, inhibiting differentiation and sustaining pluripotency (Kielman et al. 2002, Doble et al. 2007).

Furthermore deletion of Tcf3, a downstream nuclear interactor of ß-catenin mainly working as a transcriptional inhibitor, counteracts mESCs differentiation (Pereira et al. 2006, Cole et al. 2008, Wray et al. 2011), recapitulating the phenotypes observed so far.

All these evidences point for an important role of Wnt/ß-catenin activity in maintaining self-renewal and pluripotency of mESCs.

As previously discussed (Introduction pag. 56), depletion of ß-catenin in mESCs has been described by multiple labs, with different outcomes resulting either in EpiSC-like cells phenotypes (Anton et al. 2007) or unaffected self-renewal under Serum-Lif culturing conditions (Lyashenko et al. 2011, Wray et al. 2011, Wray et al. 2012, Raggioli et al. 2014). While opposite findings may as well arise from different pluripotency states of parental mESCs lines used in each experiment, to date ß-catenin requirments for mESCs self-renewal are still controversial.

Importantly, the best-characterized ß-catenin knock-out mESCs rely on conditional alleles knock-out that results in a partial loss of ß-catenin, generating N-terminally truncated proteins with unknown functions (Lyashenko et al. 2011, Wray et al. 2012, Raggioli et al. 2014).

Evidence for conditional ß-catenin alleles resulting in ΔN-ß-catenin expression has been provided previously in pre-implantation embryos (De Vries et al. 2004, Messerschmidt et al. 2016).

Here, we confirmed that N-terminally truncated ß-catenin isoforms can be detected also in mESCs and display altered subcellular localization with respect to wild-type isoforms. In principle, ΔN-ß-catenin isoforms could be responsible for the controversial findings about ß-catenin requirements in mESCs, possibly partially rescuing or interfering with wild-type ß-catenin loss.

In order to address the flaws in previous conditional ß-catenin knock-out models, we generated a complete knock-out of ß-catenin in mESCs using CRISPR/Cas9 technology.

We successfully achieved deletion of the ß-catenin locus (about 10 Kb deletion), by using a pairwise sgRNA strategy with complete CDS excision and no detectable expression of aberrant N-terminally truncated proteins.

Preliminary characterization experiments of newly generated ß-catenin knock-out cell lines (showed in Results pag. 95), however, showed no significant differences in pluripotency and self-renewal phenotypes with respect to previously characterized ß-catenin knock-out models.

Morphology and proliferation of ß-catenin knock-out cells is overall comparable to wild-type mESCs, except for subtle defects more evident cells reach confluence. As in previous knock-out models also complete ß-catenin loss is compensated through Plakoglobin upregulation.

So far our experiments indicate that ß-catenin is dispensable for mESCs self-renewal under Serum/Lif culturing conditions and that, in agreement with previous findings (Lyashenko et al. 2011, Wray et al. 2011), ß-catenin is instead required for mESCs under serum-free culturing conditions.

In short-term assays, ß-catenin knock-out cells showed impaired colony formation ability under serum-free conditions (the most severe of which being Chiron/Lif) but could ultimately not be propagated in 2i in absence of LIF, while self-renewal was possible in PD/Lif, 2i/Lif and Chiron/Lif (although with remarkable morphological defects in the latter).

ß-catenin loss completely abrogated canonical Wnt targets' (*Axin2*, *Sp5* and *Cdx1*) activation in response to Chiron treatment. Accordingly, also self-renewal enhancement in response to Gsk3 inhibition was impaired under Serum/Lif condition, demonstrating that Gsk3 inhibition mainly improves pluripotency through the Wnt/ß-catenin axis.

Nevertheless, a certain degree of AP staining enhancement was observed upon Gsk3 inhibition also in ß-catenin knock-out cells, suggesting that Gsk3 controls additional molecular mechanisms relevant for pluripotency maintenance.

Preliminary experiments with ß-catenin rescue isoforms confirm that ΔC-ß-catenin (transcriptionally incompetent) and wild-type ß-catenin are functionally equivalent in rescuing self-renewal and morphological

defects. On the other hand, ΔN-ß-catenin isoforms designed to mimic partial ß-catenin loss of previous knock-out models, fail to do so.

Taking into account these evidences, previous works concluded that TCF/LEFs functions is dispensable for mESCs pluripotency and self-renewal, however further experiments are required to exclude that, besides canonical Wnt targets which in some cases are weakly activated, ΔC-ß-catenin isoforms are truly transcriptionally silent.

With respect to previous knock-out models, however, we failed to identify any significant phenotype worsening as a consequence of complete, instead that partial, ß-catenin deletion. Preliminary experiments conducted so far, globally confirm the validity of previous ß-catenin knock-out models, suggesting that ΔN-ß-catenin isoforms are not functional with respect to self-renewal and pluripotency maintenance of mESCs.

However it has recently been proposed that ΔN-ß-catenin isoforms can partially compensate for ß-catenin loss defects in pre-implantation embryo development, suggesting that a certain degree of functionality is retained (Messerschmidt et al. 2016).

Besides the phenotypes characterised so far, it is therefore possible that also in mESCs, ΔN-ß-catenin isoforms could play a role in partially rescuing ß-catenin loss. Wnt/ß-catenin is basally active in the inner cell mass during embryo development and ß-catenin has been found to extensively bind to DNA of mESCs under Serum/Lif condition in co-operation or not with Tcf3.

Is therefore surprising how previous ß-catenin knock-out models, revealed no major transcriptomic changes upon ß-catenin loss and one possible explanation is the presence of ΔN-ß-catenin isoforms.

RNA-seq of the newly generated ß-catenin knock-out mESCs in basal Wnt/ß-catenin levels and under Chiron treatment will shed light on this point, providing more information about both TCF/LEFs independent ß-catenin functions and ß-catenin independent Gsk3 functions.

Conclusions

- Conditional knock-out alleles of ß-catenin produces N-terminally truncated isoforms in mESCs.

- CRISPR/Cas9 can be used for excision of large DNA fragments

- Plakoglobin compensates for membrane-associated defects upon ß-catenin loss.

- ß-catenin is required for mESCs self-renewal under serum-free conditions and ß-catenin knock-out cells strictly requires LIF.

Future plans

- Characterize the functions of N-terminally truncated isoforms.

- Evaluate the impact of ß-catenin loss at transcriptome level in presence or absence of Gsk3-inhibition.

CHAPTER 10 - Prolonged culture of mouse embryonic stem cells in 2i/LIF medium promotes a lapsed ground state of pluripotency.

The classification and derivation of different pluripotency states, ranging from naïve to primed, is particularly relevant, both for mouse and humans ESCs. However, ESCs may show a pluripotency spectrum in a dynamic, rather than discrete, fashion (Hackett et al. 2014, Weinberger et al. 2016), making qualitative classifications a difficult matter.

mESCs cultured in Serum/Lif media show an heterogenous expression of pluripotency genes and display metastable subpopulation with different characteristics touching diverse pluripotency states (ground state and primed cells) and a certain degree of spontaneous differentiation.

However, pluripotent sub-populations coexist under Serum/Lif culturing condition of mESCs, and interconvert over time. Heterogeneity in the expression of stem cell genes might be an important mESC feature for unbiased differentiation (MacArthur et al. 2012, Cahan et al. 2013), although this has been challenged (Martello et al. 2014).

Indeed, if heterogeneous gene expression is due only to culture conditions or it is an essential property of mESCs, is still not clear.

Culturing conditions highly influence pluripotency maintenance and the formulation of media aimed at enhancing and re-enforcing the core-pluripotency network is still under development.

2i/Lif medium is nowadays the golden standard for mESCs culturing as a principal substitute to more traditional media. 2i/Lif is a serum-free media containing two small-molecules inhibitors of ERK and Gsk3 kinases (PD and Chiron respectively) plus the Leukemia Inhibitory factor (Lif) (please see Introduction pag. 53 for a detailed description).

In contrast to Serum/Lif culture conditions, it has been reported that 2i/Lif supports homogeneity of pluripotency marker expression and counteracts differentiation stimuli, promoting uniform clone morphology and global DNA hypomethylation, ultimately enabling homogenous ground state pluripotency maintenance (Ying et al. 2008, Nichols et al. 2009, Marks et al. 2012, Leitch et al. 2013, Kumar et al. 2014, Singer et al. 2014). Moreover, it has been proposed that mESCs directly derived in 2i/Lif retain all essential features of naïve pluripotent pre-implantation epiblast cells as they first emerge in the embryo (Boroviak et al. 2014).

However, a certain level of transcriptional and functional heterogeneity has been reported also in short-term 2i/LIF cultures (Morgani et al. 2013, Abranches et al. 2014, Marucci et al. 2014); if gene expression homogeneity is beneficial for cultured mESCs, and to which extent can be maintained in 2i/Lif is currently not known. Furthermore, the majority of the experiments reported so far analyse only short-term cultures in 2i/Lif.

It has been showed that prolonged 2i/Lif cultures of mESCs results in chromosomal aberrations (Hassani et al. 2014), probably due to adverse effects of sustained Gsk3 inhibition through Chiron (Tighe et al. 2007).

Substitution of Chiron with SB431542 (a small-molecule inhibitor of TGFβ signalling) in the 2i/Lif formulation (renamed R2i) has been shown to overcome the emergence of chromosomal instability upon prolonged cultures (Hassani et al. 2014). However is not know if R2i outperforms 2i/Lif with respect to other phenotypes such as transcriptional profile, epigenetic status and differentiation potential of mESCs and more detailed studies are required to address these questions. On the other side, a detailed characterization of prolonged 2i/Lif cultures of mESCs is missing to date with respect to the mentioned phenotypes.

Here, we show that uniform expression of pluripotency genes and low number and density of nucleosomes in clutches, which correlate with ground state pluripotency, can be impaired in long-term 2i/LIF cultures.

Our results indicate that impairment of the Wnt/ß-catenin pathway could be associated with such a phenotype, which we termed ‘lapsed ground state’ as opposed to the naïve state. Of note, while inhibition of the MEK pathway is thought to reduce differentiation (Wray et al. 2010), it is not sufficient for clonal propagation of mESCs, which also requires the inhibition of the GSK3 and therefore activation of the Wnt signaling pathway (Ying et al. 2008, Wray et al. 2010, Wray et al. 2011, Dunn et al.).

The partial loss of the naïve state we observed in HP mESCs is accompanied by a decrease activity of Wnt/ß-catenin pathway (highlighted by gene-ontology analysis of RNA-seq data, reporter experiments and reduced target gene expression). Since Chiron, a Gsk3 inhibitor leading to Wnt/ß-catenin pathway activation, is constantly present in the 2i/Lif composition, it is possible that the observed impairment of Wnt signalling depends on the accumulation of Wnt pathway negative feedback loops.

We cannot definitively confirm if Wnt/ß-catenin impairment is the cause or is caused by the partial loss of the naïve state pluripotency; further work is required to fully elucidate the nature of the LP to HP transition.

Nevertheless, the influence of additional pathways, such the Hippo or p53 pathways, which we found to be differentially regulated in HP compared to LP mESCs, could be also responsible for the observed phenotype, including epigenetic, metabolism and cell-cycle related modifications due to prolonged exposure to chemical inhibitors and/or absence of serum.

Although we did not investigate the presence neither the nature of genomic aberrations in 2i/Lif cultures, we noticed a decrease of mismatch repair gene expression in the HP mESCs. However a partial rescue of the lapsed phenotype back into the naïve state can be reached, including major transcriptomic signatures and chromatin compaction status.

This suggests that stable genomic aberrations are not generated at least up to the number of passages we analysed, although it remains to be investigated whether further number of passages in 2i/Lif medium could lock the cells into an irreversible state. A detailed characterization is needed to understand to which extent aberrant chromosomal phenotypes, if any, can be rescued.

Finally, based on our results, it will be interesting to investigate long-term naïve state pluripotency maintenance in alternative media, such as a2i (in which ERK inhibition is substituted with inhibition of SRC tyrosine kinase (Shimizu et al. 2012)), 2i/LIF+PKCi (2i plus protein kinase C inhibitor (Dutta et al. 2011)) and R2i (containing PD and TGFβ inhibitor in spite of Chiron (Hassani et al. 2014)).

Such analysis might also help dissecting the relevance of cross-talks among different signaling pathways for ESC self-renewal and decision making.

Conclusions

- Prolonged culture of mESCs in 2i/Lif promotes a “lapsed” ground state of pluripotency.

- Lapsed ground state is characterized by heterogeneous expression of pluripotency markers and impairment of Wnt/ß-catenin activity, clones morphology and differentiation potential.

- At transcriptome level, lapsed ground state mESCs show impairment of metabolism and developmental genes, together with an altered expression of genes related to DNA-damage and repair.

- Lapsed ground state can be partially reverted to naïve ground state by switching mESCs to Serum/Lif and then to 2i/Lif again.

Future plans

- Evaluate the lapsed ground state mESCs in chimera formation assays.

- Identify the molecular mechanisms for the naïve-to-lapsed ground state switch.

- Characterize the pluripotency state of lapsed mESCs in alternative serum-free media.

Materials and methods

Cell culture

MEF isolation and culture

MEFs were established from E13.5 embryos from reprogrammable mice carrying two copies of the OKSM cassette and the ROSA26-M2rtTA allele (Carey et al. 2010). The embryos were isolated from the uterus and washed in phosphate-buffered saline (PBS). The head and viscera were removed, and the rest of the body was mechanically disaggregated and then incubated in 0.1% trypsin/ 0.1 mM EDTA solution for 30 min, to allow the cells to detach from the extracellular matrix and from each other. The cells were then mechanically disaggregated and plated onto a 15-cm tissue-culture dish and cultured in MEF culture medium: Dulbecco's modified Eagle's medium (DMEM) supplemented with 10% foetal bovine serum (FBS) 10 U/ml penicillin, 10 µg/ml streptomycin, 2 mM glutamine, 1 mM sodium pyruvate, and 1× non-essential amino acids. The MEFs were kept at 37 °C under 5% CO2. Wnt3a (100ng/ml) and Dkk1 (100ng/ml) were obtained from R&D systems; IWP2 (2µM) was from Stemgent and ICRT3 (25µM) was purchased from Calbiochem.

mESCs

Mouse ESCs (129/sv) were cultured on gelatin-coated plates in ESC medium: DMEM supplemented with 15% FBS (Hyclone), 1X non-essential amino acids, 1X GlutaMax, 1X penicillin/ streptomycin, 1X 2-mercaptoethanol and 1,000 U/ml LIF ESGRO (Chemicon). mESCs cultured in Serum+Lif medium were replated evey 3 days at a split ratio from 1:30 following dissociation with Trypsin 0.25% EDTA (Gibco) Accutase (Gibco).

For serum-free cultures, mESCs were cultured without feeders or serum in pre-formulated N2B27 medium (NDiff™ N2B27 base medium, Stem Cell Sciences Ltd, Cat. No. SCS-SF-NB-02) supplemented with Small molecule inhibitors PD0325901 (PD, 1 μM, Selleck) and CHIRON99021 (CH, 3 μM, Selleck) and 1000 U/ml LIF (ESGRO, Millipore). Cells were routinely propagated on 0.1% gelatin-coated plastic and replated every 3 days at a split ratio of 1 in 10 following dissociation with Accutase (Gibco) as previously reported (Wray et al. 2011).

HEK293t

Human embryonic kidney 293t (HEK293t) were purchased from ATCC (293T (ATCC® CRL-3216™) and cultured in DMEM supplemented with 10% FBS (Hyclone), 1X penicillin/ streptomycin. HEK293t were replated every 3 days at a split ratio of 1 in 6 following dissociation with Trypsin 0.25% EDTA (Gibco, Life technologies).

Embryoid bodies differentiation assay

The differentiation medium for the production of embryoid bodies (EBs) consisted of ESC culture medium without the LIF. The cells were harvested by trypsinisation, counted, and propagated in hanging drops (400 single ESCs/ 30 μl initial drop) for 2 days, before being transferred to 10 cm2 bacterial dishes. On day 5, the embryoid bodies were transferred onto gelatinised p100 dishes always in differentiation medium. For the iPSC differentiation the reprogrammed clones were detached from the feeder layer of MEFs and EBs were formed in ESC culture medium without LIF as described above. Furthermore, on day 5 the EBs were successively disaggregated and plated onto gelatin-coated dishes in ESC culture medium in absence of LIF, to allow them to differentiate into the three germ layers. For neural differentiation retinoic acid was added to the culture

Constructs

Short hairpin and sgRNAs

Short hairpins targeting ß-catenin (shß-cat1, 2 and 3), Tcf1 (shTcf1A, shTcf1B), p21 (shp21) and a short hairpin control (shScr) were cloned into the pLKO.1-Hygro lentiviral vector (Addgene plasmid #24150), following the manufacturer instructions. The oligonucleotides cloned into the pLKO vector were purchased from Sigma-Aldrich. A list of the sense oligonucleotides used to generate the short hairpins is given below (Table 9). For CRISPR/Cas9 experiments, sgRNA targeting different regions of ß-catenin locus were designed using E-CRISPR online tool (Heigwer et al. 2014). Oligos for sgRNA cloning were purchased from Sigma Aldrich. sgRNAs were sublconed using annealed oligonucleotides cloning (as previously reported for short-hairpin cloning) into px459-spCas9-Puro (Addgene # 48139) after digestion with BbsI restriction enzyme as previously described (Ran et al. 2013). A list of the sense oligonucleotides used to generate sgRNA containing vector is given in (Table 8).

sgRNA	Distance from ATG (base pairs)	Top oligo sequence (5'-3') Target sequence in bold
Ctnnb1.1	+309 (Exon 3)	**CACCGATGGAGTTGGACATGGCCA**
Ctnnb1.2	-9 (Intron 1|2 Exon2)	**CACCGGCGTGGACAATGGCTACTCA**
Ctnnb1.3	+5265 (Exon 9)	**CACCGTACGCACCGTCCTTCGTGC**
Ctnnb1.4	- 116 (Intron 1|2)	**CACCGTAGCAGAATCACGGTGACC**
Ctnnb1.5	+9572 (Exon 15)	**CACCGTCTGAACGTGCATTGTGAT**

Table 8 - List of top oligonucleotides used for cloning sgRNAs into px459-spCas9-Puro digested with BbsI. Sense target sequences are highlighted in bold

Short hairpin	ENSEMBL ID	Top oligo sequence (5'-3')
sh-ßcat1 (CDS)	ENSMUSG 00000006932	CCGG**TCTAACCTCACTTGCAATAAT**CTCGAGAT TATTGCAAGTGAGGTTAGATTTTT
sh-ßcat2 (CDS)	ENSMUSG 00000006932	CCGG**GCTGATATTGACGGGCAGTAT**CTCGAGAT ACTGCCCGTCAATA
sh-ßcat3 (3'UTR)	ENSMUSG 00000006932	CCGG**GGCGTTATCAAACCCTAGCCTT**CTCGAGA AGGCTAGGGTTTGA

sh-Tcf1A	**ENSMUSG 00000000782**	CCGG**GTTCACCCACCCATCCTTGAT**CTCGAGAT CAAGGATGGGTGGGTGAACTTTTT
sh-Tcf1B	**ENSMUSG 00000000782**	CCGG**AGAAGCCAGTCATCAAGAAAC**CTCGAGG TTTCTTGATGACTGGCTTCTTTTTT
sh-p21	**ENSMUSG 00000023067**	CCGG**TTAGGACTCAACCGTAATA**CTCGAGTATT ACGGTTGAGTCCTAATTTTTG
sh-Luciferase		CCGG**CGCTGAGTACTTCGAAATGTC**CTCGAGGA CATTTCGAAGTACTCAGCGTTTTTG
sh-Control		CCGG**GTCACGATAAGACAATGAT**CTCGAGATCA TTGTCTTATCGTGACTTTTT

Table 9 - List of top oligonucleotides used for cloning short-hairpins into pLKO-Hygro digested with AgeI/EcoRI. Sense target sequences is highlighted in bold.

pL-EF1a vectors

In order to generate lentiviral overexpression vectors, 7TGC and 7TGP reporter lentiviral plasmids (Addgene #24305; #24304, (Fuerer et al. 2010)) were repurposed for gene expression. Briefly eGFP was removed by enzymatic digestion and 7xWRE/CMV-minimal promoter were replaced by a constitutive EF1a promoter from p1494 vector (Luigi Naldini) followed by a multiple cloning site with a unique SmaI restriction site, suitable for blunt linearization and subsequent use for Gibson Assembly. eGFP was removed by 7TGP or 7TGC digestion with XbaI, plasmid was religated to generate 7TP or 7TG intermediate vectors. 7TP or 7TG were digested with SmaI to create promoterless lentiviral vectors and substituted with EF1a promoter through Gibson Assembly. SmaI 3' site was maintained for subsequent cloning of ß-catenin cDNA. Oligos for EF1a amplification and subcloning are provided below (Table 10).

Target	Template	Oligos (5'-3')
EF1a promoter	**p1494 EF1a vector**	**Forward:CGAGACTAGCCTCCTAGCCCCC AAGCTTTGCAAAGATG** **Reverse:CGACTCTAGATCTCGAGCCCCG CCGCGGTACCGTCGA**

Table 10 – Oligonucleotides for EF1a amplification.

ß-catenin isoforms generation and cloning

ß-catenin full-length cDNA was cloned from total RNA of E14 mESCs using Superscript III first-strand cDNA synthesis kit from Invitrogen. First strand synthesis was primed with oligo-dT and ß-catenin full-length was amplified with a 5' and a 3' oligos carrying 20-base pairs homology with the MCS of the TOPO-dENTR-MCS vector. TOPO-dENTR-MCS vectors was generated to facilitate Gibson Assembly cloning and subsequent cloning into multiple vectors through either Gateway cloning, Gibson Assembly or traditional cloning. Briefly TOPO-dENTR was digested with AscII and NotI, MCS was cloned using annealed oligonucleotides cloning. Full-length ß-catenin PCR was sequence-verified and subcloned into pL-EF1a digested with SmaI using Gibson Assembly kit from NEB.

ß-catenin isoforms (ΔN and ΔC) were generated by PCR using pL-EF1a ß-catenin as template with oligos carrying a 20-base pairs homology with the MCS of pL-EF1a. Finally ΔN and ΔC ß-catenin PCR were subcloned into pL-EF1a using Gibson Assembly. Oligos for ß-catenin isoforms cloning are provided below (Table 11).

Purpose	Target	Oligos sequences
TOPO-dENTR-MCS generation	-	Top:GGCCGCGGATCCCCCGGGGAATTCCTC GAGAAGCTTGTCGACGG Bottom:CGCGCCGTCGACAAGCTTCTCGAGGA ATTCCCCGGGGGATCCGC
ß-catenin full-length cDNA isolation from E14 cDNA.	Full-length ßcatenin (aa 1-781)	Forward:ATGGCTACTCAAGCTGACCTGATG Reverse:TTACAGGTCAGTATCAAACCAGGC
Subcloning into TOPO-dENTR	Full-length ß-catenin (aa 1-781)	Forward:CCGCGGATCCCCCGGGCCACATGGC TACTCAAGCTGACCT Reverse:CTTCTCGAGGAATTCCCCGGGTTACA GGTCAGTATCAAACC
Subcloning into TOPO-dENTR	ΔN-ßcatenin (aa 455-781)	Forward:CGCGGCCGCGGATCCCCCGGGCCA CATGAGGACCTACACTTATGA Reverse:CTTCTCGAGGAATTCCCCGGGTTACA GGTCAGTATCAAACC
Subcloning into TOPO-dENTR	ΔC-ßcatenin (aa 1-694)	Forward:CCGCGGATCCCCCGGGCCACATGGC TACTCAAGCTGACCT Reverse:GCTTCTCGAGGAATTCCCCGGGTTAA TCTGCAGTCTCATTCCAAG
Cloning of TOPO-dENTR inserts into pLEF1a	TOPO-dENTR inserts	Forward:ATCGACGGTACCGCGGGCCCTCCGC GGCCGCGGATCCCCC Reverse:GACTCTAGATCTCGAGCCCCAGCTTC TCGAGGAATTCCCC

Table 11 - Oligos used for generating ß-catenin isoforms overexpression vectors.

Additional constructs

pCMV-dR8.9 dvpr (Addgene #8455) and pCMV-VSV-G (Addgene #8454) were used as lentiviral packaging constructs. The FLTcf1 (p45 Tcf-B) and ΔN-Tcf1 (p54 Tcf-E) constructs were kindly provided by Hans Clevers (Van de Wetering et al, 1996). Tcf1 constructs were cloned together with the hygromycin-resistance cassette into p1494 lentiviral vectors that were kindly provided by Luigi Naldini. The 7TGP and 7TGC lentiviral reporter were purchased from Addgene (Addgene #24305; #24304) (Fuerer and Nusse, 2010).

Virus preparation, mESCs and MEFs transduction

For mESCs transduction, lentiviral particles were produced following the RNA interference Consortium (TRC) instructions for lentiviral particle production and infection in 6-well plates. Briefly 5 ×105 HEK293T cells/well were seeded in 6-well plates. The day after plating, the cells were co-transfected with 1 µg of lentiviral vector, 750 µg pCMV-dR8.9, and 250 µg pCMV-VSV-G, using Polyfect reagent (Qiagen). The day after transfection, the HEK293T culture medium was substituted with the ESC culture medium. Then 5 ×105 ESCs/well were plated onto gelatin-coated 6-well plates the day before transduction. The lentiviral-particles containing medium was harvested from HEK293T cells at 48, 72 and 96 h after transfection, filtered, and added to the ESC plates. The day after transduction, these ESCs were washed twice in PBS and hygromycin selection (50 µg/ml) was applied.

For MEFs transduction 5x106 HEK293T cells were seeded onto 10 cm plates and transfected with 10 ug pLKO-shTcf1A, pLKO-shTcf1B, or

pLKO-shScr, 6.5 ug pCMV-dR8.9 dvpr, and 3.5 ug pCMV-VSV-G packaging plasmids. After 48 and 72 hr, the supernatants were collected and centrifuged at 20,000 rpm for 1.5 hr at 20° C. The pellet with the viruses was resuspended in PBS (Life Technologies), aliquoted and stored at -80° C. For the reprogramming experiments, 2x105 MEFs were infected with either pLKO-shTcf1A, pLKO-shTcf1B, or pLKO-shScr in the MEF culture medium. After 48 hr, hygromycin selection (20 ug/ml) was applied for 3–4 days. For iPSC induction, the cells were then plated in equal numbers (5 3 104) onto gelatin-coated six-well plates in the ESC culture medium supplemented with 2 ug/ml of doxycycline.

Transient nucleofection of MEF cells

For a transient silencing of Tcf1 during reprogramming, 1x106 MEF cells were nucleofected with 10 ug of pLKO-shSCR or pLKO-shTcf1A using Amaxa reagent (Amaxa#VPD-1004) following manufacturer's instructions. After nucleofection, 1x105 cells were plated in a 35mm dish.

Alkaline phosphatase staining

Alkaline phosphatase is an enzyme expressed by ESCs and is used as a marker ofpluripotency. To evaluate the alkaline phosphatase expression, the cells were fixed in 10% Neutral Formalin Buffer for 15 min at 4°C, and washed three times with distilled water. These fixed cells were then incubated for 45 min at room temperature in 2ml of the staining solution prepared as follows: 0,005g Naphthol AS MX-PO4 (Sigma, N5000), 0,03g Red Violet LB salt (Sigma, F1625), 200 µl N,N-Dimethylformamide (DMF, Fischer Scientific, D1191), 25 ml of Tris-HCl (MW=157.6, pH 8.3, 0.2M), and 25 ml of distilled water. The alkaline-phosphatase-positive cells showed a red color and were visible under phase-contrast microscopy.

Flow cytometry and immunofluorescence

For analysis and/or sorting of intermediates, cells were trypsinised, washed once in PBS, and resuspended in PBS with 5% FBS. These harvested cells were incubated with antibodies against Thy1.2.2; 0.04 µg antibody per 1 ×106 cells (PE, eBioscience) for 20 min, washed twice in PBS plus 5% FBS, and sorted or analysed as indicated. Unstained cells were used as the negative staining control. For immunocytochemistry, the cells were fixed with 4% paraformaldehyde for 20 min at room temperature, and then washed twice with PBS. These fixed cells were then incubated in blocking solution containing 10% goat serum or 3% Bovine Serum Albumin (Sigma) and 0.1% Triton X-100 (Sigma) for 1 h at room temperature. The cells were then left overnight at 4 °C in blocking solution containing the primary antibody. The next day, the cells were washed three times with PBS and then incubated with the secondary antibody for 1 h at room temperature in PBS. The primary antibodies used are given in Table 14. Goat anti-mouse IgG, goat anti-rabbit IgG, (1:1000, Life Technologies) conjugated to Alexa Fluor-488 or Alexa Fluor-594 were used as secondary antibodies. Nuclear staining was performed with DAPI (Life Technologies).

Generation of ß-catenin KO mESCs

CRISPR/Cas9 technology was used to induce small in-dels, microdeletions or complete deletion of the Ctnnb1 locus using single sgRNA or pairwise combinations. Briefly for each experiment 5x10^6 mESCs (E14Tg2a from ATCC) per well were seeded onto gelatin-coated mw6 plates. 24 hours after seeding, 2 ml of fresh mESCs medium were provided at least 30 minutes before transfection. Transfection mix consisted of 5 ug of all-in-one vectors expressing Cas9 and previously subcloned sgRNA (px459-spCas9-Puro), 100 ul Optimem (Thermo-

Fisher) and 20 ul Polyfectamine reagent (Qiagen). For cotransfection of two sgRNA vectors 2.5 ug of each vector were used. Transfection mix was incubated 15 minutes at room temperature and then directly added to seeded mESCs. Fresh mESCs medium was added to a final volume of 2,7 ml and 24 hours after, medium was replaced. 48 hours after transfection Puromycin selection (5 ug/ml) was applied for additional 48 hours. Cells were then analysed at population level to assess the knock-out efficiency. For establishment of mESCs ßcatenin KO cell lines, transfected pools were replated at clonal density and single cell clones were manually picked and screened for homozygous Ctnnb1 deletion. For PCR assay of Ctnnb1 two or three oligonucleotides were used depending on the deletion strategy. Knock-out and screening strategies are summarised in Table 12.

Combination	Deletion	PCR assay:
Ctnnb1.1 + Ctnnb1.2	**218 bp**	**Forward:**GAATCACGGTGACCTGGGTT **Reverse:**GACCCTCTGAGCCCTAGTCA **Wild-type product: 824 bp** **Deletion product: 606 bp**
Ctnnb1.1 + Ctnnb1.3	**4970 bp**	**Forward 1:** GAATCACGGTGACCTGGGTT **Reverse 1:** GACCCTCTGAGCCCTAGTCA **Reverse 2:**CAGTTCACCTTTATCAGAGGCCAG **Wild-type product: F1+R1 -> 824 bp** **Deletion product: F1+R2 -> 595 bp*** ***Wild-type product of F1+R2 is 5565 bp, not amplified thanks to reduced extension timing.**
Ctnnb1.2 + Ctnnb1.3	**5287 bp**	**Forward 1:** GAATCACGGTGACCTGGGTT **Reverse 1:** GACCCTCTGAGCCCTAGTCA **Reverse 2:** CAGTTCACCTTTATCAGAGGCCAG **Wild-type product: F1+R1 -> 824 bp** **Deletion product: F1+R2 -> 278 bp** ***Wild-type product of F1+R2 is 5565 bp, not amplified thanks to reduced extension timing.**
Ctnnb1.4 + Ctnnb1.5	**9701 bp**	**Forward 1:** CACCGTATGCCTACAATCTGTTTCTA **Reverse 1:** GACCCTCTGAGCCCTAGTCA **Reverse 2:** CTACACAATGTTACACGTCTCCAGAT **Wild-type product: F1+R1-> 951 bp** **Deletion product: F1+R2 -> 551** ***Wild-type product of F1+R2 is 10252 bp, not amplified thanks to reduced extension timing.**

Table 12- Summary of CRISRP/Cas9 strategies and pairwise combination of sgRNAs used. For each strategy a list of the PCR primers used for genotype analysis. The expected amplicon sizes is given bp=base pairs.

RNA extraction and quantitative PCR detection of mRNA

RNA was extracted and purified using RNAeasy kits (QIAGEN) (For experiments in CHAPTER 5) or with Maxwell LEV semi-automated RNA extraction kit (Promega) (for experiments in CHAPTER 6), according to the manufacturer instructions. Total RNA was treated with DNAse I (Qiagen) to prevent DNA contamination. The cDNA was produced with SuperScript III Reverse Transcriptase kits (Life Technologies) starting from 1 µg mRNA (for experiments in CHAPTER 5) or with iScript cDNA synthesis kit (BioRad) (for experiments in CHAPTER 6). Real-time quantitative PCR reactions from 8,3 ng of cDNA were set up in triplicate using a LightCycler DNA SYBR Green I Master PCR machine (Roche). For oligos sequences see Table 13.

Target	Forward (5'-3')	Reverse (5'-3')
Axin2	GAGAGTGAGCGGCAGAGC	CGGCTGACTCGTTCTCCT
Brachyury	TGCAGATTGTCTTTGGCTACTTTG	CTCTAATGTCCTCCCTTGTTGCC
Cdh1	AACAACTGCATGAAGGCGGGAATC	CCTGTGCAGCTGGCTCAAATCAAA
Cdkn1a	CGCAGGAGCTGGTATCTTTC	CCTTGAGGCTCAGCTCATCTA
Ctnnb1	CGACACTGCATAATCTCCTGCTCC	GGTCCACCACTGGCCAGAATGAT
Cyclin D1	GAGATTGTGCCATCCATGC	CTCCTCTTCGCACTTCTGCT
Dppa3	GATGCAACGATCCAGATTT	TGGAAATTAGAACGTACATACTCCAA
Epcam	GCTGGCAACAAGTTGCTCTCTGAA	CGTTGCACTGGTTGGCTTTGAAGA
Fgf5	AATATTTGCTGTGTCTCAGG	TAAATTTGGCACTTGCATGG
Flk1	CGGTGAGAAAGCCTTGAT	CAAGCATACGGGCTTGTTTG
Foxa2	CTGAAGCCCGAGCACCATTA	CCCTGGGTAGTGCATGAC
GAPDH	GTATGACTCCACTCACGGCAAA	TTCCATTCTCGGCCTTG
Gata4	GTCGTAATGCCGAGGGTGA	TCCTTCCGCATTGCAAGAG
Nanog	AACCAAAGGATGAAGTGCAAG	TCCAAGTTGGGTTGGTCCA

p16	**TGATGATGATGGGCAACG**	**ACGGGAACGCAAATATCG**
p19	**TCCATTGAAGAAGGGAGTGG**	**CACCAAAGGGGTGAGAAAA**
Pax6	**AACAACCTGCCTATGCAACC**	**CATAACTCCGCCCATTCACT**
Oct4	**CGTGGAGACTTTGCAGCCTG**	**GCTTGGCAAACTGTTCTAGCTCCT**
Oct4 (UTR)	**GTTGGAGAAGGTGGAACCAA**	**CTCCTTCTGCAGGGCTTTC**
Sall1	**ACCCGGAAGAGGGAGTACAG**	**TGGAAATGTTGAGGCTTCG**
Snai1	**TTGTGTCTGCACGACCTGTGGAAA**	**TCTTCACATCCGAGTGGGTTTGGA**
Snai2 (Slug)	**CACATTCGAACCCACACATTGCCT**	**TGTGCCCTCAGGTTTGATCTGTCT**
Tcf7 (Tcf1)	**GCTGCCTGAGGTCAGAGAAT**	**CCCCAGCTTTCTCCACTCTA**
Tcf7 (Tcf1 human)	**ACCTGGTCACCCAGCAGCCA**	**TCAGGTTGCGGTCGAAGGGC**
Tcf7l1 (Tcf3)	**GAAATCCCAGTTACGGTC**	**CAGGTTGGGTAGAGCTGC**
Thy1.2	**AACTCTTGGCACCATGAACC**	**TCAGGCTGGTCACCTTCTG**
Vimentin	**CCCAGATTCAGGAACAGCAT**	**TCCGGTACTCGTTTGATCC**
Zfp42	**AGGAAATAGGTAGAGCGCATCGCA**	**AGGCGATCCTGCTTTCTTCTGTGT**

Table 13 – List of oligonucleotides used for qRT-PCR experiments

Western blot

Cells were harvested and washed twice with PBS. Cell lysis was performed on ice for 25 min, in RIPA buffer (150 mM NaCl, 1% Nonidet P40, 0.5% sodium deoxycholate, 0.1% sodium dodecyl sulphate, 50 mM Tris-HCl, pH 8.0) containing a protease inhibitory cocktail (Roche). Insoluble material was pelleted by centrifugation at 16,000× g for 3 min at 4 °C. Protein concentrations were determined using the Bradford assay (Bio-Rad). Thirty micrograms extract was mixed with 4× sample buffer (40% glycerol, 240 mM Tris/HCl, pH 6.8, 8% SDS, 0.04% bromophenol blue, 5% β-mercaptoethanol), denatured at 96ºC for 5 minutes, separated by SDS-PAGE, and transferred to nitrocellulose membranes (PROTRAN-Whatman, Schleicher&Schuell). The membranes were blocked with 5% non-fat dry milk in TBS-T for 60 min, incubated with primary antibodies overnight at 4 °C, washed three times with TBS-T for 10 min, incubated with the peroxidase-conjugated secondary antibody (1:2000; Amersham

Biosciences) in TBST with 5% non-fat dry milk for 60 min, and washed three times with TBST for 10 min. Immunoreactive proteins were detected using Supersignal West Dura HRP Detection kits (Pierce). A list of the primary antibodies is provided in Table 14

Chromatin immunoprecipitation assay (ChIP)

ChIP was carried out as described in (Morey et al, 2012). Briefly, ESCs were trypsinised and crosslinked in 1% formaldehyde for 10 min at room temperature. Crosslinking was quenched with 0.125 M glycine for 5 min. The pelleted cells were lysed in 1 ml ChIP buffer and sonicated for 10 min in a Bioruptor sonicator (Diagenode). The soluble material was quantified using Bradford assays. To immunoprecipitate the transcription factors, 500 µg protein was used. Antibodies were incubated overnight with the chromatin. The immunocomplexes were recovered with 30 µl protein A or G agarose bead slurries. The immunoprecipitated material was washed three times with low-salt buffer and one time with high-salt buffer. DNA complexes were decrosslinked at 65 °C for 3 h, and the DNA was then eluted in 200 µl water using the PCR purification kit (QIAGEN). Two microliters DNA was used for each qPCR reaction, using SYBR green (Fermentas), a list of the oligonucleotides used is provided in Table 15. Details for primary antibodies used for ChIP is provided in Table 14.

Antibody	Raised in	Working dilution	Supplier and catalogue number
MAP2	Mouse	1:200 (IF)	Abcam (ab11267)
CD90.2 (Thy-1.2) APC-conjugated	Mouse	0,06 µg x 106 cells (FACS)	eBioscience (12-0902)
β-catenin (anti C-terminal)	Mouse	1:500 /1:1000 (WB) 1:100/1:500 (IF)	BD (MAB-318)
ß-catenin (anti-N-terminal)	Rabbit		Sigma Aldrich (CC2206)

ß-catenin unphosphorylated	**Rabbit**	**1:500 (WB)**	**Millipore (#05-665)**
SSEA-1	**Mouse**	**1:100 (IF)**	**Santa Cruz (sc- 21701)**
Oct4	**Mouse**	**1:100/1:200 (IF) 1:500/1:1000 (WB)**	**Santa Cruz (sc-5279)**
Nestin	**Mouse**	**1:200 (IF)**	**Abcam (ab6142)**
Albumin	**Mouse**	**1:500 (IF)**	**Abcam (ab19196-2)**
Tubulin	**Mouse**	**1:1000/1:2000 (WB)**	**Sigma (T0198)**
Actin	**Mouse**	**1:2000 (WB)**	**Abcam (ab8226)**
Gata4	**Rabbit**	**1:200 (IF)**	**Abcam (ab61170)**
Sox2	**Rabbit**	**1:500 (IF)**	**Abcam (ab97959)**
Nanog	**Rabbit**	**1:300 (IF)**	**Calbiochem (#SC1000)**
Nanog	**Rabbit**		**Bethil**
Plakoglobin	**Mouse**	**1:1000 (WB) 1:100 (IF)**	**BD (610253)**
GFP	**Rabbit**	**1:500 (IF)**	**Santa Cruz (sc-8332)**
TCF1 FL (C6D9)	**Rabbit**	**1:1000 (WB)**	**Cell Signaling (#2203)**
TCF1 Total (C46C7)	**Rabbit**	**1:1000 (WB) 5 µg (ChIP)**	**Cell Signaling (#2206)**
E-cadherin		**(WB)**	**Abcam (ab15148)**
E-cadherin APC-conjugated		**(FACS)**	**Thermofisher**
H3 (total)	**Rabbit**	**1:10000 (WB)**	**Abcam (ab1791)**

Table 14 - List of the primary antibodies used for immune-fluorescence (IF), western-blot (WB), chromatin immune-precipitation (ChIP) and flow-citometry/fluorescence-activated cell sorting (FACS) experiments.

Target	Genomic region (mm10)	Oligonucleotides sequences
Axin2	chr11:108920349+108920569	Forward:GAGCGCCTCTGTGATTGG Reverse: GACCCCACCTTTTACAGCAA
Snai1	chr2:167540114+167540263	Forward:TGCTAAGCTGTGGGGCTCTA Reverse: GAGAACTGGGTGGTGCATTT
Cdkn1a (p21)	chr17:29093835+29093977	Forward:TCCACAGCGATATCCAGACA Reverse: TCCACTCATCACCACACACA
Control 1	chr6:9794157+9794307	Forward: AGAGAAGTGCTGTGCAGAC Reverse: CATGCACAGTTCAGCAGCT
Control 2 (IgX1a)	IgX1a locus (Qiagen) Chr RefSe NC_000072.5 assay position 9746274	-

Table 15 – List of qPCR oligonucleotides used for Chromatin Immuno-precipitation assays (ChIP).

Cell cycle analysis

For cell cycle analysis of mESCs, cells were detached with Accutase (Gibco) and collected by centrifugation at 300 rcf for 5 min. The cell pellet was resuspended and fixed overnight in 3ml ice-cold 70% ethanol. After fixation, the cells were centrifuged at 300rcf for 10 min at room

temperature. The pellet was washed twice in 1ml PBS. During each wash, the cells were pelleted at 300rcf for 5 min at room temperature. Then cells were resuspended in DAPI solution (SIGMA 09542) (5**µ**g/ml/10_6 cells in PBS) and incubated for 30 min on ice. Samples were processed with BD LSR Fortessa and analysed with FlowJo software.

Growth curve analysis

For growth curve analysis 7x10^4 mESCs per well were plated in triplicates in mw12 well plates. Each day, for the following 96 hours, cells were detached, diluted in propidium iodide (PI) containing medium to stain dead cells and transferred into mw96 U-bottom plates (Falcon) for through flow-cytometry using FACS-canto.

For cell counts by FACS cells were trypsinized, diluted in serum containing media and propidium iodide (PI) to detect dead cells. Diluted cells were plated in 96-well plates and counted using FACScanto. Exponential growth curves were calculated setting the intercept equal to the number of cells counted at 24 hours after plating (pc) and the growth rate (gr) was used to calculate the doubling time (dt).

$$y = pc \cdot e^{gr \cdot time}; \quad dt = \frac{\ln(2)}{gr};$$

Flow cytometry analysis of mESCs

Mouse ESCs were trypsinized and the pelleted cells were resuspended in PBS with 2% FBS with DAPI. The GFP of the E14-TOP7x-dGFP and Rex1GFPd2 cells was analyzed using a BD LSR Fortessa.

Neural differentiation assay

For monolayer neural differentiation we adapted a protocol previously reported (Marks et al. 2012). Mouse ESCs cultured in Serum/LIF (S) or 2i/LIF (LP, HP, HP/S/2i) were plated at a density

of 5,000 cells per cm^2. After plating, media were switched to N2B27 to induce neural differentiation. Sox1 expression was measured by qPCR.

Epiblast differentiation assay

For Epiblast differentiation we adapted a protocol previously reported in (Guo et al. 2011). Briefly, mESCs (S, LP, HP and HP/S/2i) were plated at $3X10^4$ cells/cm^2 in N2B27 media (DMEM/F12 1:1 GIBCO; N2 [Cat. 17502-048] and B27 [Cat. 10880-038] Invitrogen) containing 20ng/ml activin A (R&D System) and 12ng/ml Fgf2 (R&D System) on fibronectin (Millipore)-coated plates. Medium was replaced every 24 hours. RNA was extracted from cells collected every 24 hours to measure Fgf5 expression by qPCR.

RNA Sequencing and analysis

We use poly-A pull-down to enrich mRNAs from total RNA samples and proceed on library preparation by using Illumina TruSeq RNA prep kit. Libraries were then sequenced using Illumina HiSeq2000 at Columbia Genome Center producing more than 340 million single reads long 101 bases. We use RTA (Illumina) for base calling and CASAVA (version 1.8.2) for converting BCL to fastq format, coupled with adaptor trimming. We mapped the reads to a reference transcriptome (mouse transcriptome from Ensembl v80) using kallisto (v0.42.5, (Bray et al. 2016)), to generate counts and "transcripts per million" (TPM) values. We tested for differentially expressed genes for all pairwise conditions using edgeR (Robinson et al. 2010) from raw counts, filtering for genes with p values < 0.001 and a fold change greater than 1.

To measure the transcriptomic differences between all samples, raw counts were normalised for library size and transformed using "variance stabilising transformation" in DESeq (Anders et al. 2010), before calculating distance (dist; using euclidean distances; Fig. 2A left) and principle components (princomp; Fig 2A right [PCA]) in R using only genes with variance greater than 1.

For heatmaps of lineage marker expression (Figure 4), we plotted log2 (TPM+1), in order to avoid logarithm of null values.

GO and KEGG analysis were performed using DAVID (6.8 beta version) (Huang et al. 2007, Huang da et al. 2009).

Gene set enrichment analysis was performed with GSEA v2.2.2 (Broad Institute, (Subramanian et al. 2005)) using the following settings: Expression datasets = raw counts; Gene sets database = c2.cp.kegg.v5.1.symbols.gmt; Number of permutations = 1000; Permutation type = gene_set. Gene sets with a nominal p Value < 1% were considered significantly enriched.

Immuno-staining for STORM.

For the imaging experiments, cells were plated on 8-well Lab-tek 1 coverglass chamber (Nunc) at a seeding density of 20,000-50,000 cells per well, fixed and permeabilized with Methanol-Ethanol (1:1) solution at -20^{O}C for 6 min. After 1 h incubation at room temperature with blocking buffer containing 10% (wt/vol) BSA (Sigma) in PBS, samples were incubated overnight with the rabbit polyclonal anti-H2B (Abcam, abcam 1790) diluted 1:50 in blocking buffer and then for 40 min with the same dilution of secondary donkey anti-rabbit (Jackson ImmunoResearch), labeled with Alexa Fluor 405-Alexa Fluor 647 (Invitrogen) pair dyes. Repeated washing were done at every step.

STORM Imaging.

Imaging was done using a commercial microscope system from Nikon Instruments (NSTORM). 647 nm laser light was used for exciting the reporter dye (Alexa Fluor 647, Invitrogen) and switching it to the dark state, and 405 nm laser light was used for reactivating the Alexa Fluor 647 into a fluorescent state via an activator dye (Alexa Fluor 405)–facilitated manner. An imaging cycle was used in which one frame belonging to the activating light pulse (405 nm) was alternated with three frames belonging to the imaging light pulse (647 nm). Activation laser (405 nm) power was increased over time in an identical way up to 60 μW as in (Ricci et al. 2015).

Imaging was done using a previously described imaging buffer (Cysteamine MEA [SigmaAldrich, #30070-50G], Glox Solution: 0.5 mgmL-1 glucose oxidase, 40 mgmL-1catalase [all Sigma], 10% Glucose in PBS) (Bates et al. 2007).

STORM images analysis and cluster quantification.

STORM images were analyzed and rendered as previously described (Bates et al. 2007, Huang et al. 2008, Huang et al. 2008) by fitting the fluorophore images in each frame to a simple Gaussian to determine *x-y* coordinates. Number of localizations per clutch was quantified as previously explained (Ricci et al. 2015) by means of custom code originally written in Matlab by Carlo Manzo.

Statistical Analysis

Averages from three independent experiments were calculated for most of the shown experiments, unless where specifically indicated, and Student's t-tests were performed for statistical analysis. P Value <0.05 was used to determine statistical significance.

Bibliography

A

Abranches, E., et al. (2013). "*Generation and characterization of a novel mouse embryonic stem cell line with a dynamic reporter of Nanog expression*." PLoS One 8(3): e59928.

Abranches, E., et al. (2014). "*Stochastic NANOG fluctuations allow mouse embryonic stem cells to explore pluripotency*." Development 141(14): 2770-2779.

Ahumada, A., et al. (2002). "*Signaling of rat Frizzled-2 through phosphodiesterase and cyclic GMP*." Science 298(5600): 2006-2010.

Anders, S. and W. Huber (2010). "*Differential expression analysis for sequence count data*." Genome Biol 11(10): R106.

Anton, R., et al. (2007). "*Beta-catenin signaling contributes to stemness and regulates early differentiation in murine embryonic stem cells*." FEBS Lett 581(27): 5247-5254.

Arce, L., et al. (2006). "*Diversity of LEF/TCF action in development and disease*." Oncogene 25(57): 7492-7504.

Atcha, F. A., et al. (2003). "*A new beta-catenin-dependent activation domain in T cell factor*." J Biol Chem 278(18): 16169-16175.

Aulehla, A., et al. (2003). "*Wnt3a plays a major role in the segmentation clock controlling somitogenesis*." Dev Cell 4(3): 395-406.

Aulicino, F., et al. (2014). "*Temporal perturbation of the Wnt signaling pathway in the control of cell reprogramming is modulated by TCF1*." Stem Cell Reports 2(5): 707-720.

Avior, Y., et al. (2016). "*Pluripotent stem cells in disease modelling and drug discovery*." Nat Rev Mol Cell Biol 17(3): 170-182.

B

Banito, A., et al. (2009). "*Senescence impairs successful reprogramming to pluripotent stem cells*." Genes Dev 23(18): 2134-2139.

Banziger, C., et al. (2006). "*Wntless, a conserved membrane protein dedicated to the secretion of Wnt proteins from signaling cells*." Cell 125(3): 509-522.

Barker, N., et al. (2001). "*The chromatin remodelling factor Brg-1 interacts with beta-catenin to promote target gene activation*." EMBO J 20(17): 4935-4943.

Bates, M., et al. (2007). "*Multicolor super-resolution imaging with photo-switchable fluorescent probes*." Science 317(5845): 1749-1753.

Batlle, E., et al. (2000). "*The transcription factor snail is a repressor of E-cadherin gene expression in epithelial tumour cells*." Nat Cell Biol 2(2): 84-89.

Bauer, A., et al. (2000). "*Pontin52 and reptin52 function as antagonistic regulators of beta-catenin signalling activity*." EMBO J 19(22): 6121-6130.

Behrens, J., et al. (1996). "*Functional interaction of beta-catenin with the transcription factor LEF-1*." Nature 382(6592): 638-642.

Bhat, B. M., et al. (2007). "*Structure-based mutation analysis shows the importance of LRP5 beta-propeller 1 in modulating Dkk1-mediated inhibition of Wnt signaling*." Gene 391(1-2): 103-112.
Biechele, T. L. and R. T. Moon (2008). "*Assaying beta-catenin/TCF transcription with beta-catenin/TCF transcription-based reporter constructs*." Methods Mol Biol 468: 99-110.
Bienz, M. and H. Clevers (2000). "*Linking colorectal cancer to Wnt signaling*." Cell 103(2): 311-320.
Bienz, M. and H. Clevers (2003). "*Armadillo/beta-catenin signals in the nucleus--proof beyond a reasonable doubt?*" Nat Cell Biol 5(3): 179-182.
Binari, R. C., et al. (1997). "*Genetic evidence that heparin-like glycosaminoglycans are involved in wingless signaling*." Development 124(13): 2623-2632.
Bodine, P. V., et al. (2009). "*A small molecule inhibitor of the Wnt antagonist secreted frizzled-related protein-1 stimulates bone formation*." Bone 44(6): 1063-1068.
Boroviak, T., et al. (2014). "*The ability of inner-cell-mass cells to self-renew as embryonic stem cells is acquired following epiblast specification*." Nat Cell Biol 16(6): 516-528.
Brambrink, T., et al. (2008). "*Sequential expression of pluripotency markers during direct reprogramming of mouse somatic cells*." Cell Stem Cell 2(2): 151-159.
Brannon, M., et al. (1999). "*XCtBP is a XTcf-3 co-repressor with roles throughout Xenopus development*." Development 126(14): 3159-3170.
Brault, V., et al. (2001). "*Inactivation of the beta-catenin gene by Wnt1-Cre-mediated deletion results in dramatic brain malformation and failure of craniofacial development*." Development 128(8): 1253-1264.
Bray, N. L., et al. (2016). "*Near-optimal probabilistic RNA-seq quantification*." Nat Biotechnol 34(5): 525-527.
Brembeck, F. H., et al. (2006). "*Balancing cell adhesion and Wnt signaling, the key role of beta-catenin*." Curr Opin Genet Dev 16(1): 51-59.
Brons, I. G., et al. (2007). "*Derivation of pluripotent epiblast stem cells from mammalian embryos*." Nature 448(7150): 191-195.
Buechling, T., et al. (2011). "*p24 proteins are required for secretion of Wnt ligands*." EMBO Rep 12(12): 1265-1272.

C

Cadigan, K. M. (2002). "*Wnt signaling--20 years and counting*." Trends Genet 18(7): 340-342.
Cadigan, K. M. and Y. I. Liu (2006). "*Wnt signaling: complexity at the surface*." J Cell Sci 119(Pt 3): 395-402.
Cadigan, K. M. and M. L. Waterman (2012). "*TCF/LEFs and Wnt signaling in the nucleus*." Cold Spring Harb Perspect Biol 4(11).

Cahan, P. and G. Q. Daley (2013). "*Origins and implications of pluripotent stem cell variability and heterogeneity*." Nat Rev Mol Cell Biol 14(6): 357-368.
Carey, B. W., et al. (2010). "*Single-gene transgenic mouse strains for reprogramming adult somatic cells*." Nat Methods 7(1): 56-59.
Carlsson, P., et al. (1993). "*The hLEF/TCF-1 alpha HMG protein contains a context-dependent transcriptional activation domain that induces the TCR alpha enhancer in T cells*." Genes Dev 7(12A): 2418-2430.
Chambers, I., et al. (2007). "*Nanog safeguards pluripotency and mediates germline development*." Nature 450(7173): 1230-1234.
Chan, K. C., et al. (2015). "*Therapeutic targeting of CBP/beta-catenin signaling reduces cancer stem-like population and synergistically suppresses growth of EBV-positive nasopharyngeal carcinoma cells with cisplatin*." Sci Rep 5: 9979.
Chinnadurai, G. (2002). "*CtBP, an unconventional transcriptional corepressor in development and oncogenesis*." Mol Cell 9(2): 213-224.
Cole, M. F., et al. (2008). "*Tcf3 is an integral component of the core regulatory circuitry of embryonic stem cells*." Genes Dev 22(6): 746-755.
Cong, F. and H. Varmus (2004). "*Nuclear-cytoplasmic shuttling of Axin regulates subcellular localization of beta-catenin*." Proc Natl Acad Sci U S A 101(9): 2882-2887.
Coronado, D., et al. (2013). "*A short G1 phase is an intrinsic determinant of naive embryonic stem cell pluripotency*." Stem Cell Res 10(1): 118-131.
Coudreuse, D. Y., et al. (2006). "*Wnt gradient formation requires retromer function in Wnt-producing cells*." Science 312(5775): 921-924.

D

Davidson, G., et al. (2005). "*Casein kinase 1 gamma couples Wnt receptor activation to cytoplasmic signal transduction*." Nature 438(7069): 867-872.
Davidson, K. C., et al. (2015). "*The pluripotent state in mouse and human*." Development 142(18): 3090-3099.
Davis, R. L., et al. (1987). "*Expression of a single transfected cDNA converts fibroblasts to myoblasts*." Cell 51(6): 987-1000.
De, A. (2011). "*Wnt/Ca2+ signaling pathway: a brief overview*." Acta Biochim Biophys Sin (Shanghai) 43(10): 745-756.
De Vries, W. N., et al. (2004). "*Maternal beta-catenin and E-cadherin in mouse development*." Development 131(18): 4435-4445.
Di Stefano, B., et al. (2014). "*C/EBPalpha poises B cells for rapid reprogramming into induced pluripotent stem cells*." Nature 506(7487): 235-239.

Doble, B. W., et al. (2007). "*Functional redundancy of GSK-3alpha and GSK-3beta in Wnt/beta-catenin signaling shown by using an allelic series of embryonic stem cell lines*." Dev Cell 12(6): 957-971.
Du, S. J., et al. (1995). "*Identification of distinct classes and functional domains of Wnts through expression of wild-type and chimeric proteins in Xenopus embryos*." Mol Cell Biol 15(5): 2625-2634.
Dunn, S. J., et al. (2014). "*Defining an essential transcription factor program for naive pluripotency*." Science 344(6188): 1156-1160.
Dutta, D., et al. (2011). "*Self-renewal versus lineage commitment of embryonic stem cells: protein kinase C signaling shifts the balance*." Stem Cells 29(4): 618-628.

E

Edel, M. J., et al. (2010). "*Rem2 GTPase maintains survival of human embryonic stem cells as well as enhancing reprogramming by regulating p53 and cyclin D1*." Genes Dev 24(6): 561-573.
Eldar-Finkelman, H. and A. Martinez (2011). "*GSK-3 Inhibitors: Preclinical and Clinical Focus on CNS*." Front Mol Neurosci 4: 32.
Esteban, M. A., et al. (2012). "*The mesenchymal-to-epithelial transition in somatic cell reprogramming*." Curr Opin Genet Dev 22(5): 423-428.
Esteban, M. A., et al. (2010). "*Vitamin C enhances the generation of mouse and human induced pluripotent stem cells*." Cell Stem Cell 6(1): 71-79.
Evans, M. J. and M. H. Kaufman (1981). "*Establishment in culture of pluripotential cells from mouse embryos*." Nature 292(5819): 154-156.
Factor, D. C., et al. (2014). "*Epigenomic comparison reveals activation of "seed" enhancers during transition from naive to primed pluripotency*." Cell Stem Cell 14(6): 854-863.

F, G,

Fagotto, F., et al. (1998). "*Nuclear localization signal-independent and importin/karyopherin-independent nuclear import of beta-catenin*." Curr Biol 8(4): 181-190.
Fuerer, C. and R. Nusse (2010). "*Lentiviral vectors to probe and manipulate the Wnt signaling pathway*." PLoS One 5(2): e9370.
Gallahan, D., et al. (1987). "*A new common integration region (int-3) for mouse mammary tumor virus on mouse chromosome 17*." J Virol 61(1): 218-220.
Gao, C., et al. (2014). "*Regulation of Wnt/beta-catenin signaling by posttranslational modifications*." Cell Biosci 4(1): 13.
Giese, K., et al. (1991). "*DNA-binding properties of the HMG domain of the lymphoid-specific transcriptional regulator LEF-1*." Genes Dev 5(12B): 2567-2578.
Gradl, D., et al. (2002). "*Functional diversity of Xenopus lymphoid enhancer factor/T-cell factor transcription factors relies on combinations*

of activating and repressing elements." J Biol Chem 277(16): 14159-14171.
Graf, T. (2011). "*Historical origins of transdifferentiation and reprogramming*." Cell Stem Cell 9(6): 504-516.
Guo, G., et al. (2011). "*A PiggyBac-based recessive screening method to identify pluripotency regulators*." PLoS One 6(4): e18189.
Gurdon, J. B., et al. (1958). "*Sexually mature individuals of Xenopus laevis from the transplantation of single somatic nuclei*." Nature 182(4627): 64-65.

H, I

Ha, N. C., et al. (2004). "*Mechanism of phosphorylation-dependent binding of APC to beta-catenin and its role in beta-catenin degradation*." Mol Cell 15(4): 511-521.
Hackett, J. A. and M. A. Surani (2014). "*Regulatory principles of pluripotency: from the ground state up*." Cell Stem Cell 15(4): 416-430.
Hall, J., et al. (2009). "*Oct4 and LIF/Stat3 additively induce Kruppel factors to sustain embryonic stem cell self-renewal*." Cell Stem Cell 5(6): 597-609.
Hao, J., et al. (2006). "*WNT/beta-catenin pathway up-regulates Stat3 and converges on LIF to prevent differentiation of mouse embryonic stem cells*." Dev Biol 290(1): 81-91.
Hassani, S. N., et al. (2014). "*Inhibition of TGFbeta signaling promotes ground state pluripotency*." Stem Cell Rev 10(1): 16-30.
Hawkins, K., et al. (2014). "*Cell signalling pathways underlying induced pluripotent stem cell reprogramming*." World J Stem Cells 6(5): 620-628.
He, T. C., et al. (1998). "*Identification of c-MYC as a target of the APC pathway*." Science 281(5382): 1509-1512.
He, X., et al. (2004). "*LDL receptor-related proteins 5 and 6 in Wnt/beta-catenin signaling: arrows point the way*." Development 131(8): 1663-1677.
Heigwer, F., et al. (2014). "*E-CRISP: fast CRISPR target site identification*." Nat Methods 11(2): 122-123.
Hikasa, H., et al. (2002). "*The Xenopus receptor tyrosine kinase Xror2 modulates morphogenetic movements of the axial mesoderm and neuroectoderm via Wnt signaling*." Development 129(22): 5227-5239.
Ho, R., et al. (2013). "*Stage-specific regulation of reprogramming to induced pluripotent stem cells by Wnt signaling and T cell factor proteins*." Cell Rep 3(6): 2113-2126.
Hoppler, S., et al. (1996). "*Expression of a dominant-negative Wnt blocks induction of MyoD in Xenopus embryos*." Genes Dev 10(21): 2805-2817.
Hoppler, S. and C. L. Kavanagh (2007). "*Wnt signalling: variety at the core*." J Cell Sci 120(Pt 3): 385-393.

Hovanes, K., et al. (2001). "*Beta-catenin-sensitive isoforms of lymphoid enhancer factor-1 are selectively expressed in colon cancer*." Nat Genet 28(1): 53-57.
Hsu, S. C., et al. (1998). "*Modulation of transcriptional regulation by LEF-1 in response to Wnt-1 signaling and association with beta-catenin*." Mol Cell Biol 18(8): 4807-4818.
Huang, B., et al. (2008). "*Whole-cell 3D STORM reveals interactions between cellular structures with nanometer-scale resolution*." Nat Methods 5(12): 1047-1052.
Huang, B., et al. (2008). "*Three-dimensional super-resolution imaging by stochastic optical reconstruction microscopy*." Science 319(5864): 810-813.
Huang da, W., et al. (2009). "*Systematic and integrative analysis of large gene lists using DAVID bioinformatics resources*." Nat Protoc 4(1): 44-57.
Huang, D. W., et al. (2007). "*DAVID Bioinformatics Resources: expanded annotation database and novel algorithms to better extract biology from large gene lists*." Nucleic Acids Res 35(Web Server issue): W169-175.
Huang, Y., et al. (2014). "*Telomere regulation in pluripotent stem cells*." Protein Cell 5(3): 194-202.
Huber, A. H., et al. (1997). "*Three-dimensional structure of the armadillo repeat region of beta-catenin*." Cell 90(5): 871-882.
Huber, O., et al. (1996). "*Nuclear localization of beta-catenin by interaction with transcription factor LEF-1*." Mech Dev 59(1): 3-10.
Huelsken, J., et al. (2000). "*Requirement for beta-catenin in anterior-posterior axis formation in mice*." J Cell Biol 148(3): 567-578.
Ikeya, M., et al. (1997). "*Wnt signalling required for expansion of neural crest and CNS progenitors*." Nature 389(6654): 966-970.

J

Jamieson, C., et al. (2011). "*Regulation of beta-catenin nuclear dynamics by GSK-3beta involves a LEF-1 positive feedback loop*." Traffic 12(8): 983-999.
Janda, C. Y., et al. (2012). "*Structural basis of Wnt recognition by Frizzled*." Science 337(6090): 59-64.
Jernigan, K. K., et al. (2010). "*Gbetagamma activates GSK3 to promote LRP6-mediated beta-catenin transcriptional activity*." Sci Signal 3(121): ra37.
Jho, E. H., et al. (2002). "*Wnt/beta-catenin/Tcf signaling induces the transcription of Axin2, a negative regulator of the signaling pathway*." Mol Cell Biol 22(4): 1172-1183.
Jirmanova, L., et al. (2002). "*Differential contributions of ERK and PI3-kinase to the regulation of cyclin D1 expression and to the control of the G1/S transition in mouse embryonic stem cells*." Oncogene 21(36): 5515-5528.

K

Kahan, B. W. and B. Ephrussi (1970). "*Developmental potentialities of clonal in vitro cultures of mouse testicular teratoma*." J Natl Cancer Inst 44(5): 1015-1036.

Kawamura, T., et al. (2009). "*Linking the p53 tumour suppressor pathway to somatic cell reprogramming*." Nature 460(7259): 1140-1144.

Kielman, M. F., et al. (2002). "*Apc modulates embryonic stem-cell differentiation by controlling the dosage of beta-catenin signaling*." Nat Genet 32(4): 594-605.

Kim, D. H., et al. (2015). "*Single-cell transcriptome analysis reveals dynamic changes in lncRNA expression during reprogramming*." Cell Stem Cell 16(1): 88-101.

Kim, H., et al. (2013). "*Modulation of beta-catenin function maintains mouse epiblast stem cell and human embryonic stem cell self-renewal*." Nat Commun 4: 2403.

Kim, Y. E., et al. (2008). "*Upregulation of NF-kappaB upon differentiation of mouse embryonic stem cells*." BMB Rep 41(10): 705-709.

Kishida, S., et al. (1999). "*DIX domains of Dvl and axin are necessary for protein interactions and their ability to regulate beta-catenin stability*." Mol Cell Biol 19(6): 4414-4422.

Klaus, A. and W. Birchmeier (2008). "*Wnt signalling and its impact on development and cancer*." Nat Rev Cancer 8(5): 387-398.

Klein, P. S. and D. A. Melton (1996). "*A molecular mechanism for the effect of lithium on development*." Proc Natl Acad Sci U S A 93(16): 8455-8459.

Kohn, A. D. and R. T. Moon (2005). "*Wnt and calcium signaling: beta-catenin-independent pathways*." Cell Calcium 38(3-4): 439-446.

Kolodziejczyk, A. A., et al. (2015). "*Single Cell RNA-Sequencing of Pluripotent States Unlocks Modular Transcriptional Variation*." Cell Stem Cell 17(4): 471-485.

Komiya, Y. and R. Habas (2008). "*Wnt signal transduction pathways*." Organogenesis 4(2): 68-75.

Korinek, V., et al. (1998). "*Depletion of epithelial stem-cell compartments in the small intestine of mice lacking Tcf-4*." Nat Genet 19(4): 379-383.

Kramps, T., et al. (2002). "*Wnt/wingless signaling requires BCL9/legless-mediated recruitment of pygopus to the nuclear beta-catenin-TCF complex*." Cell 109(1): 47-60.

Kuhl, M., et al. (2000). "*Ca(2+)/calmodulin-dependent protein kinase II is stimulated by Wnt and Frizzled homologs and promotes ventral cell fates in Xenopus*." J Biol Chem 275(17): 12701-12711.

Kulak, O., et al. (2015). "*Disruption of Wnt/beta-Catenin Signaling and Telomeric Shortening Are Inextricable Consequences of Tankyrase Inhibition in Human Cells*." Mol Cell Biol 35(14): 2425-2435.
Kumar, R. M., et al. (2014). "*Deconstructing transcriptional heterogeneity in pluripotent stem cells*." Nature 516(7529): 56-61.
Kunath, T., et al. (2007). "*FGF stimulation of the Erk1/2 signalling cascade triggers transition of pluripotent embryonic stem cells from self-renewal to lineage commitment*." Development 134(16): 2895-2902.

L

Lee, E., et al. (2003). "*The roles of APC and Axin derived from experimental and theoretical analysis of the Wnt pathway*." PLoS Biol 1(1): E10.
Leitch, H. G., et al. (2013). "*Naive pluripotency is associated with global DNA hypomethylation*." Nat Struct Mol Biol 20(3): 311-316.
Leitch, H. G., et al. (2013). "*Rebuilding pluripotency from primordial germ cells*." Stem Cell Reports 1(1): 66-78.
Li, H., et al. (2009). "*The Ink4/Arf locus is a barrier for iPS cell reprogramming*." Nature 460(7259): 1136-1139.
Li, R., et al. (2010). "*A mesenchymal-to-epithelial transition initiates and is required for the nuclear reprogramming of mouse fibroblasts*." Cell Stem Cell 7(1): 51-63.
Li, T. W., et al. (2006). "*Wnt activation and alternative promoter repression of LEF1 in colon cancer*." Mol Cell Biol 26(14): 5284-5299.
Liu, T., et al. (2001). "*G protein signaling from activated rat frizzled-1 to the beta-catenin-Lef-Tcf pathway*." Science 292(5522): 1718-1722.
Lluis, F., et al. (2011). "*T-cell factor 3 (Tcf3) deletion increases somatic cell reprogramming by inducing epigenome modifications*." Proc Natl Acad Sci U S A 108(29): 11912-11917.
Lluis, F., et al. (2008). "*Periodic activation of Wnt/beta-catenin signaling enhances somatic cell reprogramming mediated by cell fusion*." Cell Stem Cell 3(5): 493-507.
Logan, C. Y. and R. Nusse (2004). "*The Wnt signaling pathway in development and disease*." Annu Rev Cell Dev Biol 20: 781-810.
Lustig, B., et al. (2002). "*Negative feedback loop of Wnt signaling through upregulation of conductin/axin2 in colorectal and liver tumors*." Mol Cell Biol 22(4): 1184-1193.
Lyashenko, N., et al. (2011). "*Differential requirement for the dual functions of beta-catenin in embryonic stem cell self-renewal and germ layer formation*." Nat Cell Biol 13(7): 753-761.

M

MacArthur, B. D., et al. (2012). "*Nanog-dependent feedback loops regulate murine embryonic stem cell heterogeneity*." Nat Cell Biol 14(11): 1139-1147.

MacDonald, B. T., et al. (2009). "*Wnt/beta-catenin signaling: components, mechanisms, and diseases*." Dev Cell 17(1): 9-26.
Madan, B. and D. M. Virshup (2015). "*Targeting Wnts at the source--new mechanisms, new biomarkers, new drugs*." Mol Cancer Ther 14(5): 1087-1094.
Maeda, O., et al. (2004). "*Plakoglobin (gamma-catenin) has TCF/LEF family-dependent transcriptional activity in beta-catenin-deficient cell line*." Oncogene 23(4): 964-972.
Maherali, N. and K. Hochedlinger (2009). "*Tgfbeta signal inhibition cooperates in the induction of iPSCs and replaces Sox2 and cMyc*." Curr Biol 19(20): 1718-1723.
Mahmoudi, S. and A. Brunet (2012). "*Aging and reprogramming: a two-way street*." Curr Opin Cell Biol 24(6): 744-756.
Marks, H., et al. (2012). "*The transcriptional and epigenomic foundations of ground state pluripotency*." Cell 149(3): 590-604.
Marlow, F., et al. (2002). "*Zebrafish Rho kinase 2 acts downstream of Wnt11 to mediate cell polarity and effective convergence and extension movements*." Curr Biol 12(11): 876-884.
Marson, A., et al. (2008). "*Wnt signaling promotes reprogramming of somatic cells to pluripotency*." Cell Stem Cell 3(2): 132-135.
Martello, G. and A. Smith (2014). "*The nature of embryonic stem cells*." Annu Rev Cell Dev Biol 30: 647-675.
Martin, G. R. and M. J. Evans (1975). "*Differentiation of clonal lines of teratocarcinoma cells: formation of embryoid bodies in vitro*." Proc Natl Acad Sci U S A 72(4): 1441-1445.
Marucci, L., et al. (2014). "*beta-catenin fluctuates in mouse ESCs and is essential for Nanog-mediated reprogramming of somatic cells to pluripotency*." Cell Rep 8(6): 1686-1696.
Matsui, Y., et al. (1992). "*Derivation of pluripotential embryonic stem cells from murine primordial germ cells in culture*." Cell 70(5): 841-847.
Mauviel, A., et al. (2012). "*Integrating developmental signals: a Hippo in the (path)way*." Oncogene 31(14): 1743-1756.
Merrill, B. J., et al. (2001). "*Tcf3 and Lef1 regulate lineage differentiation of multipotent stem cells in skin*." Genes Dev 15(13): 1688-1705.
Merrill, B. J., et al. (2004). "*Tcf3: a transcriptional regulator of axis induction in the early embryo*." Development 131(2): 263-274.
Messerschmidt, D., et al. (2016). "*beta-catenin-mediated adhesion is required for successful preimplantation mouse embryo development*." Development 143(11): 1993-1999.
Metcalfe, C., et al. (2010). "*Stability elements in the LRP6 cytoplasmic tail confer efficient signalling upon DIX-dependent polymerization*." J Cell Sci 123(Pt 9): 1588-1599.

Mikels, A. J. and R. Nusse (2006). "*Wnts as ligands: processing, secretion and reception*." Oncogene 25(57): 7461-7468.
Miller, J. R. (2002). "*The Wnts*." Genome Biol 3(1): REVIEWS3001.
Mlodzik, M. (2002). "*Tissue polarity in the retina*." Results Probl Cell Differ 37: 89-106.
Molenaar, M., et al. (1998). "*Differential expression of the HMG box transcription factors XTcf-3 and XLef-1 during early xenopus development*." Mech Dev 75(1-2): 151-154.
Moon, R. T., et al. (2004). "*WNT and beta-catenin signalling: diseases and therapies*." Nat Rev Genet 5(9): 691-701.
Morgani, S. M., et al. (2013). "*Totipotent embryonic stem cells arise in ground-state culture conditions*." Cell Rep 3(6): 1945-1957.

N

Nichols, J. and A. Smith (2009). "*Naive and primed pluripotent states*." Cell Stem Cell 4(6): 487-492.
Niehrs, C. (2006). "*Function and biological roles of the Dickkopf family of Wnt modulators*." Oncogene 25(57): 7469-7481.
Niida, A., et al. (2004). "*DKK1, a negative regulator of Wnt signaling, is a target of the beta-catenin/TCF pathway*." Oncogene 23(52): 8520-8526.
Niwa, H. (2007). "*How is pluripotency determined and maintained?*" Development 134(4): 635-646.
Niwa, H., et al. (2009). "*A parallel circuit of LIF signalling pathways maintains pluripotency of mouse ES cells*." Nature 460(7251): 118-122.
Nusse, R. "The Wnt Homepage." Retrieved 06/02/2016, 2016, from http://web.stanford.edu/group/nusselab/cgi-bin/wnt/.
Nusse, R., et al. (1991). "*A new nomenclature for int-1 and related genes: the Wnt gene family*." Cell 64(2): 231.
Nusse, R., et al. (1984). "*Mode of proviral activation of a putative mammary oncogene (int-1) on mouse chromosome 15*." Nature 307(5947): 131-136.
Nusslein-Volhard, C. and E. Wieschaus (1980). "*Mutations affecting segment number and polarity in Drosophila*." Nature 287(5785): 795-801.

O

Ogawa, K., et al. (2006). "*Synergistic action of Wnt and LIF in maintaining pluripotency of mouse ES cells*." Biochem Biophys Res Commun 343(1): 159-166.
Okamura, R. M., et al. (1998). "*Redundant regulation of T cell differentiation and TCRalpha gene expression by the transcription factors LEF-1 and TCF-1*." Immunity 8(1): 11-20.
Orsulic, S., et al. (1999). "*E-cadherin binding prevents beta-catenin nuclear localization and beta-catenin/LEF-1-mediated transactivation*." J Cell Sci 112 (Pt 8): 1237-1245.

P

Pai, R., et al. (2004). "*Deoxycholic acid activates beta-catenin signaling pathway and increases colon cell cancer growth and invasiveness*." Mol Biol Cell 15(5): 2156-2163.

Pauklin, S. and L. Vallier (2013). "*The cell-cycle state of stem cells determines cell fate propensity*." Cell 155(1): 135-147.

Pereira, L., et al. (2006). "*Repression of Nanog gene transcription by Tcf3 limits embryonic stem cell self-renewal*." Mol Cell Biol 26(20): 7479-7491.

Peters, G., et al. (1983). "*Tumorigenesis by mouse mammary tumor virus: evidence for a common region for provirus integration in mammary tumors*." Cell 33(2): 369-377.

Polo, J. M., et al. (2012). "*A molecular roadmap of reprogramming somatic cells into iPS cells*." Cell 151(7): 1617-1632.

Price, F. D., et al. (2013). "*Canonical Wnt signaling induces a primitive endoderm metastable state in mouse embryonic stem cells*." Stem Cells 31(4): 752-764.

Price, L. S., et al. (2004). "*Rap1 regulates E-cadherin-mediated cell-cell adhesion*." J Biol Chem 279(34): 35127-35132.

Price, M. A. (2006). "*CKI, there's more than one: casein kinase I family members in Wnt and Hedgehog signaling*." Genes Dev 20(4): 399-410.

R

Raggioli, A., et al. (2014). "*Beta-catenin is vital for the integrity of mouse embryonic stem cells*." PLoS One 9(1): e86691.

Rais, Y., et al. (2013). "*Deterministic direct reprogramming of somatic cells to pluripotency*." Nature 502(7469): 65-70.

Ran, F. A., et al. (2013). "*Genome engineering using the CRISPR-Cas9 system*." Nat Protoc 8(11): 2281-2308.

Rao, T. P. and M. Kuhl (2010). "*An updated overview on Wnt signaling pathways: a prelude for more*." Circ Res 106(12): 1798-1806.

Reya, T. and H. Clevers (2005). "*Wnt signalling in stem cells and cancer*." Nature 434(7035): 843-850.

Reya, T., et al. (2003). "*A role for Wnt signalling in self-renewal of haematopoietic stem cells*." Nature 423(6938): 409-414.

Ricci, M. A., et al. (2015). "*Chromatin fibers are formed by heterogeneous groups of nucleosomes in vivo*." Cell 160(6): 1145-1158.

Rijsewijk, F., et al. (1987). "*The Drosophila homolog of the mouse mammary oncogene int-1 is identical to the segment polarity gene wingless*." Cell 50(4): 649-657.

Robinson, M. D., et al. (2010). "*edgeR: a Bioconductor package for differential expression analysis of digital gene expression data*." Bioinformatics 26(1): 139-140.

Roccio, M., et al. (2013). "*Predicting stem cell fate changes by differential cell cycle progression patterns*." Development 140(2): 459-470.
Roose, J., et al. (1999). "*Synergy between tumor suppressor APC and the beta-catenin-Tcf4 target Tcf1*." Science 285(5435): 1923-1926.
Roose, J., et al. (1998). "*The Xenopus Wnt effector XTcf-3 interacts with Groucho-related transcriptional repressors*." Nature 395(6702): 608-612.
Ross, J., et al. (2014). "*A rare human syndrome provides genetic evidence that WNT signaling is required for reprogramming of fibroblasts to induced pluripotent stem cells*." Cell Rep 9(5): 1770-1780.

S

Samavarchi-Tehrani, P., et al. (2010). "*Functional genomics reveals a BMP-driven mesenchymal-to-epithelial transition in the initiation of somatic cell reprogramming*." Cell Stem Cell 7(1): 64-77.
Sato, N., et al. (2004). "*Maintenance of pluripotency in human and mouse embryonic stem cells through activation of Wnt signaling by a pharmacological GSK-3-specific inhibitor*." Nat Med 10(1): 55-63.
Schifferli, J. A. and D. K. Peters (1983). "*Immune adherence and staphylococcus protein A binding of soluble immune complexes produced by complement activation*." Clin Exp Immunol 54(3): 827-833.
Seifert, J. R. and M. Mlodzik (2007). "*Frizzled/PCP signalling: a conserved mechanism regulating cell polarity and directed motility*." Nat Rev Genet 8(2): 126-138.
Sharma, R. P. (1973). "*Wingless a new mutant in Drosophila melanogaster*." Drosophila information service(50): p. 134.
Sharma, R. P. and V. L. Chopra (1976). "*Effect of the Wingless (wg1) mutation on wing and haltere development in Drosophila melanogaster*." Dev Biol 48(2): 461-465.
Sheldahl, L. C., et al. (1999). "*Protein kinase C is differentially stimulated by Wnt and Frizzled homologs in a G-protein-dependent manner*." Curr Biol 9(13): 695-698.
Shimizu, T., et al. (2012). "*Dual inhibition of Src and GSK3 maintains mouse embryonic stem cells, whose differentiation is mechanically regulated by Src signaling*." Stem Cells 30(7): 1394-1404.
Sierra, J., et al. (2006). "*The APC tumor suppressor counteracts beta-catenin activation and H3K4 methylation at Wnt target genes*." Genes Dev 20(5): 586-600.
Sims, R. J., 3rd, et al. (2004). "*Recent highlights of RNA-polymerase-II-mediated transcription*." Curr Opin Cell Biol 16(3): 263-271.
Singer, Z. S., et al. (2014). "*Dynamic heterogeneity and DNA methylation in embryonic stem cells*." Mol Cell 55(2): 319-331.
Smith, A. G., et al. (1988). "*Inhibition of pluripotential embryonic stem cell differentiation by purified polypeptides*." Nature 336(6200): 688-690.

Soufi, A., et al. (2012). "*Facilitators and impediments of the pluripotency reprogramming factors' initial engagement with the genome*." Cell 151(5): 994-1004.
Staal, F. J., et al. (1999). "*Tcf-1-mediated transcription in T lymphocytes: differential role for glycogen synthase kinase-3 in fibroblasts and T cells*." Int Immunol 11(3): 317-323.
Stadeli, R. and K. Basler (2005). "*Dissecting nuclear Wingless signalling: recruitment of the transcriptional co-activator Pygopus by a chain of adaptor proteins*." Mech Dev 122(11): 1171-1182.
Stadeli, R., et al. (2006). "*Transcription under the control of nuclear Arm/beta-catenin*." Curr Biol 16(10): R378-385.
Stadtfeld, M., et al. (2008). "*Defining molecular cornerstones during fibroblast to iPS cell reprogramming in mouse*." Cell Stem Cell 2(3): 230-240.
Stevens, L. C. and C. C. Little (1954). "*Spontaneous Testicular Teratomas in an Inbred Strain of Mice*." Proc Natl Acad Sci U S A 40(11): 1080-1087.
Subramanian, A., et al. (2005). "*Gene set enrichment analysis: a knowledge-based approach for interpreting genome-wide expression profiles*." Proc Natl Acad Sci U S A 102(43): 15545-15550.

T

Tada, M., et al. (2001). "*Nuclear reprogramming of somatic cells by in vitro hybridization with ES cells*." Curr Biol 11(19): 1553-1558.
Tai, C. I. and Q. L. Ying (2013). "*Gbx2, a LIF/Stat3 target, promotes reprogramming to and retention of the pluripotent ground state*." J Cell Sci 126(Pt 5): 1093-1098.
Takahashi, K., et al. (2007). "*Induction of pluripotent stem cells from adult human fibroblasts by defined factors*." Cell 131(5): 861-872.
Takahashi, K. and S. Yamanaka (2006). "*Induction of pluripotent stem cells from mouse embryonic and adult fibroblast cultures by defined factors*." Cell 126(4): 663-676.
Takahashi, K. and S. Yamanaka (2016). "*A decade of transcription factor-mediated reprogramming to pluripotency*." Nat Rev Mol Cell Biol 17(3): 183-193.
Takeda, H., et al. (2006). "*Human sebaceous tumors harbor inactivating mutations in LEF1*." Nat Med 12(4): 395-397.
Tamai, K., et al. (2000). "*LDL-receptor-related proteins in Wnt signal transduction*." Nature 407(6803): 530-535.
Tanaka, K., et al. (2000). "*The evolutionarily conserved porcupine gene family is involved in the processing of the Wnt family*." Eur J Biochem 267(13): 4300-4311.
Tang, X., et al. (2012). "*Roles of N-glycosylation and lipidation in Wg secretion and signaling*." Dev Biol 364(1): 32-41.

Tao, Q., et al. (2005). "*Maternal wnt11 activates the canonical wnt signaling pathway required for axis formation in Xenopus embryos*." Cell 120(6): 857-871.
ten Berge, D., et al. (2008). "*Wnt signaling mediates self-organization and axis formation in embryoid bodies*." Cell Stem Cell 3(5): 508-518.
ten Berge, D., et al. (2011). "*Embryonic stem cells require Wnt proteins to prevent differentiation to epiblast stem cells*." Nat Cell Biol 13(9): 1070-1075.
Tesar, P. J., et al. (2007). "*New cell lines from mouse epiblast share defining features with human embryonic stem cells*." Nature 448(7150): 196-199.
Thorne, C. A., et al. (2010). "*Small-molecule inhibition of Wnt signaling through activation of casein kinase 1alpha*." Nat Chem Biol 6(11): 829-836.
Tighe, A., et al. (2007). "*GSK-3 inhibitors induce chromosome instability*." BMC Cell Biol 8: 34.
Topczewski, J., et al. (2001). "*The zebrafish glypican knypek controls cell polarity during gastrulation movements of convergent extension*." Dev Cell 1(2): 251-264.
Townsley, F. M., et al. (2004). "*Pygopus and Legless target Armadillo/beta-catenin to the nucleus to enable its transcriptional co-activator function*." Nat Cell Biol 6(7): 626-633.
Toyooka, Y., et al. (2008). "*Identification and characterization of subpopulations in undifferentiated ES cell culture*." Development 135(5): 909-918.
Travis, A., et al. (1991). "*LEF-1, a gene encoding a lymphoid-specific protein with an HMG domain, regulates T-cell receptor alpha enhancer function [corrected]*." Genes Dev 5(5): 880-894.

U, V

Utikal, J., et al. (2009). "*Immortalization eliminates a roadblock during cellular reprogramming into iPS cells*." Nature 460(7259): 1145-1148.
van Beest, M., et al. (2000). "*Sequence-specific high mobility group box factors recognize 10-12-base pair minor groove motifs*." J Biol Chem 275(35): 27266-27273.
Van de Wetering, M., et al. (1996). "*Extensive alternative splicing and dual promoter usage generate Tcf-1 protein isoforms with differential transcription control properties*." Mol Cell Biol 16(3): 745-752.
van de Wetering, M., et al. (1991). "*Identification and cloning of TCF-1, a T lymphocyte-specific transcription factor containing a sequence-specific HMG box*." EMBO J 10(1): 123-132.

W, X

Waddington, C. H. (1957). "*The strategy of the genes. A discussion of some aspects of theoretical biology*." George Allen & Unwin.

Wagner, R. T., et al. (2010). "*Canonical Wnt/beta-catenin regulation of liver receptor homolog-1 mediates pluripotency gene expression*." Stem Cells 28(10): 1794-1804.
Wang, J., et al. (2006). "*A protein interaction network for pluripotency of embryonic stem cells*." Nature 444(7117): 364-368.
Wang, T., et al. (2011). "*The histone demethylases Jhdm1a/1b enhance somatic cell reprogramming in a vitamin-C-dependent manner*." Cell Stem Cell 9(6): 575-587.
Wang, Y. and J. Nathans (2007). "*Tissue/planar cell polarity in vertebrates: new insights and new questions*." Development 134(4): 647-658.
Waterman, M. L. (2004). "*Lymphoid enhancer factor/T cell factor expression in colorectal cancer*." Cancer Metastasis Rev 23(1-2): 41-52.
Wehrli, M., et al. (2000). "*arrow encodes an LDL-receptor-related protein essential for Wingless signalling*." Nature 407(6803): 527-530.
Weinberger, L., et al. (2016). "*Dynamic stem cell states: naive to primed pluripotency in rodents and humans*." Nat Rev Mol Cell Biol 17(3): 155-169.
White, J. and S. Dalton (2005). "*Cell cycle control of embryonic stem cells*." Stem Cell Rev 1(2): 131-138.
Willert, K., et al. (2003). "*Wnt proteins are lipid-modified and can act as stem cell growth factors*." Nature 423(6938): 448-452.
Willert, K. and K. A. Jones (2006). "*Wnt signaling: is the party in the nucleus?*" Genes Dev 20(11): 1394-1404.
Willert, K. and R. Nusse (2012). "*Wnt proteins*." Cold Spring Harb Perspect Biol 4(9): a007864.
Williams, B. O. and K. L. Insogna (2009). "*Where Wnts went: the exploding field of Lrp5 and Lrp6 signaling in bone*." J Bone Miner Res 24(2): 171-178.
Wilmut, I., et al. (1997). "*Viable offspring derived from fetal and adult mammalian cells*." Nature 385(6619): 810-813.
Wray, J. and C. Hartmann (2012). "*WNTing embryonic stem cells*." Trends Cell Biol 22(3): 159-168.
Wray, J., et al. (2011). "*Inhibition of glycogen synthase kinase-3 alleviates Tcf3 repression of the pluripotency network and increases embryonic stem cell resistance to differentiation*." Nat Cell Biol 13(7): 838-845.
Wray, J., et al. (2010). "*The ground state of pluripotency*." Biochem Soc Trans 38(4): 1027-1032.
Wu, G., et al. (2003). "*Structure of a beta-TrCP1-Skp1-beta-catenin complex: destruction motif binding and lysine specificity of the SCF(beta-TrCP1) ubiquitin ligase*." Mol Cell 11(6): 1445-1456.
Wu, Y., et al. (2013). "*CHIR99021 promotes self-renewal of mouse embryonic stem cells by modulation of protein-encoding gene and long*

intergenic non-coding RNA expression." Exp Cell Res 319(17): 2684-2699.

Xing, Y., et al. (2008). "*Crystal structure of a full-length beta-catenin*." Structure 16(3): 478-487.

Y

Yamada, S., et al. (2005). "*Deconstructing the cadherin-catenin-actin complex*." Cell 123(5): 889-901.

Yamanaka, S. and H. M. Blau (2010). "*Nuclear reprogramming to a pluripotent state by three approaches*." Nature 465(7299): 704-712.

Yao, D., et al. (2011). "*Mechanism of the mesenchymal-epithelial transition and its relationship with metastatic tumor formation*." Mol Cancer Res 9(12): 1608-1620.

Ye, S., et al. (2013). "*Embryonic stem cell self-renewal pathways converge on the transcription factor Tfcp2l1*." EMBO J 32(19): 2548-2560.

Yeo, J. C., et al. (2014). "*Klf2 is an essential factor that sustains ground state pluripotency*." Cell Stem Cell 14(6): 864-872.

Yi, F., et al. (2011). "*Opposing effects of Tcf3 and Tcf1 control Wnt stimulation of embryonic stem cell self-renewal*." Nat Cell Biol 13(7): 762-770.

Yi, F., et al. (2008). "*Tcf3 functions as a steady-state limiter of transcriptional programs of mouse embryonic stem cell self-renewal*." Stem Cells 26(8): 1951-1960.

Ying, Q. L., et al. (2003). "*BMP induction of Id proteins suppresses differentiation and sustains embryonic stem cell self-renewal in collaboration with STAT3*." Cell 115(3): 281-292.

Ying, Q. L., et al. (2008). "*The ground state of embryonic stem cell self-renewal*." Nature 453(7194): 519-523.

Yoshida, K., et al. (1994). "*Maintenance of the pluripotential phenotype of embryonic stem cells through direct activation of gp130 signalling pathways*." Mech Dev 45(2): 163-171.

Yu, J., et al. (2007). "*Induced pluripotent stem cell lines derived from human somatic cells*." Science 318(5858): 1917-1920.

Z

Zeng, X., et al. (2005). "*A dual-kinase mechanism for Wnt co-receptor phosphorylation and activation*." Nature 438(7069): 873-877.

Zhai, L., et al. (2004). "*Drosophila wnt-1 undergoes a hydrophobic modification and is targeted to lipid rafts, a process that requires porcupine*." J Biol Chem 279(32): 33220-33227.

Zhang, Q., et al. (2007). "*Small-molecule synergist of the Wnt/beta-catenin signaling pathway*." Proc Natl Acad Sci U S A 104(18): 7444-7448.

Zhang, X., et al. (2013). "*Gene regulatory networks mediating canonical Wnt signal-directed control of pluripotency and differentiation in embryo stem cells*." Stem Cells 31(12): 2667-2679.
Zhen, Y., et al. (2007). "*Indirubin-3'-monoxime inhibits autophosphorylation of FGFR1 and stimulates ERK1/2 activity via p38 MAPK*." Oncogene 26(44): 6372-6385.
Zorn, A. M., et al. (1999). "*Regulation of Wnt signaling by Sox proteins: XSox17 alpha/beta and XSox3 physically interact with beta-catenin*." Mol Cell 4(4): 487-498.
Zunder, E. R., et al. (2015). "*A continuous molecular roadmap to iPSC reprogramming through progression analysis of single-cell mass cytometry*." Cell Stem Cell 16(3): 323-337.